Effect of catheter motion on ultrasound M-mode images and corresponding velocity profiles

Development and validation of a simulation model

Bente de Lat | April, 2014

TU Delft | PHILIPS

Graduation committee & supervisors:

Prof. Dr. J. Dankelman, BMechE, 3ME

Dr. Ir. G.J.M. Tuijthof, BMechE, 3ME

Dr. G.A. Delgado Lopes, Intelligent Control & Robotics, DCSC

Dr. Ir. A.J. Loeve, BMechE, 3ME

Dr. A. Kolen, Philips Research, Minimally Invasive Healthcare

Dr. F. Zuo, Philips Research, Video & Image Processing

Effect of catheter motion on ultrasound M-mode images and corresponding velocity profiles

Development and validation of a simulation model

Bente de Lat[1,2], Gabrielle Tuijthof[1], Arjo Loeve[1], Alex Kolen[2], Fei Zuo[2], and Jenny Dankelman[1]

[1]Delft University of Technology, Faculty of 3ME, Department of Biomechanical Engineering
[2]Philips Research Eindhoven, Department of Minimally Invasive Healthcare

Background An ablation catheter with integrated high-frequency single element ultrasound transducers has been developed by Philips Research, which makes it possible to assess tissue-depth and lesion formation in real-time. The interpretation of the acquired ultrasound M-mode images is difficult due to a combination of cardiac motion and motion of the catheter itself.
Objective The aim of this study is to develop and validate a simulation model that includes catheter and tissue motion and use this as a tool to gain insights in the effects of catheter motion on M-mode images and corresponding velocity profiles.
Method A 2D simulation model, of a moving catheter with three integrated ultrasound transducers that observe contracting tissue, was developed. Comparison of simulated data with real ultrasound data was performed, among other tests, to validate the 2D simulation model. Validation criteria were based on predefined requirements. The validated simulation model was used to generate seventeen different output datasets varying with the frequency and amplitude of the cardiac & catheter motion input signals. These datasets were used to analyse the effect of catheter motion on M-mode images and corresponding velocity profiles.
Results The validation tests imply that the simulated data can serve as reliable replacements for real ultrasound data. Findings from the analysis of the simulated data suggest that cardiac velocity is underestimated when the catheter angle deviates from its perpendicular state in relation to the tissue and is overestimated when the catheter angle moves back to its perpendicular state. Moreover, when catheter motion dominates over cardiac motion the cardiac velocity may be estimated in the opposite direction as the actual direction of cardiac motion.
Conclusion The validation tests insinuate that the simulation model meets the predefined requirements. The simulation increases understanding of the relation between catheter & cardiac motion in M-mode images. The information that can be derived from an M-mode image can be used to estimate if catheter motion is dominating over cardiac motion. Furthermore, the findings obtained within this study can be used to evaluate if the estimated direction of the velocity of cardiac motion is correct and if the cardiac velocity is under- or overestimated.
Keywords: Catheter ablation; Ultrasound; Catheter motion; M-mode interpretation; Velocity profile

1. Introduction

Atrial fibrillation (AF) is the most common cardiac arrhythmia disease worldwide associated with an adverse prognosis [1, 2]. AF occurs when undesired electrical signals arise around the pulmonary veins (PVs) and disturb the normal heart rhythm [3]. The prevalence of people suffering AF is increasing in relation to age. For patients aged 60-69 the estimated prevalence ranges from 1.2% to 2.8%, for patients older than 80 years the prevalence ranges from 7.3% to 13.7% [3,4]. Moreover, a significant increase of the prevalence is expected in the coming fifty years [4, 5]. AF is a costly health problem and will become even more costly as a result of the increasing prevalence. Developments in the treatment of AF could contribute to limit these rising rates [3]. (Appendix D)

Cardiac radiofrequency (RF) ablation has become the surgical treatment of choice to treat AF permanently. In order to make this treatment successful for AF, contiguous lesions are required to totally isolate the PVs and block undesired electrical signals. These lesions need to be transmural, which means that the lesion covers the entire thickness of the heart wall. Currently, observing a decrease in local electro gram amplitude, intracardiac echocardiography, electrical impedance and contact force are used to assess the success rate of a lesion. However, these methods, in combination with the delivered power and duration of ablation, do not give a direct measurement of the lesion size, which makes it difficult to determine in real-time if a lesion is transmural [6]. Moreover, because of the shortcomings of the current assessment possibilities, gaps in ablation lines around the PVs that are supposed to be contiguous are a reality of current clinical practice, which constrain the success rate of AF ablation [7]. (Appendix E)

To be able to assess tissue-depth and lesion formation in real-time, an ablation catheter with integrated high-frequency single element ultrasound (US) transducers has been developed by Philips Research, shown in Figure 1. (Appendix F) This type of catheter has one transducer at the tip and three transducers at the side, respectively

named transducer A, B and C. Ultrasound pulses with a frequency of 30 MHz are transmitted into the tissue by each transducer. These pulses interact with the scanned tissue and are reflected back towards the catheter tip. These reflected signals cause deformation of the piezoelectric element, which is the essential element in the transducer that has the property to convert ultrasound waves into electrical signals and vice versa. Deformation of this piezoelectric element generates an unprocessed electrical RF signal. (Appendix F.3) This RF signal contains information about the reflections, propagation of the US waves and their interaction with the observed moving tissue. The RF signal consists of a carrier wave, shown at the left side of Figure 2, which has the same frequency as the transmitted pulse if a stationary object is observed.

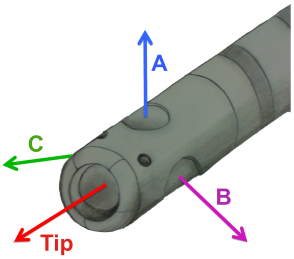

Figure 1: *The 'Cameleo' ablation catheter with four integrated ultrasound transducers, developed and manufactured by Philips Research*

Extraction of the envelope of this RF signal, also shown in Figure 2, makes RF data suitable for interpretation. The envelop signal can be visualised in an A-mode image, see Figure 2, of which the amplitude of the envelope signal determines the brightness of the grey scaled A-mode image. [8] An M-mode consists of multiple A-modes that are displayed over time, see the grey scaled image in Figure 3. Changes that occur in the observed tissue can be monitored with an M-mode image. The catheter shown in Figure 1 generates a single M-mode image per integrated transducer.

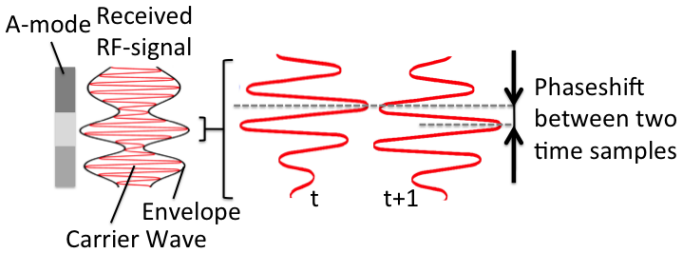

Figure 2: *Phaseshift between the RF signals of two subsequent time samples, which can be used to measure the velocity of the observed tissue in relation to the transducer*

The received RF data can also be used to obtain a velocity profile of the moving tissue that shows the velocities of the tissue particles in relation to the transducer. This can be done with the Temporal-Spectral-Mean (TSM) algorithm, developed by Philips research. This algorithm calculates the velocities based on the phase shifts between the RF signals of two subsequent time samples with an accuracy of 2 %, see Figure 2. A visual representation of this velocity profile, from now on referred to as TSM, can be displayed as an overlay image over the M-mode image, see Figure 3. In the TSM image, tissue that moves towards the transducer is a positive velocity indicated with the colour red whereas tissue that moves away from the transducer is a negative velocity indicated with the colour blue. In case of cardiac motion this means that when the heart contracts, the cardiac wall becomes thicker, and consequently the tissue will move away from the transducer, which results in a negative estimated velocity. When the heart relaxes, the wall thickness decreases, which results in a positive estimated velocity.

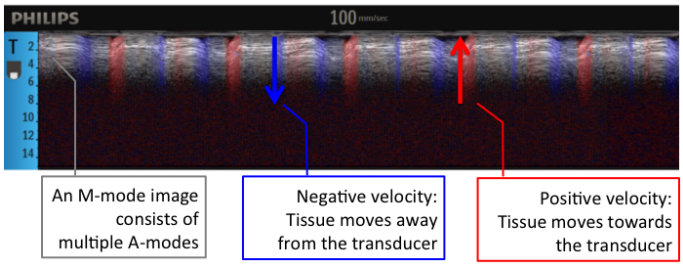

Figure 3: *M-mode image with a TSM image as an overlay, which presents the direction and velocity of the tissue motion.*

The visualisation processes of converting the RF data into these M-mode and TSM images are performed with the Cameleo software (Philips, Version 904, Eindhoven The Netherlands).

With the generated M-mode images the progression of a lesion formation can be monitored. The TSM is used to observe a decrease in velocity of the ablated tissue, since ablated tissue is stiffer and consequently the tissue velocity decreases. This intraprocedural method allows a physician to adapt the ablation parameters in real-time in order to safely perform successful transmural lesions [6,9]. However, for new physicians it is challenging to get familiar with these M-modes and TSM images.

The main problem with this novel system is that the M-mode images of moving cardiac tissue are acquired with a moving catheter. This undesired, but also unknown movement, makes the interpretation of M-mode images difficult, since it is unknown how the M-mode pattern relates to cardiac and catheter motion. It is also unknown how catheter motion influences the TSM estimations. (Appendix G) Therefore, the aim of this study is to:

- Develop and validate a 2D simulation model that simulates a moving catheter, including integrated US transducers that generate RF-data of naturally moving cardiac tissue
- Use this simulation model as a tool to gain insight about how catheter and cardiac motion relates to patterns in M-mode images and subsequent velocity profiles

First, the development of the 2D simulation model will be explained in Section 2. Second, the performed validation of this model is evaluated in Section 3. Finally, insight about the effect of catheter motion on an M-mode image and corresponding TSM, based on the analysis of simulated data, will be discussed in Section 4.

2. Development of Simulation Model

2.1. Method of Simulation Development

To gain insight into the effects of catheter and cardiac motion on M-mode images, a simplified simulation model was

developed, see Figure 4. First, a naturally moving cardiac tissue model was generated in a 2D space using a Cartesian coordinate system. Secondly, a moving catheter, including three integrated US transducers, was added to this model. Finally, per modelled transducer the received RF signal of the moving tissue was generated and displayed in a single M-mode image.

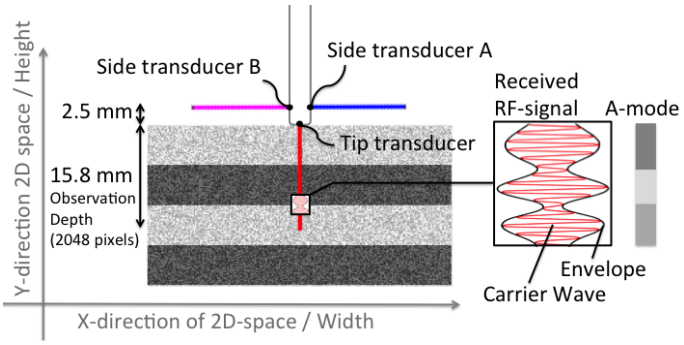

Figure 4: *Schematic overview of the specifications of the 2D simulation model*

In clinical practise their is a limited understanding how the catheter is moving, which makes it hard to determine the relation between the M-mode images and catheter motion. This model could be used as a tool to provide insight in the effects of catheter and cardiac motion on M-mode images since effects of these motions can be observed directly.

Matlab (Mathworks,version R2012b, Natick, United States of America (USA)) was used for programming the simulation model. The 2D simulation model was developed based on predefined requirements, specifications and assumptions. (Appendix I)

2.1.1. Requirements & Specifications Model

To be able to simulate the interaction between the cardiac tissue and catheter as desired, the 2D simulation model should meet the following predefined requirements (Appendix J), which were based on the physiology of a beating heart, the working principles of the Cameleo catheter (Figure 1) and the corresponding visualisation processes:

1. Motion of the modelled cardiac tissue, which represents a beating heart, should at least contain motion in the axial direction, which is defined as perpendicular direction in relation to the tissue surface, in other words, the Y direction of the 2D space, see Figure 4 and 5
2. At least three catheter motions should be modelled, representing translation in lateral and axial direction, respectively X and Y direction of the 2D space, see Figure 4, and rotation along the Z-axis, see Figure 5
3. Every transducer integrated in the catheter tip should provide a single M-mode image
4. If identical catheter and cardiac motion is used to generate data, then simulated M-mode images should present the same patterns compared to real M-mode images, which can be quantified by comparing the frequency, amplitude and slope that can be derived from the geometry of the M-mode patterns
5. The simulation model should display directly the observed moving tissue as result of a changing catheter orientation, which can be compared with a real M-mode image, or should generate a received RF signal that contains information about the reflections and motions in the observed tissue
6. The velocities that occur in the tissue as result of cardiac or catheter motion should be able to be measured from the simulated RF data with an accuracy of 98% using the TSM algorithm (Philips, Eindhoven The Netherlands)
7. If identical catheter and cardiac motion are used to generate data, the TSM of the simulated RF data should be similar to the TSM of real RF data, which can be quantified by comparing if identical velocity directions are determined
8. The simulated RF data should be generated in 16-bit integers, which is required in order to use the simulated data as input for the visualisation Cameleo software (Philips, Version 904, Eindhoven The Netherlands)
9. The values of all parameters in the simulation model should be adjustable

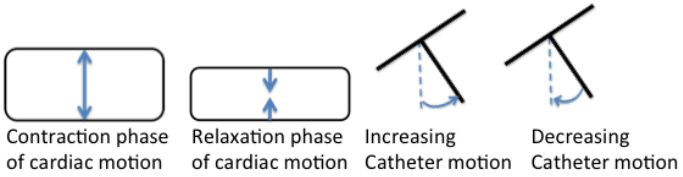

Figure 5: *When the heart contracts, the heart wall expands, when the heart relaxes, the heart wall becomes thinner.(Appendix J) Rotational Catheter motion around Z-axis can be described dependent of the changing angle with respect to the perpendicular orientation to the tissue.*

Throughout this entire study, the adjustable parameters were set according to the following specifications, which are schematically shown in Figure 4. (Appendix K) These values were based on the settings of the MUVIC 444-H Cameleo catheter, shown in Figure 1, and accessory US system, developed and manufactured by Philips research.

10. The tip of the catheter should contain one single element transducer
11. Two single element transducers should be placed at the side of the catheter tip, orientated with a fixed angle of 90° in relation to the orientation of the tip transducer
12. Distance between the side transducers and tip transducer should be 2.5 mm
13. The carrier wave of the received RF signal should be modelled with a frequency of 30 MHz and a sample frequency of 100 MHz
14. The observation depth of the transducers should be 15.8 mm, which relates to a RF signal consisting of 2048 samples
15. The frequency for both catheter and cardiac motion should be comparable to an average heart rate of 60 beats per second, which relates to a frequency of 1 Hz of the motion input signals

16. The tissue should consist of at least a two layer structure with different reflection coefficients

2.1.2. Assumptions

The following assumptions were made to simplify the model: (Appendix L)

- The density and compressibility of the tissue are not determined, but assumed to be equal in the entire tissue
- The speed of sound is assumed to be equal in the entire tissue, since the speed of sound is a function of density and compressibility
- The acoustic impedance is assumed to be equal in the entire tissue, since the acoustic impedance is a function of density and speed of sound
- In practise, the reflection coefficient is determined by the differences in acoustic impedance between tissue structures. In a real US image, these differences in reflection coefficients are represented with different shades of grey. Since for this simulation model is assumed that the acoustic impedance is equal in the entire tissue, the reflection coefficients are determined with a value in the range of 16-bit, independent of any physical properties. The value 0 relates to no reflection and the value 2^{16} relates to maximal reflection, visualised as respectively black and white in an M-mode image
- Differences in reflection coefficients within one tissue layer, a speckle pattern, are introduced in the simulation for detailed visual purposes, but are also not in relation with any physical properties of the tissue
- The RF signal of a transducer does only contain information about the tissue on which the transducer is oriented
- There is no reduction of the amplitude and intensity of the RF signal as a function of depth
- No frequency shift of the carrier wave occurs as a result of interaction with a moving tissue particle

2.2. Results of Simulation Model Development

The 2D simulation model can generate two different types of output depending on the purpose of the simulation results:

- The Movie-generator, Figure 6, generates a movie of the observed moving tissue as result of a changing catheter orientation, which can be used to obtain graphical data for qualitative analysis.
- The RF-generator, Figure 7, generates RF data that is not directly suitable for interpretation, but can be used for applications as calculating a TSM or can serve as input for the Cameleo software

Figure 6 shows an edited screenshot of a movie obtained with the Movie-generator. The cardiac motion and catheter motion input signals are displayed in the upper right corner. The red dots in these graphs represent the current time sample. For each time sample, tissue changes and changes of the catheter orientation are showed in the upper left corner. The red, blue and pink lines represent the sightlines of the transducers. For each transducer, these sightlines per time sample are displayed in the three lower images, where the horizontal axis represents the time, the vertical axis represents the observation depth and the coloured dot at the top represents the transducer. So, for each time sample the grey values that are observed are directly plotted. This way of presenting data is representative for M-modes images acquired with the Cameleo catheter.

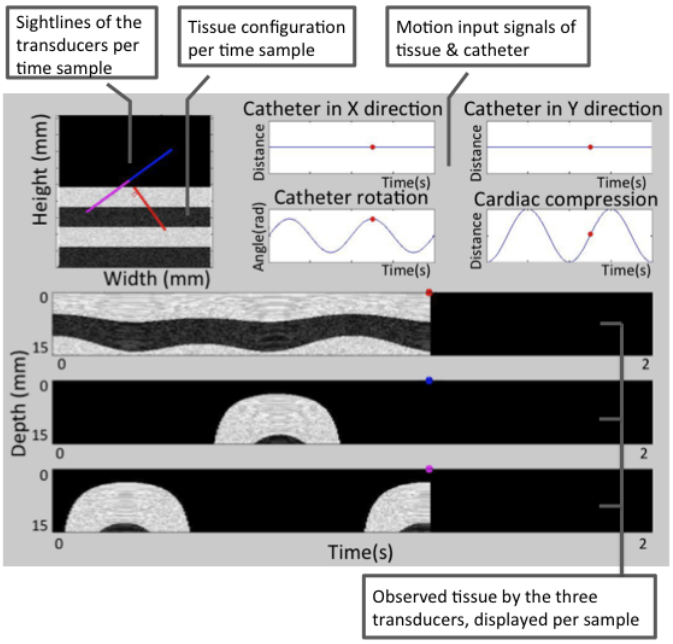

Figure 6: *Movie generator: In the upper left corner the tissue composition and catheter orientation, including three US transducers, is shown per time sample, which are determined by the motion signals shown in the upper right corner. The three bottom images corresponds to the three transducers and show per time sample the temporal changes of the observed tissue*

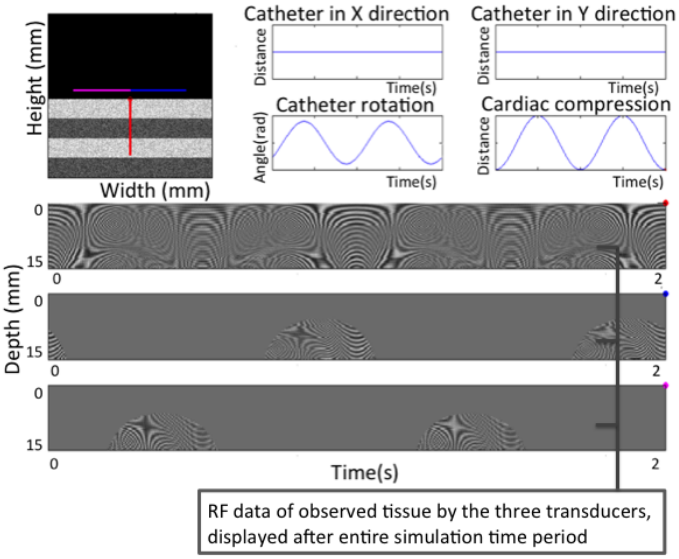

Figure 7: *RF data generator: Generates representative RF data of the observed tissue as shown in Figure 6. After processing the RF data it can be used for interpretation.*

The RF data generator shows the RF data after running the simulation for a set time period, see Figure 7. That

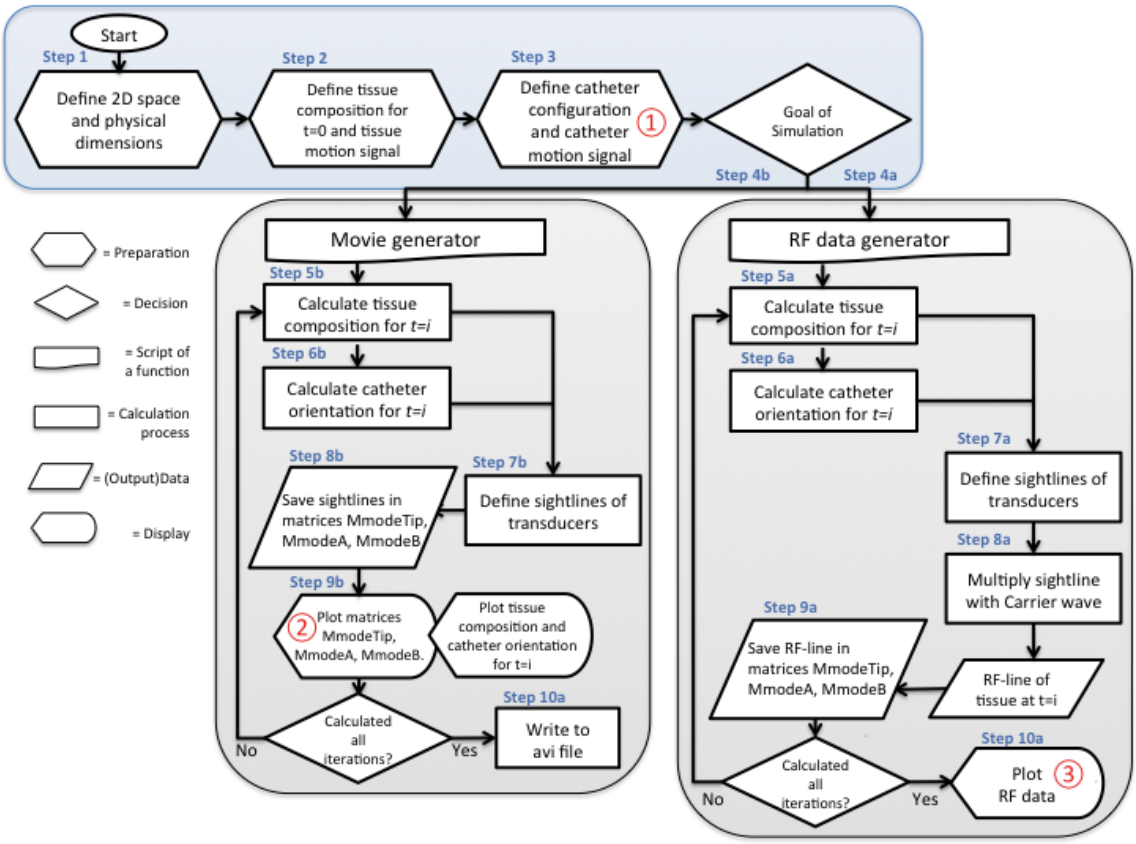

Figure 8: *Simplified workflow of model explained in Section 2.2. Circled numbers corresponds with output images of Figure 11*

means that the data are not displayed per time sample, as is the case for the Movie-generator. The RF-generator displays the RF data in a separate image per transducer.

To run this simulation model, some preparations tasks have to be fulfilled before the simulation can be run for a set time period. The workflow of the simulation model is shown in a schematic overview in Figure 8, and will be explained in more detail. (Appendix M)

Initialisation (Figure 8, step 1)
First, an empty 2D space is generated, which is represented by the graph size of the image in the upper left corner of Figure 6 and 7. The physical dimensions of this 2D space are discretized in a number of pixels, which determines the resolution of the 2D space. Also, the simulation time period and sample frequency are defined that automatically determine the number of time samples, which is the number of iterations that must be completed when running the simulation model.

Define the cardiac tissue and motion input signal (Figure 8, step 2)
Second, the cardiac tissue is modelled, shown in the upper left corner of Figure 6 and 7. To achieve simulated output that can be compared with real images, a routine is created that generates a set number of tissue layers for which different reflection coefficients can be determined that are independent of any physical properties. The reflection coefficients are visualised in shades of grey, of which black determines no reflection and white means maximal reflection, see Figure 6 and 7. Additionally, the cardiac motion input signal is defined, which determines the tissue height of one tissue layer over time, shown in the upper right corner of Figure 6 and 7.

Define the catheter configuration and motion input signal (Figure 8, step 3)
The third step is to define the properties and configuration of the transducers. First, the starting position and orientation of the tip transducer is defined. The orientation and position of the two remaining transducers are defined in relation to the tip transducer. As a consequence, all transducers will move as one object. Next, the movement of the catheter is defined by means of three motion input signals, displayed in the upper right corner of Figure 6 and 7. Furthermore, the watching depth of the transducers is defined, which relates to the number of pixels in which the sightline or RF signal of one time sample is expressed.

Goal of simulation (Figure 8, step 4).
The prepared parameter settings defined at this point are essential for both the Movie-generator and the RF-generator. Depending on the desired output the choice is made which generator will be used to run for all the time samples.

Run simulation as RF-generator (Figure 8, step 4a)
For each iteration an entire process need to be repeated, see Figure 8. First of all, for the current iteration that should be completed, from now on referred to as $t = i$, the tissue is deformed as is determined with the cardiac motion input signal (Figure 8, step 5a).

Next (Figure 8, step 6a), the three catheter motion input signals are expressed in a 4x4 translation-rotation matrix, see Equation 1 that can be used to calculate the orientation and position of the transducers for $t = i$. In this 4x4 matrix the three dimensional coordinate (x, y, z) of the catheter tip is written as $(x, y, z, 1)$, which makes it possible to include translations in this matrix, presented in the fourth column.

$$\begin{bmatrix} x' \\ y' \\ z' \\ 1 \end{bmatrix} = \begin{bmatrix} \cos\theta_z & -\sin\theta_z & 0 & dx \\ \sin\theta_z & \cos\theta_z & 0 & dy \\ 0 & 0 & 1 & dz \\ 0 & 0 & 0 & 1 \end{bmatrix} \begin{bmatrix} x \\ y \\ z \\ 1 \end{bmatrix} \quad (1)$$

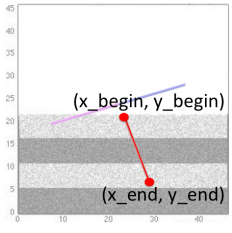

Figure 9: *Coordinates sightline*

Subsequently, the deformed tissue data and the changed position and orientation of the catheter are used to determine the sightlines of all the transducers for $t = i$ (Figure 8, step 7a). To achieve this, two coordinates are determined for every transducer; the spatial begin-position and end-position of the sightline for $t = i$, see Figure 9. The intermediate coordinates between the begin- and end-position are determined based on the set number of pixels that the sightline or RF signal should contain. Next, these series of coordinates are used to find the corresponding reflection coefficients in the deformed tissue data, which results in the sightline per transducer for $t = i$. The sightline at any given time t resembles an A-mode image of a real US image.

To make these data comparable to real RF data the simulated sightline is multiplied with a carrier wave, which resembles the inverse operation of the envelope extraction (Figure 8, step 8a). In order to also include information about motions to this carrier wave a routine is created that generates a carrier wave signal that is modified depending on the cardiac and catheter motion signal at $t = i$. This carrier wave consists of a series of generated Gaussian pulses of which the distance between these pulses varies as a function of the cardiac motion or catheter motion, see Figure 10. The change of this carrier wave signal provides a measurable phase shift between two iterations.

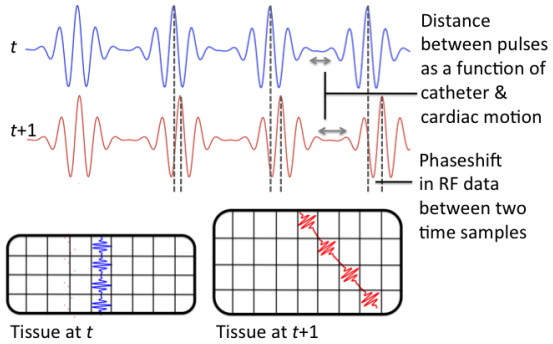

Figure 10: *Schematic representation of modelled carrier wave signal of two time samples. The distance between the pulses of the carrier signal at $t+1$ are increased in relation to t as a result of cardiac and catheter motion, which causes a measurable phase shift*

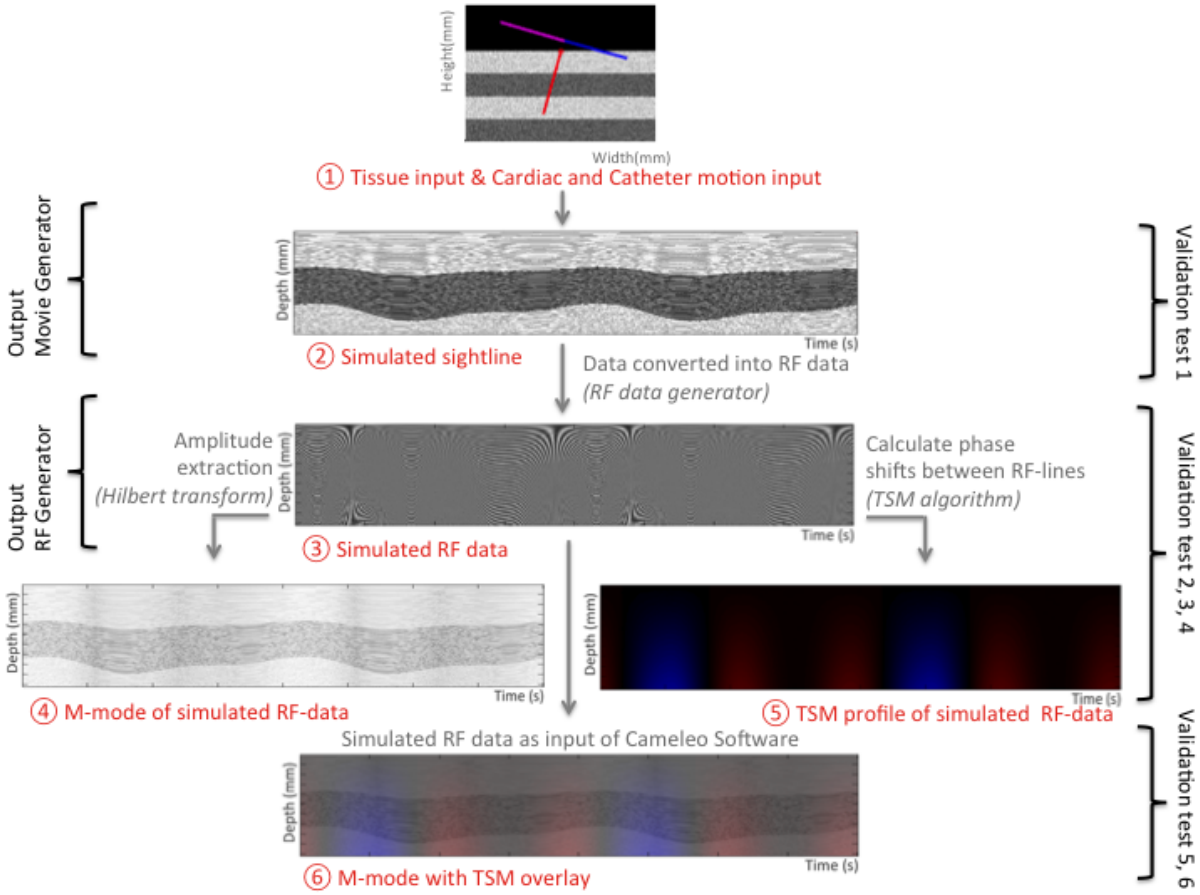

Figure 11: *Schematic overview of the outputs of the simulation model and possible applications of the RF data.*

The simulated RF signal for $t = i$ is then saved in the matrices MmodeTip, MmodeA and MmodeB, representing the output of the different transducers. (Figure 8, step 9a) When this entire process is completed for each time sample, then these matrices are plotted as shown in Figure 7.

Run simulation as Movie-generator (Figure 8, step 4b)
The processes that need to be accomplished to generate the output of the Movie generator are the same as step 5a, 6a, 7a that are performed for the RF-generator, see Figure 8. The main difference is that the determined sightlines of the three transducers are immediately displayed after completion of an iteration (Figure 8, step 9b), directly next to the sightlines of the previous iterations, which resembles an M-mode image as has been shown in Figure 6.

The user of the simulation model can set the values of all the parameters, which makes it possible to simulate a large variety of cases. The motion input signals that are used in the examples shown in Figure 6 and 7 are modelled with a (co)sine function. It is also possible to use a multi-sine or a representative simulated ECG signal (Appendix M.2) as motion input signal. Comprehensive user manuals of the Movie generator and RF data generator are provided in Appendix M.2.5 and Appendix M.2.6.

In Figure 11 an overview is shown of the outputs that can be created with the simulation model and for which applications the RF data can be used.

3. Validation of Simulation Model

3.1. Method of the Validation

To provide confidence in the described simulation model, a validation should be performed [10] and should prove whether the simulation model meets the predefined requirements. Figure 11 shows the relation between the validation tests and the used output data of the simulation model. (see Appendix N for additional validation tests)

3.1.1. Test set-up

For some of the validation tests real US image where generated. A test set-up was build to be able to apply the same motions as used in the simulation model.

A tissue phantom was created with comparable visual properties as the tissue in the simulation model. This phantom consisted of 4 layers with a difference in reflection behaviour caused by using aluminium oxide (Al_2O_3) powder with different particles size. The layers were created by using 80 grams of gelatine, in 800 ml water and 1.6 gram of Al_2O_3 9 μm for the blue coloured layers and 1.6 gram Al_2O_3 3 μm for the red coloured layers, see Figure 12.

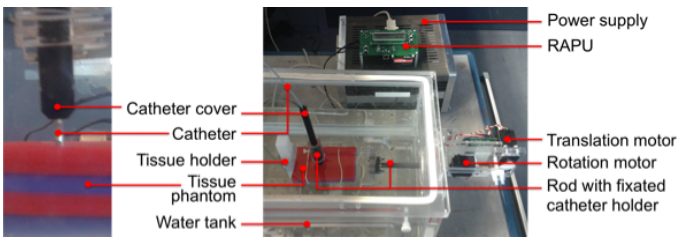

Figure 12: *Test set-up to acquire real US with motorized controlled catheter motion*

The test set up, Figure 12, consisted of two Hitec HS-815BB stepper motors, which have a range of rotation of 180° in 127 steps. These motors were controlled with the Remote Advanced Playback Unit (RAPU) (Brookshire software, version 4.0, Springfield). Identical motion signals as were used in the simulation model were generated with the Visual Show Automation (VSA) (Brookshire software, version 5.0, Springfield) and then uploaded to the RAPU. The motors were connected to a rod, which was able to translate or rotate depending of the motor that was used. The cardiac motion was performed with a palpating movement controlled by hand. The catheter holder, which was fixed to the rod, was designed in such a way that the tip transducer was oriented exactly in the extension of the rod. As a result, the tip transducer was the pivot of the rotational motions, which is also the case in the simulation model. The MUVIC 444-H Cameleo catheter was used, of which only the data acquired with the tip transducer and transducer A were used, since these transducers lie in one 2D-plane. Furthermore, the acquisition was done in a water tank to prevent that the transmitted US pulses were reflected by air before reaching the tissue. (Appendix N.1)

3.1.2. Test 1: Simulated sightline compared to real US data

To test if the model meets Requirement 4, the simulated sightline (Figure 11, simulated sightline) generated with the simulation model was compared with real US data.

The real US data and the simulated sightlines that were compared with each other, were generated according to the parameter settings of cases I to VI given in Table 1. These real US data were compared with simulated data based on the following criteria;

- Y translation, X translation, cardiac and catheter motion; can the same amplitude and frequency be determined from the simulated data and US data and is this information correct compared to the input parameters?
- Is the geometry of the acquired data with the side transducers comparable for the simulated data and US data based on the form of the observed tissue surface area?

3.1.3. Test 2: Envelope of simulated RF data compared to simulated sightline

This test was developed to test if the same motion patterns can be extracted from the simulated RF data as shown by the simulated sightline (Figure 11, simulated RF data, simulated sightline). The Hilbert transformation was used to obtain the envelope signal from the simulated RF data, with an M-mode image as result (Figure 11, M-mode). This M-mode image was compared with the simulated sightline. The validity of the simulated RF data can be supported when no dissimilarities are found between the geometry of those two images. In that case it is demonstrated that the correct motion patterns are stored in the simulated RF data. Test 2 was performed for simulated RF data with parameter settings of cases III to V given in Table 1, of which the thickness of the middle layer was measured for $t = 0.25\ sec$, $t = 0.5\ sec$ and $t = 1\ sec$.

3.1.4. Test 3: Simulated RF data of cardiac motion compared with velocity profile

The velocities that occur in the tissue can be calculated with two different methods: with the derivative of the predefined cardiac motion input signal or with the TSM algorithm.

These velocities were compared to test if the simulated RF data meet Requirement 6, which asserts that the velocity should be estimated by the TSM with an accuracy of 98 %. In this test should be taken into account that the velocity distribution in relation to the catheter tip is not equal in the entire tissue when the heart wall deforms homogeneously. Tissue particles that are located nearby the transducer are less translated in relation to the catheter tip compared to the tissue particles located further away from the catheter tip, see Figure 13. Consequently, the (absolute) velocities that are measured increase as a function of depth. Therefore, it is important that velocities that are calculated based on the input signal and measured with the TSM are compared at the same depth in the tissue. The validity of the RF data is demonstrated if less than 2% difference is measured between the velocity based on the input signal and the velocity based on the TSM. Test 3 was performed for simulated RF data with parameter settings of case III given in Table 1.

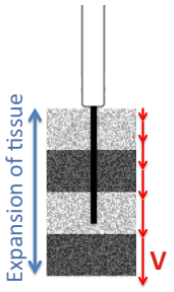

Figure 13: *Absolute velocities of tissue particles in relation to the catheter tip increase as a function of depth*

3.1.5. Test 4: Simulated RF data of catheter motion compared with velocity profile

Both cardiac motion and catheter motion cause phase shifts between the RF data of two time samples. Test 3 was focussed on the validity of the simulated RF data in case of cardiac motion, the following test was done to demonstrate if the simulated RF data were also modelled correctly with respect to catheter motion and if the simulation model meets Requirement 6.

When the catheter is orientated with a constant angle in relation to moving tissue, the observed movement in the tissue would differ in comparison to a catheter that is placed perpendicular to the tissue. The TSM algorithm was used to calculate the velocity of the observed tissue, measured at a constant angle, see Figure 14. In this test the Y-component of this estimated velocity was compared to the velocity at depth Y_{angle} according to derivative of the predefined input signal. The depth Y_{angle} is 11.17 mm when an angle of 0.25π is used. The validity of the simulated RF data is demonstrated if less than 2% difference is measured between the velocity based on the input signal and the velocity based on the TSM. Test 4 was performed for simulated RF data with parameter settings of case VII given in Table 1.

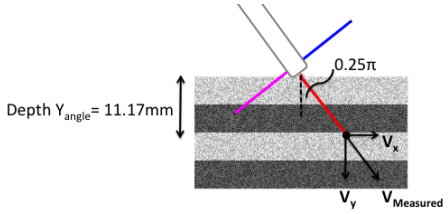

Figure 14: *Schematic overview of validation test 4, in which the Y-component of the estimated velocity by the TSM is compared with the velocity according to the input signal*

3.1.6. Test 5: Compatibility of simulated RF data with Cameleo software

To test if the model meets Requirement 8, the simulated RF data were converted to a .cam file (Appendix M.2.6), which is the input for the Cameleo software. The validity of the simulated RF data is demonstrated if the data can be displayed as an M-mode and if the TSM algorithm works in real-time on the simulated RF data. When RF data are generated or converted incorrectly into an input file of the Cameleo software, then the data would not be displayed correctly. Figure 3 shows a correct presentation of a TSM. Figure 15 shows some examples of incorrectly displayed RF data. In the RF data of Figure 15A an undesired frequency shift occurs, with as result that phase shifts in the RF data can not be measured correctly. Figure 15B shows an example of aliasing. This means that the velocities that are measured in the RF data are too high to measure with the TSM, which is probably a result of incorrectly simulated RF data. Figure 15C shows an example of RF data that is converted incorrectly to 16-bit data. In this example the data are not scaled in a range of 16-bit, which can be indicated as bit-reduction. As a result, the amplitude information, and consequently the shades of grey of an M-mode image are in the same order of magnitude. In this example the TSM is shown correctly, but the M-mode shows limited differences in brightness. Figure 15D shows an image where information stored in the RF signal has been lost due to incorrect demodulation parameters in the Cameleo software.

Table 1: *Settings of performed acquisitions with the simulation model and/or real US that were used for several validation tests. A=amplitude and F=frequency*

Case	Cardiac motion controlled by hand	Catheter motion motorised	Catheter motion controlled by hand	Y motion controlled by hand	X motion controlled by hand
I				A=±2 mm, F=±1 Hz	
II			A=constantly ±0.125π		A=±4 mm, F=±0.5 Hz
III	A=±0.5 mm, F=±1 Hz				
IV		A=±0.125π, F=±1 Hz			
V	A=±0.5 mm, F=±1 Hz	A=±0.125π, F=±1 Hz			
VI	A=±0.5 mm, F=±1 Hz		A=±0.125π, F=±1 Hz		
VII	A=±0.5 mm, F=±1 Hz		A=constantly ±0.25π		
VIII			A=±0.125π, F=±1 Hz		

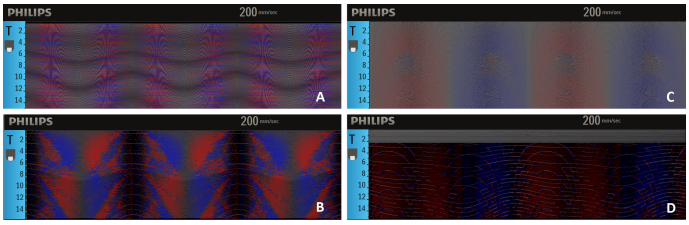

Figure 15: *Examples of incorrect RF data displayed in Cameleo Software. A: Frequency shift in RF data. B: Aliasing occurs as a result of incorrect input data. C: RF data are converted incorrectly to 16-bit data, with as a result that there is no difference visible in reflection coefficient. D: Information stored in the RF signal has been lost due to incorrect used parameters in the Cameleo software.*

3.1.7. Test 6: TSM of simulated RF data compared to TSM of real US data in Cameleo Software

To test if the model meets Requirement 7, the TSM of simulated RF data generated with the simulation model and displayed in the Cameleo software (Figure 11, M-mode with TSM overlay) was compared with the TSM of real US data. The real US data and the simulated data were generated according to the parameter settings of cases III & VIII given in Table 1.

The real US data acquisition applied with catheter motion was done by hand since the TSM tracked the undesired shocking movements of the stepper motor instead of the more rough catheter movements, see Figure 16. A disadvantage of the hand controlled catheter motion was that the frequency and amplitude could be less accurately controlled in comparison with the motor driven catheter movements.

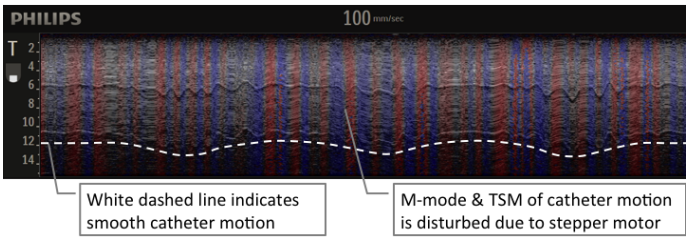

Figure 16: *TSM of catheter motion acquired with stepper motor. The TSM tracks the shocking movements of the motor instead of the rough catheter movements*

3.2. Results of the Validation

3.2.1. Test 1: Simulated sightline compared to real US data

The graphical results of test 1 are presented in Figure 17, 18, 19 and 20, as determined by the settings from respectively case I, II, III,IV of Table 1. In these Figures is specified how the peak-to-peak amplitude and period of one movement can be determined based on the geometry of the simulated data and real US data. The derived frequency and amplitude of the motion signals are presented in Table 2 for the four different cases. These determined values are equal to the input signals shown in Table 1, excluding the amplitude determined in case IV for real US data. Other comparisons between the simulated and real US data are discussed per Figure.

Table 2: *Determined frequency and amplitude from geometry of simulated data and real US data for cases I, II, III and IV, respectively Figure 17, 18, 19 and 20*

Test	Case	Data	Frequency	Amplitude
1	I	Simulated	1 Hz	2 mm
		Real US	1 Hz	2 mm
	II	Simulated	0.5 Hz	4 mm
		Real US	0.5 Hz	-
	III	Simulated	1 Hz	0.5 mm (one layer)
		Real US	1 Hz	0.5 mm (one layer)
	IV	Simulated	1 Hz	0.1257π
		Real US	1 Hz	0.1780π

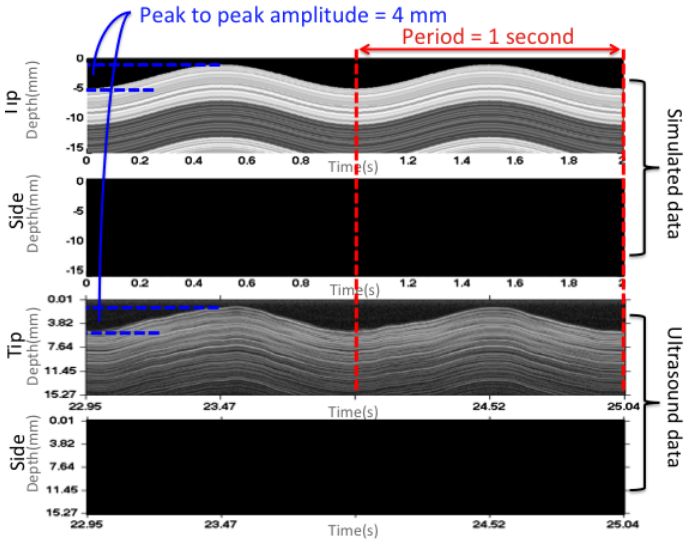

Figure 17: *Catheter motion in Y-direction: Simulated data compared to real US data, both acquired with 1 Hz frequency and 2 mm amplitude, which can be derived from this Figure as presented in Table 2*

Figure 17 shows acquired data with a translating catheter in Y-direction. It can be seen that for both the simulated data and real US data the tissue is only observed with the tip transducer, since the side transducers do not show any data. This is because motion is only applied in the Y-direction. Characteristic for Y-motion are the black areas above the observed tissue which means that there is no reflective signal, which in this case indicates water. Consequently, this means that there is no catheter-tissue contact.

Figure 18 shows translation of the catheter in the X-direction acquired with a constant catheter angle. It can be seen that for both the simulated data and real US data the tissue is observed with the tip transducer and side transducer, since the catheter was placed with a constant angle on the tissue surface while it moved from left to right. The distance from the transducer to the tissue surface, which is water, is visible in the images of the side transducers and is 3 mm for both the simulated and real US data. Furthermore, it can be seen that for both the simulated and real US data the slope of the speckle patterns of the tip transducer and side transducer are in opposite directions, indicated with the black arrows. When the transducer moves in direction to the tissue, the slope of the speckle pattern is increasing, while the slope is decreasing when the transducer moves away from the tissue.

A difference that can be noticed in Figure 18 is that the peak-to-peak amplitude can be determined from the simulated data, but is hard to determine from the real US data. Another remarkable difference is the circled black spot in the M-mode of the tip transducer from the real US data. This spot is caused by the catheter that has been moved too far to the edge of the tissue, with as result that the tip transducer observes through the tissue wall, as shown in Figure 18, this detail is not an indication that the simulated data is incorrect.

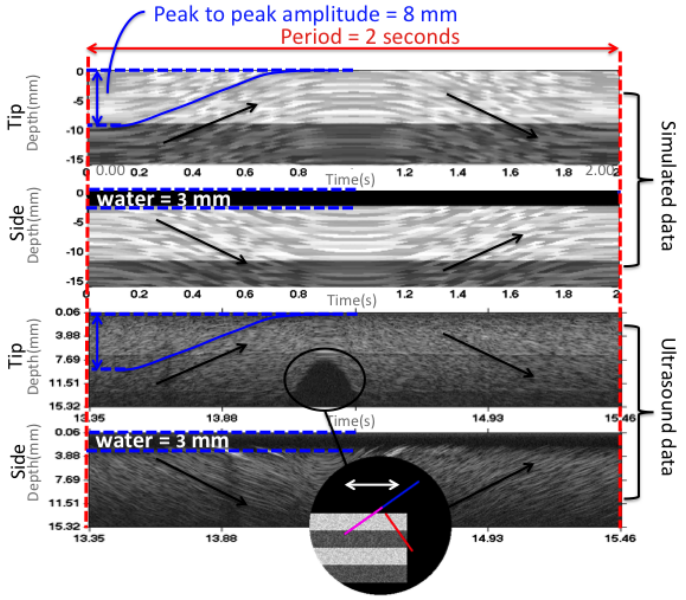

Figure 18: *Catheter motion in X-direction: Simulated data compared to real US data, both acquired with 0.5 Hz frequency and 4 mm amplitude, which can be derived from this Figure as presented in Table 2*

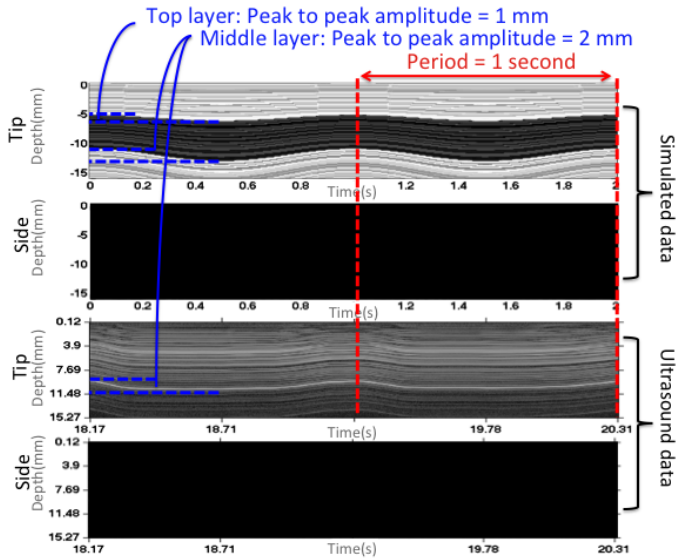

Figure 19: *Cardiac motion: Simulated data compared to real US data, both acquired by palpating with 1 Hz frequency and 0.5 mm amplitude in Y direction, which can be derived from this Figure as presented in Table 2*

Figure 19 shows data acquired with only simulated cardiac motion. It can be seen that for both the simulated data and real US data the tissue is only observed with the tip transducer, since cardiac motion is only applied in Y-direction. This cardiac motion signal is defined per tissue layer. In case of the real US data, the first layer border crossing is hard to determine, therefore the peak-to-peak amplitude of the second border crossing is used, which gives the amplitude of two layers. In Table 2 the amplitude for one tissue layer is presented.

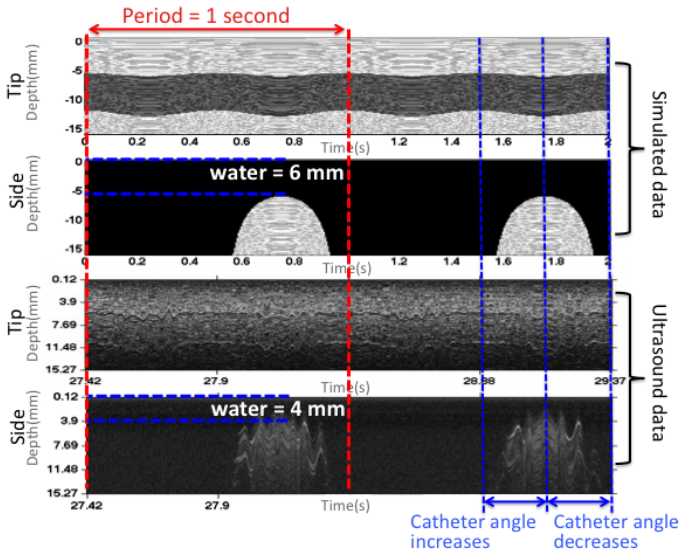

Figure 20: *Catheter rotation: Simulated data compared to real US data, both acquired with 1 Hz frequency and* 0.125π *amplitude of the rotation around Z-axis, which can be derived from this Figure as presented in Table 2*

Figure 20 shows data acquired with only catheter motion. In the images of the tip transducers a visual thickening of the tissue layers takes place at the same time for simulated data and real US data. These motion patterns are a result of a change in catheter angle and consequently, the images of the side transducer show a curve-shaped tissue surface area. When the catheter angle increases or decreases, presented as α_2 in Figure 21, the observed tissue by the side transducer respectively also increases or decreases per A-mode, with a curved shaped surface area in the M-mode image as result.

Figure 21, Equation 2 and 3 present how the maximum catheter angles can be determined from Figure 20, as is presented in Table 2.

$$\alpha_1 = \tan^{-1}(\frac{6\ mm}{2.5\ mm}) = 0.3742\pi \tag{2}$$

$$\alpha_2 = 0.5\pi - 0.3742\pi = 0.1257\pi \tag{3}$$

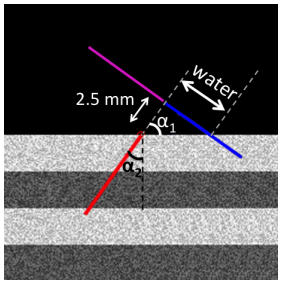

Figure 21: *The amplitude of catheter rotational motion, here indicated as* α_2*, can be determined based on the distance from the side transducer to the tissue surface that can be seen on the M-mode, here indicated as 'water'*

3.2.2. Test 2: Envelope of simulated RF data compared to simulated sightline

Figure 22 shows the M-mode derived from simulated RF data and the simulated sightline (Figure 11, M-mode, simulated sightline) of case V. The thickness of the middle tissue layer of the simulated M-mode corresponds to the thickness measured in the simulated sightline. The thickening of the tissue layers occur at the same time and show that the simulated RF data and simulated sightline do not show any dissimilarity in the observed motion patterns caused by cardiac or catheter motion. However, a clear difference can be seen in the brightness between the two images, which relates to a loss in amplitude of the simulated M-mode image in comparison to the simulated sightline. Moreover, in the simulated M-mode image patterns are visible which suggest that the data still contain a carrier wave after envelope extraction. Table 3 presents the comparison of the simulated M-mode and the simulated sightline for the other tested cases.

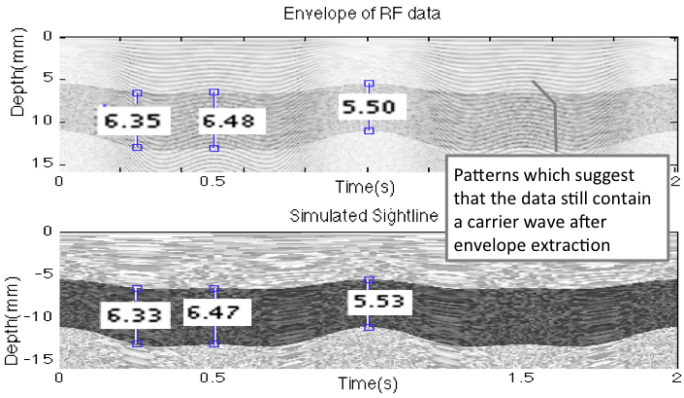

Figure 22: *Top: M-mode image derived from simulated RF data. Bottom: Simulated sightline. Both were acquired by settings of case V from Table 1*

Table 3: *Results of validation test 2. Comparison of the thickness of the middle layer of the M-mode derived from simulated RF data (envelope) and the simulated sightline. Case V is displayed in Figure 22 (and case III and IV in Appendix N.3).*

Test	Case	Data	t = 0.25	t = 0.5	t = 1
2	III	Envelope	5.91 *mm*	6.47 *mm*	5.38*mm*
		Sightline	5.94 *mm*	6.46*mm*	5.36*mm*
	IV	Envelope	6.31*mm*	5.53 *mm*	5.50*mm*
		Sightline	6.33 *mm*	5.51*mm*	5.51*mm*
	V	Envelope	6.35 *mm*	6.48*mm*	5.50*mm*
		Sightline	6.33 *mm*	6.47*mm*	5.53*mm*

3.2.3. Test 3: Simulated RF data of cardiac motion compared with velocity profile

Table 4 shows the results from test 3, where the fourth column presents the maximum velocity that occurs in the tissue at the corresponding depth according to the motion input signal and its derivative, shown in Figure 23. These values are used to calculate the velocity that occurs at the maximal observation depth of the transducer, presented in the fifth column of Table 4. This value should correspond with the maximum absolute velocity that is measured with the TSM of case III, see Figure 24 and presented in the sixth column of Table 4.

According to the input signal, the velocity is 8.27 mm/s at a depth of 15.8 mm. The TSM, estimates a velocity of 8.18 mm/s from the simulated RF data. This means that the velocity can be estimated from the simulated RF data with an accuracy of 98.9%, which meets the validation criteria.

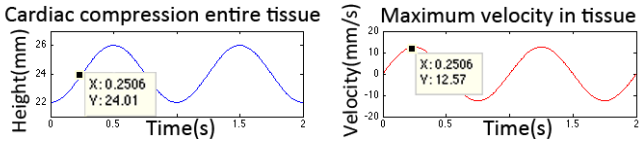

Figure 23: *Left: Input signal of simulation model, that shows the thickness of entire tissue over time. Right: Derivative of input signal, which shows maximum velocity in tissue. Combining information from these graphs shows that a maximum velocity of 12.57 mm/s occurs at a depth of 24.01 mm at t=0.2506 sec*

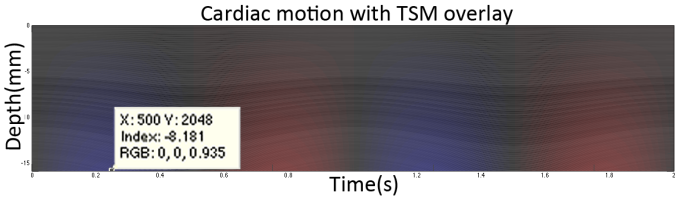

Figure 24: *TSM profile of cardiac motion, case III from Table 1, with the data cursor placed where the velocity is maximum*

3.2.4. Test 4: Simulated RF data of catheter motion compared with velocity profile

Table 4 also shows the results from test 4. An additional seventh column presents the Y-component of the maximum estimated velocity by the TSM of case VII, Figure 25, which is measured at a depth of 11.17 mm, see Figure 14. This estimated velocity should correspond to the velocity that is determined at the same depth based on the input signal, presented in the fifth column.

Table 4: *Comparison of the tissue velocities estimated with the TSM and derived from the input signal to test the reliability of the simulated RF data*

Test	Case	Variable	Determined with input signal		Determined with TSM	
			Maximum velocity that occurs in tissue at corresponding depth (Figure 23)	Velocity in tissue at maximal depth that can be observed by transducer	Aboslute velocity in tissue at maximal depth that can be observed by transducer (Figure 24 and 25)	Y-component of absolute velocity measured with catheter angle of 0.25π
3	III	Velocity	12.57 mm/s	**8.27 mm/s**	**8.181 mm/s**	N/A
		Depth	24.01 mm	15.8 mm	15.8 mm	N/A
4	VII	Velocity	12.57 mm/s	**5.85 mm/s**	8.199 mm/s	**5.80 mm/s**
		Depth	24.01 mm	11.17 mm	11.17 mm	11.17 mm

According to the input signal, the velocity is $5.85\,mm/s$ at a depth of $11.17\,mm$. The TSM estimates a velocity of $5.80\,mm/s$ from the simulated RF data. This means that the velocity can be estimated from the simulated RF data with an accuracy of 99.2%, which meets the validation criteria.

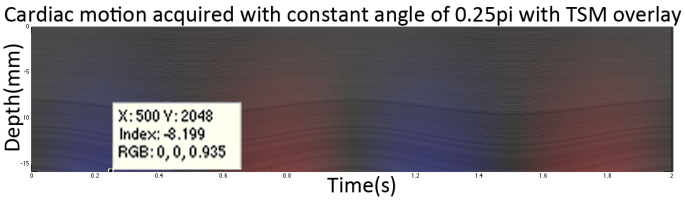

Figure 25: *TSM profile of cardiac motion acquired with a constant catheter angle of* 0.25π*, case VII from Table 1, with the data cursor placed where the velocity is maximum*

3.2.5. Test 5: Compatibility of simulated RF data with Cameleo software

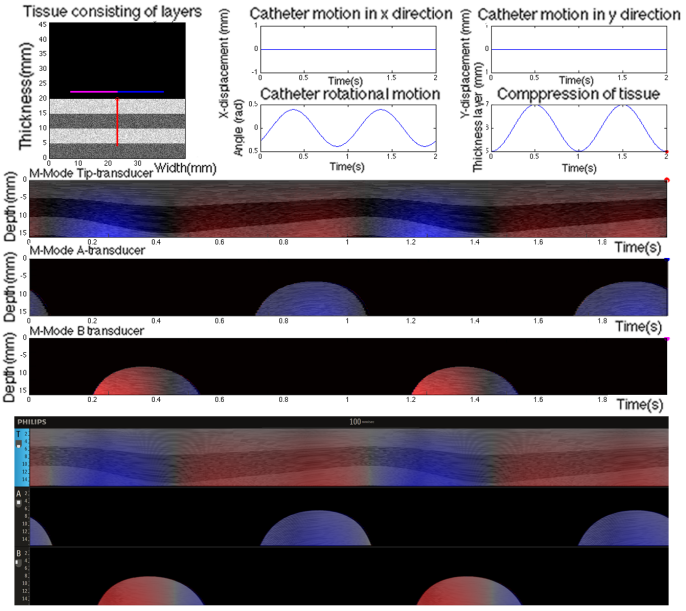

Figure 26: *Top: Output simulation model for cardiac motion and catheter motion with TSM as overlay. Bottom: Simulated RF data displayed in Cameleo software with TSM overlay*

In this test the simulated RF data are used as input for the Cameleo Software. Figure 26 shows how the data are presented by the simulation model and how the simulated RF data are displayed with the Cameleo software. The output in the Cameleo Software does not show any of the artefacts shown in Figure 15 and are similar in relation to the simulation output. Moreover, the TSM algorithm works in real-time. These facts support that the simulated RF data are compatibly with the Cameleo Software.

3.2.6. Test 6: TSM of simulated RF data compared to TSM of real US data in Cameleo Software

The results of validation test 6 are presented in Figure 27 and Figure 28, these figures show the difference between the M-mode and TSM of simulated RF data and real ultrasound data. Figure 27 is acquired with only cardiac motion and Figure 28 is acquired with only catheter motion, respectively case III and VIII from Table 1. As already demonstrated in previous tests, the simulated data and real US data show comparable motion patterns in the M-mode images.

Figure 27 shows that for the simulated data and real US data similar findings can be made. When the tissue becomes thicker, the tissue particles move away from the transducer with as result that the TSM estimates a negative velocity. When the tissue thickness decreases, the tissue particles move towards the transducer, then the TSM will determine a positive velocity. This result corresponds to the input parameters and working principle of the TSM.

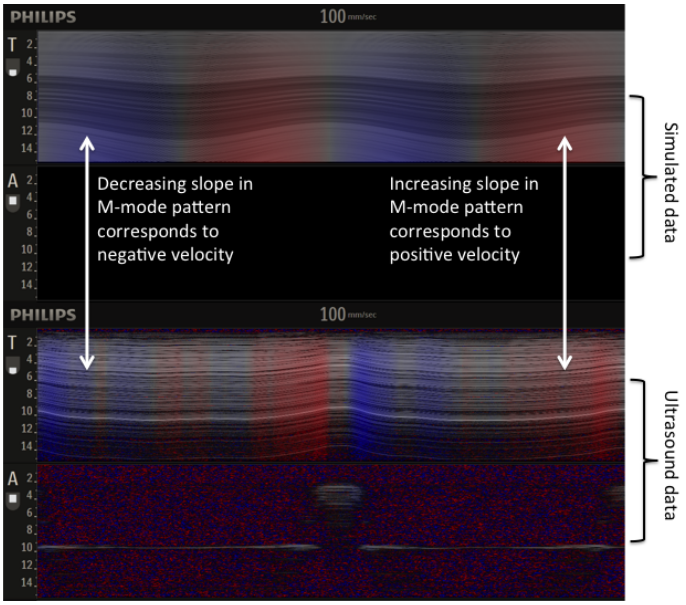

Figure 27: *M-mode images with a TSM overlay of cardiac motion generated with simulated data (top) and real US data (bottom) displayed in Cameleo Software, where T indicates the tip transducer and A indicates the side transducer A*

In Figure 28 the results acquired with only catheter motion are displayed for both simulated data and real US data. For the data observed by the tip transducers can be noticed, like it is the case for cardiac motion, that when it seems that the tissue becomes thicker and the slope of the M-mode pattern increases, a positive velocity is estimated by the TSM and for a decreasing slope a negative velocity is estimated. Another similarity for both simulated data and real US data is that the velocity determined with the side transducer is the opposite direction of what is determined by the TSM of the tip transducer. Furthermore, Figure 28 shows that the velocity direction estimated for the side transducer changes at the top of the curved shaped observed tissue. This is supported with Figure 20 where has been shown that at this point the catheter motion changes in direction. (Appendix N.4 supports the comparison between the simulated data and real US data with images on more detailed level)

Although the results are comparable, differences can be noticed. For example, in the simulation model the motions of the tissue and catheter can be accurately controlled in comparison to the acquisition of real US data, with as result that the motion patterns in the simulated M-mode and TSM images are more consistent in comparison to the real US data. The TSM of the real US data has a lot of interruptions, since the motion is not as smooth applied as

in the simulated data. Also the velocity measured in the curve-shaped TSM of the side transducer of the real US data, especially for an increasing catheter angle, seems to be less than in the simulated data, which indicates that the increasing catheter angle was applied with less velocity than the decreasing catheter angle.

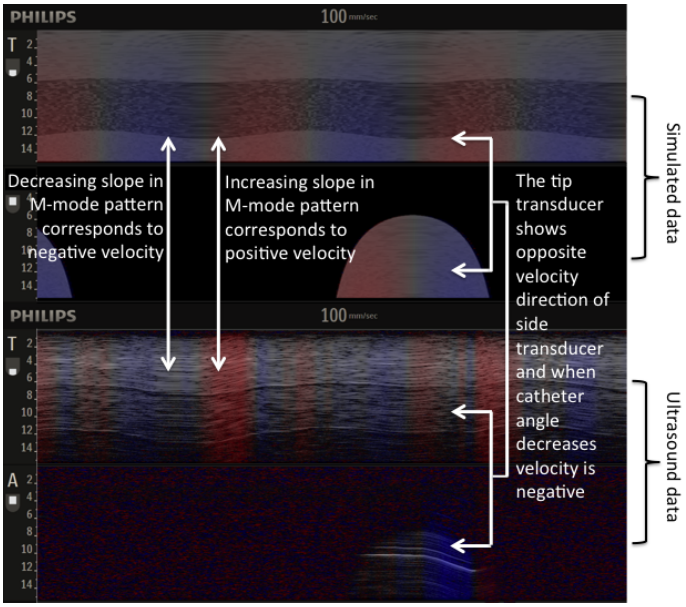

Figure 28: *M-mode images with a TSM overlay of catheter motion generated with simulated data (top) and real US data (bottom) displayed in Cameleo Software, where T indicates the tip transducer and A indicates the side transducer A*

4. Analysis of Output Data from Simulation Model

4.1. Method of Analysis

Observation of output data from the validated simulation model had to indicate how cardiac and catheter motion relates to characteristic patterns in M-mode images and corresponding velocity profile. To obtain these insights, the focus was on the following points:

- How does acquisition with only cardiac motion or only catheter motion relates to M-mode images and TSM of the tip and side transducers?
- How does catheter motion affects data that is acquired with only cardiac motion and vice versa?
- Can be indicated if catheter or cardiac motion is dominant from the M-mode or TSM?

In this study the term 'dominating catheter motion' refers to the situation in which the absolute velocity of a changing catheter angle between two time samples is larger then the absolute velocity of a change in tissue thickness between two time samples. When calculating this absolute velocity of both motions, as schematically shown in Figure 29, it is essential to divide the largest value (of tissue thickness or catheter angle) by the smallest value, to be sure that every situation, including decreasing or increasing motion, can be compared with each other.

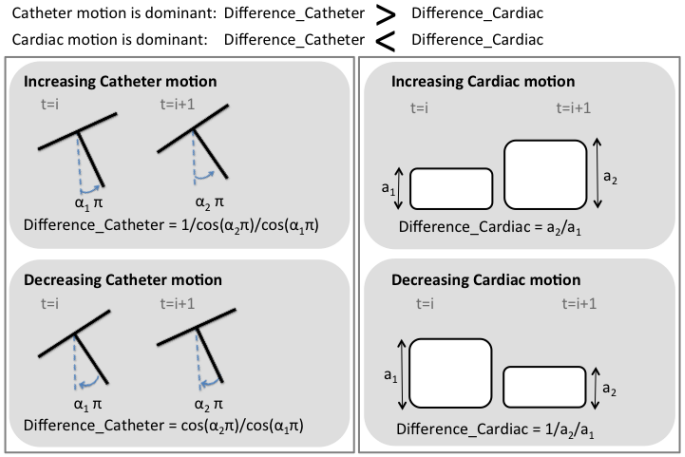

Figure 29: *Overview of calculation method to determine if catheter motion or cardiac motion is dominant*

To perform this analysis, output data were generated by varying the settings of the motion input signals of cardiac and catheter motion. For cardiac motion the total growth of one tissue layer was varied with 1 mm and 2 mm, for catheter motion the angle was varied with the values 0.125π, 0.2π and 0.25π, with as result that in data sets are acquired with both dominating cardiac motion and catheter motion. Moreover, phase shifts of 0.25π and 0.5π were used between the cardiac motion signal and catheter motion signal, to investigate how dominating motion could be determined from the output data. Table 8 in Appendix O.1 shows the complete overview of settings that were used.

4.2. Results of Analysis

Figure 30 and 31 show an overview of the findings that have been made from the acquired simulated data. (Appendix O.2) The overviews will be discussed per Figure.

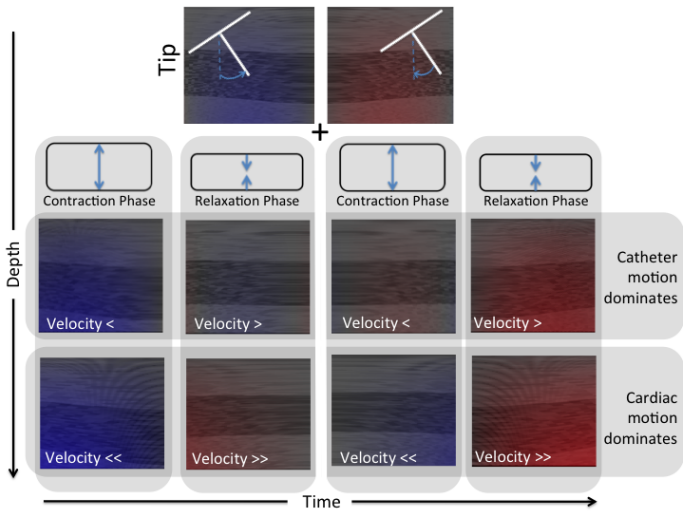

Figure 30: *Overview that shows how the M-mode and TSM of the tip transducer, acquired with only catheter motion, can be influenced by cardiac motion*

The image displayed at the top of Figure 30 shows the M-mode image and TSM of the tip transducer when only catheter motion is applied. This M-mode image is used as a starting point to show which changes occur when also cardiac motion is simulated. If cardiac motion is added to

catheter motion, shown in the lower images of Figure 30, the M-mode and TSM can be influenced in two different ways: If the cardiac motion is in contraction phase (cardiac wall becomes thicker), then the tissue particles move away from the transducer, with a decreasing velocity as result. If the cardiac motion is in relaxation phase (cardiac wall becomes thinner), then the tissue particles move towards the transducer and the velocity will increase. Moreover, if cardiac motion is dominant over catheter motion it would dominate the M-mode patterns and corresponding TSM. This means that the TSM could estimate the opposite velocity direction as the actual applied catheter motion.

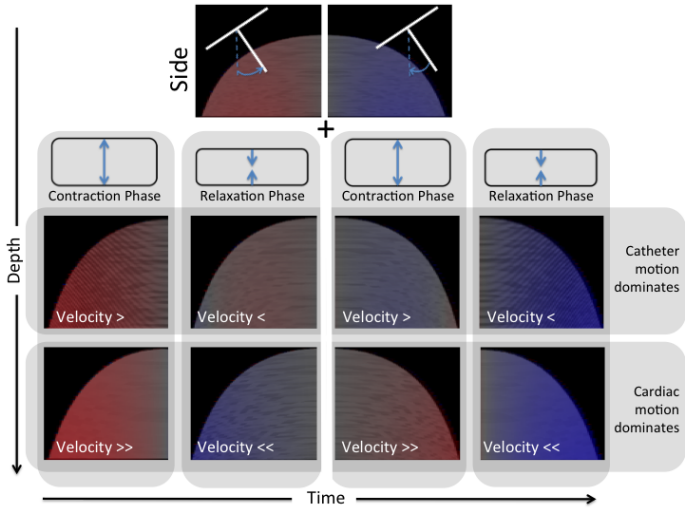

Figure 31: *Overview that shows how the M-mode and TSM of the side transducer, acquired with only catheter motion, can be influenced by cardiac motion*

The image displayed at the top of Figure 31 shows the M-mode image and TSM of a side transducer when only catheter motion is simulated. From the curve shaped surface area can be determined if the catheter motion is increasing or decreasing, as have been explained with Figure 21. When the catheter angle increases, a positive velocity is estimated by the TSM. When the catheter angle decreases, a negative velocity is estimated by the TSM.

This M-mode image and TSM is used as a starting point to show which changes occur when also cardiac motion is applied. If cardiac motion is added to the catheter motion, shown in the lower images of Figure **??**, the surface area of the observed tissue does not change, which means that the surface area is fully dependent on the catheter motion. On the other hand, the speckle pattern of the M-mode and the TSM will be influenced by cardiac motion. If the cardiac motion is in contraction phase, the observed tissue changes and the steepness of the speckle pattern in the M-mode increases, which results in an increasing velocity. If the cardiac motion is in relaxation phase, the speckle pattern in the M-mode decreases, which results in a decreasing velocity.

Also for the simulated M-mode of the side transducer applies that if cardiac motion is dominant over catheter motion it would dominate the M-mode patterns and TSM, which can cause an opposite estimated velocity direction as the actual applied catheter motion. Since the direction of catheter motion could also be determined from the curved shape surface area, based on the available simulated data the conclusion can be made that when an increasing M-mode surface area has a blue TSM this should be caused by dominating cardiac motion. The same also applies for a decreasing M-mode area that has a red TSM.

Furthermore should be noticed that the side transducer estimates the opposite velocity direction in relation to the tip transducer. This knowledge can be used, with all of the previously mentioned, to gain knowledge about which motion is dominating.

Figure 96 in Appendix O.3 supports the observations shown in Figure 30.

4.3. Example Case

All the findings schematically shown in 30 and 31 are applied on an example, see Figure 32, to demonstrate how these observations can be combined and how they can give more insight in the motions patterns in M-mode images and corresponding TSM. First, a possible action plan will be explained, which can be used to apply the find observations in order to evaluate an M-mode and TSM.

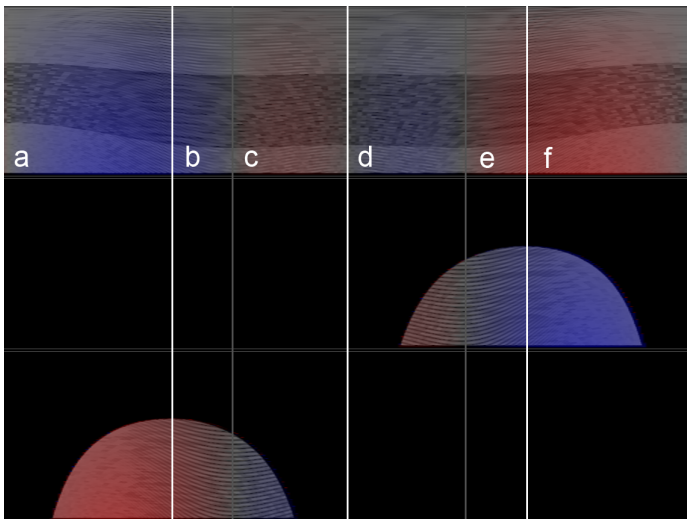

Figure 32: *Simulated output data, acquired with both cardiac motion and catheter motion, divided in six segments in order to evaluate effects of catheter motion and cardiac motion*

1. Determine based on the geometry of the curved shaped surface area displayed by the side transducer what the influence of catheter motion should be on the tissue velocity estimation of the tip transducer. An increasing surface area of the side transducer M-mode means that the estimated velocity with the tip transducer decreases and vice versa.
2. Determine if it can be said for sure that cardiac motion is dominant. This is the case when the estimated TSM of the side transducer is blue while the surface area of the M-mode is increasing ór when the estimated TSM of the side transducer is red while the surface area of the M-mode is decreasing. If so, it is for sure that the velocity direction of the tip transducer is properly estimated in relation to cardiac motion, but the estimated velocity is over or under estimated, depending on the direction of catheter motion, which can be determined based on the geometry of the curved shape surface area shown by the side-transducer.

3. This third step is only relevant if it cannot be said for sure that cardiac motion is dominant (step 2).If so, two considerations are left;
   First, if cardiac motion is in relaxation phase & catheter motion has an increasing effect on the tip transducer velocity (determined by step 1) ór if cardiac motion is in contraction phase & catheter motion has a decreasing effect on the estimated velocity by the tip transducer (determined by step 1), then it is for sure that the TSM of the tip transducer estimated the correct direction of cardiac motion, but the velocity will be over or under estimated depending on the direction of catheter motion.
   Second, if cardiac motion is in contraction phase & catheter motion has an increasing effect on the tip transducer velocity (determined by step 1) ór if cardiac motion is in relaxation phase & catheter motion has a decreasing effect on the estimated velocity by the tip transducer (determined by step 1), then the motions have an opposite result on the M-mode image and corresponding TSM. The velocity estimated by the TSM of the tip transducer would probably be a wrong interpretation of the cardiac velocity direction (then is catheter motion dominant) or is cancelled out by cardiac motion (then nor catheter motion, nor cardiac motion is dominant).

The example of Figure 32 is divided into several segments. The white lines are placed where the direction of catheter motion turns, which is based on the geometry of the M-mode image of the side transducers. The grey lines are placed where the velocity direction changes based on the TSM. All these segments will be evaluated based on the previously mentioned action plan.

a) Step 1) Catheter motion decreases the estimated velocity by the tip transducer.
   Step 2) Side transducer is red, so it cannot be said for sure if cardiac motion is dominant.
   Step 3) If cardiac motion is in contraction phase, the cardiac velocity direction is correct, but underestimated, if cardiac motion is in relaxation phase, the cardiac velocity direction is cancelled out or even incorrect.
b) Step 1) Catheter motion increases the estimated velocity by the tip transducer.
   Step 2) Side transducer is red, so it is for sure that cardiac motion is dominant. Cardiac velocity direction in tip transducer is correct, but overestimated due to catheter motion.
c) Step 1) Catheter motion increases the estimated velocity by the tip transducer.
   Step 2) Side transducer is blue, so it cannot be said for sure if cardiac motion is dominant.
   Step 3) If cardiac motion is in relaxation phase, the cardiac velocity direction is correct, but overestimated, if cardiac motion is in contraction phase, the cardiac velocity direction is cancelled out or even incorrect.
d) Step 1) Catheter motion decreases the estimated velocity by the tip transducer.
   Step 2) Side transducer is red, so it cannot be said for sure if cardiac motion is dominant.
   Step 3) If cardiac motion is in contraction phase, the cardiac velocity direction is correct, but underestimated, if cardiac motion is in relaxation phase, the cardiac velocity direction is cancelled out or even incorrect.
e) Step 1) Catheter motion decreases the estimated velocity by the tip transducer.
   Step 2) Side transducer is blue, so it is for sure that cardiac motion is dominant. Cardiac velocity direction in tip transducer is correct, but underestimated due to catheter motion.
f) Step 1) Catheter motion increases the estimated velocity by the tip transducer.
   Step 2) Side transducer is blue, so it cannot be said for sure if cardiac motion is dominant.
   Step 3) If cardiac motion is in relaxation phase, the cardiac velocity direction is correct, but overestimated, if cardiac motion is in contraction phase, the cardiac velocity direction is cancelled out or even incorrect.

(Appendix O.4 and O.4 show two more example cases)

5. Discussion

The aim of this study was to develop and validate a 2D simulation model of a catheter, including simulated US transducers, that moves during M-mode acquisition and to use this simulation model as a tool to gain insight into the effects of catheter motion on M-mode images and corresponding TSM.

Development of Simulation Model

A 2D model has been developed that is able to simulate moving cardiac tissue that is observed by a catheter including integrated US transducers. All the settings of the simulation model can be set as desired, which makes it possible to simulate a large variety of situations and experiment with different catheter configurations.

The advantage of having this simulation, is that the impact of certain motions can be investigated by changing the settings of motion input signals. Since these signals can be set by the user, the user can directly observe how a change in the input parameters affects the output of the simulation model.

The output of the simulation model, which depends on the interaction between the cardiac tissue and catheter, can be visualised in a movie. In this movie the changes in tissue and catheter orientation are shown, but also the observed tissue by the transducers is displayed over time, which is comparable with a real US M-mode image. Such a movie can be used to train physicians to intrepet M-modes and TSM images for an intraprocedural procedure and to get familiar with the M-mode images acquired with a moving catheter in a moving environment.

The purpose of this simulation was to use the simulation model as a tool to gain insight into the effects of motion, rather than building a fully realistic simulation that includes the impact of all different physical tissue properties. This motivation has led to a simulation model that

is a simplification of the reality, due to multiple assumptions that have been made. For example, propagation of an US wave in a homogeneous medium is normally described with the visco-elastic wave equation [11]. The high degree of complexity of the visco-elastic wave equation would not contribute to the scope of this study. Nevertheless, if in the future the scope of a study also includes the impact of physical properties, this simulation lends itself to be extended with these aspects.

Moreover, almost all the parameters in the simulation model are based on measurable dimensions of the Cameleo catheter or physical properties of real US. The distance between pulses of the simulated carrier signal as function of cardiac and catheter motion is based on the changes in tissue thickness and catheter orientation, as shown in Figure 10. This way of modelling seems to be properly since the motion patterns in the RF data exactly follow the motion patterns of the M-mode image (see Appendix N.4). However, further research should prove whether this way of modelling is correct. This can for example be investigated by comparing the velocities measured from real US data with the velocities measured from the simulated data using an accurate test set-up to perform catheter motion as generated in the simulation model. (Appendix P.1.1)

Another fact that should be reconsidered in further research is that no scattering occurs during acquisition, while it may be possible that also using scattering information may provide insight about present motions.

Validation of Simulation model

The validation tests show for the tested cases that the geometry of the motion patterns in the M-mode of simulated data corresponds to real US data when same input parameters are used. The tissue velocity derived from the simulated RF data has been estimated with an accuracy higher than 98% in this study, which demonstrates the reliability of the simulated RF data. Furthermore, the simulated data works properly as input for the currently used Cameleo software. In conclusion, the performed validation tests suggest that the simulated data meet the predefined requirements and suggest that the simulated data can be used as reliable replacements for real US data.

However, the results of the validation process of this simulation model does not guarantee that this simulation is completely valid. An attempt was made to find a balance between confidences in the model and the time spent on the validation process, as advised by Robinson, 1997 [10]. For example, the designed test set-up shown in Figure 12 turned out not to be ideal and unexpected problems occurred during the validation tests.

One problem that occurred with this test set-up was that the stepper motor introduced undesired disruptions in the TSM, shown in Figure 16. Using a servomotor that operates with a continuous position feedback control may solve this problem. Eventually, given the time limitations of this study, the catheter motion that was applied during the data acquisition of real US data for validation test 6, was controlled by hand. Nevertheless, a test set up that can control motions more accurately will generate data that would be more suitable for comparison with the simulated data.

On the other hand, the simulation model gives also the opportunity to add these stepper motor disturbances to the input signal of the simulation model (as done in Appendix P). In that case disturbances would be added to the motion input signals of the simulation model. However, this could lead to other difficulties, like estimating the exact disturbances of the stepper motor. (Appendix P.2.1)

A result of the shortcomings of the test set-up was that the real US data of case V and VI from Table 1 where cardiac and catheter motion were combined, were not utilizable for comparison with simulated data. These data sets were excluded since it was impossible to perform the combined motions with a constant frequency and amplitude as was intended with the current used test set-up. (Appendix N.2)

In summary, more confidence in this simulation model can be gained when the validation set-up will be further developed in such a way that cardiac and catheter motion can be accurately controlled at the same time. An additional benefit of a more accurate controlled test set-up is that it also creates the opportunity to compare the value of the velocities estimated from the simulated and real US data, instead of only comparing the directions. As a final, repetition of validation tests should be performed in order to also statistically demonstrate the reliability of the simulation model [10].

Analysis of Output Data from Simulation Model

From the analysis of the simulated output data turned out that the estimated cardiac velocity seems to be overestimated when the catheter angle is decreasing and seems to be underestimated when the catheter angle is increasing. When catheter motion is dominant over cardiac motion the estimated velocity by the TSM could even be estimated in the opposite direction as the actual direction of the cardiac motion. It is possible that cardiac and catheter motion are alternating in dominance, since both motions increase and decrease.

In section 4.3 has been showed how these findings can be applied on an example case. For the samples a, c, d, and f there are still uncertainties about the correctness of the estimated velocity, since this depends on whether this cardiac motion is in contraction or relaxation phase. An ECG signal can be used to determine if the cardiac motion is in relaxation or contraction phase. This extra information could be used to establish whether the TSM shows the correct velocity direction, see part a, c, d and f of example in Figure 32.

Currently, the velocities that are displayed by the TSM are assumed to be the velocities that occur in the cardiac tissue. The insights obtained with this study imply that catheter motion certainly influences the M-mode images and corresponding TSM. These insights can be used as a starting point to develop an inverse algorithm that can compensate for the catheter motion. With such a compensation algorithm it may be possible to display the actual cardiac tissue velocities. Such an algorithm could contribute to a better assessment of a lesion formation, since the estimated tissue velocities are used to determine if the tissue is ablated successfully. Besides, this simulation model lends itself as a development and validation tool for such an algorithm, since the motion input signals and output are both known.

A possible solution to compensate for catheter motion is to use the catheter angle that can be calculated as shown in Figure 21. Based on this information it should be possible to calculate the velocities that are caused by catheter motion. When subtracting the value of these velocities from the estimated velocity by the TSM the actual velocities of the cardiac tissue are determined. Further research must show the feasibility of this theory. Nevertheless, this solution will only compensate for the estimated velocities by the TSM. It will be challenging to compensate for the influences of catheter motion on the acquired M-mode images, which is supported by the vision of Gibson, 2011 [12].

Furthermore, the question is whether these findings are also valuable for more complicated motions, as is the case for clinical data. First of all, the motion inputs that are used during this study are simplified motion signals, but since the findings are based on geometric relations, it is expected that the findings should also maintain for more complicated motions.

Another challenge that is already being provided when applying these findings in clinical practise is that in some clinical cases the tip of the catheter is pushed into the tissue, with as a result that you will constantly have side transducer M-mode images. As a result, it is not possible to calculate the catheter angle and no distinction can be made if the catheter angle is increasing or decreasing, which is information that is required to determine, according to the findings adressed in this study, if cardiac motion is dominant. A solution for this may be to add extra side transducers in the catheter that are placed with a larger distance in relation to the catheter tip (Appendix P.3.1). A drawback of a larger distance is that the estimation of the catheter angle may be less accurate, since cardiac tissue is not a straight surface as simulated in this model. In fact, for the most accurate catheter angle estimation this distance should be as small as possible, but to retain the ability to measure the catheter angle from the M-mode of the side-transducer a larger distance is needed. This simulation model can be used to experiment with varying the configuration of the transducers, to investigate which possible solutions are reliable. In conclusion, more research is needed to investigate if the findings of this study remain intact for more complicated motion patterns in clinical practise.

Compared to other studies

As far as known, this is the first study that simulates a moving catheter with integrated US transducers, which observes moving cardiac tissue, and that analyses the effects of catheter motion on M-mode images and corresponding velocity profile. Information that can be found in the literature that is related to this topic is for example the study of Klemm et al, 2007, [13] where the effect of catheter motion, as a result of cardiac and respiratory motion, effects three-dimensional mapping systems during ablation. The results show that the catheter motion has a significant effect on the displacement during three-dimensional mapping of the heart.

Another related study to this topic is from Caspari et al, 2001. [14] They also designed a catheter with integrated ultrasound. They did not mention anything about the effect of catheter motion on their acquired B-mode US images. They only mentioned that rhythmical motion of the catheter may cause uncontrolled movements of the intraventricular septum. According Caspari et al this phenomenon must be considered as a limitation of catheter motion.

Lastly, the study of Chiang et al [15] is related to the interaction between cardiac tissue and an ablation catheter, where they focussed especially on the fact whether the catheter slips during ablation. In this study it is not US that is used, but the catheter motion in relation to the cardiac wall is determined by looking at the deformation of the catheter. Therefore, the catheter is marked with several markers. The deformation of the catheter and the interaction with the cardiac wall is determined based on the transformations of these markers.

The focus of these related studies shows that the presented insights in this article have in all probability not been investigated before and supports the added value of this research. Besides the added value for the development of the Cameleo catheter, the gained knowledge could be used or inspire other scientists to apply or investigate effects of catheter motion in their application.

6. Recommendations

As with the development of new technologies or analysis methods, development uncovers many new challenges. Some of these challenges have already been addressed, however, some potential future expansion possibilities of this simulation model should be mentioned as well.

First, it would be interesting to add the possibility to simulate tissue ablation. As a result, the tissue where the catheter tip is placed will change over time. This can be used to gain even more insights about the effect of catheter motion on the assessment of lesion forming during ablation. (Appendix Q.1) Moreover, this added feature can be used to train physicians to adapt the ablation parameters in real-time while safely performing successful transmural lesions during this intraprocedural method. [6, 9]

Second, the currently used Cameleo catheter consists of four single element transducers, which results in four M-modes. The catheter, as modelled in the simulation model, consists only of 3 transducers and moves in a 2D space. It will be interesting to extend the simulation model to a 3D version that will better mimic the reality and can be used to investigate how the insights from this study maintain in a 3D space. A disadvantage for a 3D model could be the calculation time, since the amount of data will be tripled. (Appendix M.3 and Q).

Furthermore, the cardiac motion is only modelled in one dimension, the thickness of the tissue changes only in Y direction. It would be recommended to model the cardiac motion in more dimensions, which gives a more realistic representation that may support the findings of this study or may lead to new insights about less simplified motions.

Finally, to make the simulation more user friendly, a user interface could be designed. Additionally, it is recommended to make it possible that the user could adapt the input signals in real time and would immediately see the effect of these changes in the M-mode. (Appendix Q.2)

7. Conclusion

A 2D simulation model of a catheter, including simulated US transducers, that moves during M-mode acquisition has been developed and validated. The validation tests insinuate that the simulation model meets the predetermined requirements and suggest that the simulated data can be used as reliable replacements of real US data.

With the simulation model a large variety of cardiac motion and catheter motion interaction can be simulated with predefined settings. The output of the simulation model increases understanding of the correlation between cardiac and catheter motion in M-mode images.

The insights that were gained in this study imply that dominating catheter motion over cardiac motion can lead to wrong interpretation of the velocity direction of cardiac motion. Additionally, from the side transducer M-modes it can be estimated if cardiac motion is dominating over catheter motion or vice versa. The information gained from the side transducers can be used to obtain information about motions patterns in the tip transducer. These insights about the effects of catheter motion on M-mode images provide new directions for further research.

Furthermore, the simulated data are compatible with the currently used Cameleo software for real ultrasound. This enables using the simulated data as input when new versions of the Cameleo Software are tested. Moreover, the interactive simulation model can be used for education of physicians who need to get familiar with M-mode images of a moving catheter in a moving environment.

References

[1] E. J. Benjamin, P. a. Wolf, R. B. D'Agostino, H. Silbershatz, W. B. Kannel, and D. Levy. Impact of Atrial Fibrillation on the Risk of Death : The Framingham Heart Study. *Circulation*, 98(10):946–952, September 1998.

[2] D Conen, S Osswald, and C M Albert. Epidemiology of atrial fibrillation. *Swiss medical weekly*, 139(25-26):346–52, June 2009.

[3] Valentin Fuster, Lars E Rydén, David S Cannom, Harry J Crijns, Anne B Curtis, and et al. ACC/AHA/ESC 2006 Guidelines for the Management of Patients with Atrial Fibrillation: a report of the American College of Cardiology/American Heart Association Task Force on Practice Guidelines and the European Society of Cardiology Committee for Practice . *Circulation*, 114(7):e257–354, August 2006.

[4] Alan S. Go, Elaine M. Hylek, Kathleen a. Phillips, YuChiao Chang, Lori E. Henault, Joe V. Selby, and Daniel E. Singer. Prevalence of Diagnosed Atrial Fibrillation in Adults. *Jama*, 285(18):2370, May 2001.

[5] Donald Lloyd-Jones, Robert J Adams, Todd M Brown, Mercedes Carnethon, Shifan Dai, and et al. Heart disease and stroke statistics–2010 update: a report from the American Heart Association. *Circulation*, 121(7):e46–e215, February 2010.

[6] Matthew Wright, Erik Harks, Szabolcs Deladi, Freek Suijver, Maya Barley, Anneke van Dusschoten, Steven Fokkenrood, Fei Zuo, Frédéric Sacher, Mélèze Hocini, Michel Haïssaguerre, and Pierre Jaïs. Real-time lesion assessment using a novel combined ultrasound and radiofrequency ablation catheter. *Heart rhythm : the official journal of the Heart Rhythm Society*, 8(2):304–12, February 2011.

[7] Mark a Wood. Exposing gaps in linear radiofrequency lesions: form before function. *Circulation. Arrhythmia and electrophysiology*, 4(3):257–9, June 2011.

[8] Christian Cachard Jean Martial Mari. Acquire real-time rf digital ultrasound data from a commercial scanner. *Electrical Journal Technical Acoustics*, 3, 2007.

[9] Hugh Calkins, Josep Brugada, Douglas L Packer, Riccardo Cappato, and et al. Chen. Hrs/ehra/ecas expert consensus statement on catheter and surgical ablation of atrial fibrillation: Recommendations for personnel, policy, procedures and follow-up. *Europace*, 9(6):335–379, June 2007.

[10] Stewart Robinson. Simulation model verification and validation: Increasing the user's confidence. *Proceedings of the 1997 Winter Simulation Conference*, pages 53–59, 1997.

[11] JM Prince, JL Links. *Medical imaging signals and systems*. Pearson Prentice Hall, 2006.

[12] Douglas Gibson. Visualization of lesion transmurality and depth of necrosis using an ablation catheter that incorporates ultrasound imaging: a small step or a major leap forward on the road to a more durable catheter ablation procedure for treatment of atrial fibrillation? *Heart rhythm : the official journal of the Heart Rhythm Society*, 8(2):313–4, February 2011.

[13] Hanno U Klemm, Daniel Steven, Christin Johnsen, Rodolfo Ventura, Thomas Rostock, Boris Lutomsky, Tim Risius, Thomas Meinertz, and Stephan Willems. Catheter motion during atrial ablation due to the beating heart and respiration: impact on accuracy and spatial referencing in three-dimensional mapping. *Heart rhythm : the official journal of the Heart Rhythm Society*, 4(5):587–92, May 2007.

[14] G H Caspari, S Müller, T Bartel, J Koopmann, and R Erbel. Full performance of modern echocardiography within the heart: in-vivo feasibility study with a new intracardiac, phased-array ultrasound-tipped catheter. *European journal of echocardiography : the journal of the Working Group on Echocardiography of the European Society of Cardiology*, 2(2):100–7, June 2001.

[15] Patricia Chiang, Yiyu Cai, Koon Hou Mak, Ei Mon Soe, Chee Kong Chui, and Jianmin Zheng. A geometric approach to the modeling of the catheter–heart interaction for VR simulation of intra-cardiac intervention. *Computers & Graphics*, 35(5):1013–1022, October 2011.

[16] Paul A Iaizzo. *Handbook of Cardiac Anatomy, Physiology, and Devices*. Springer, 2009.

[17] Ruud B van Heeswijk, Gabriele Bonanno, Simone Coppo, Andrew Coristine, Tobias Kober, and Matthias Stuber. Motion compensation strategies MRI.pdf. *Critical reviews in biomedical engineering*, 40(2):99–119, January 2012.

[18] Donald Lloyd-Jones, Robert J Adams, Todd M Brown, Mercedes Carnethon, and et al. Heart disease and stroke statistics–2010 update: a report from the American Heart Association. *Circulation*, 121(7):e46–e215, February 2010.

[19] Grace Frankel, Rejina Kamrul, Lynette Kosar, and Brent Jensen. Rate versus rhythm control in atrial fibrillation. *Canadian family physician Mdecin de famille canadien*, 59:161–8, 2013.

[20] Riccardo Cappato, Hugh Calkins, Shih-Ann Chen, Wyn Davies, Yoshito Iesaka, and et al. Worldwide survey on the methods, efficacy, and safety of catheter ablation for human atrial fibrillation. *Circulation*, 111-9:1100–5, 2005.

[21] Riccardo Cappato, Hugh Calkins, Shih-Ann Chen, Wyn Davies, Yoshito Iesaka, and et al. Updated worldwide survey on the methods, efficacy, and safety of catheter ablation for human atrial fibrillation. *Circulation. Arrhythmia and electrophysiology*, 3(1):32–8, February 2010.

[22] OpenStaxCollege. http://cnx.org/content/m46676, Februari 2014.

A. Acknowledgments

This graduation project was conducted on behalf of Philips Research, Minimally Invasive Healthcare department.

I would like to thank my supervisors from the TU Delft; Gabrielle Tuijthof, Arjo Loeve and Jenny Dankelman. Without Gabrielle I had never made the decisive decision to take this large challenge. She has given me the faith to complete this successfully and gave me the advice to tackle the difficulties during such a project step by step. Although she was not able to be my daily mentor she was really concerned in this project. Arjo Loeve carried out the task as daily supervisor and he did a really helpful job. He gave me every meeting new insights and especially taught me to observe complicated matter from a simple perspective. I will never forget his vision that you especially understand a topic when you can explain it clearly to a little child. I also want to thank him for giving me courage to continue when I was worried again about the progression of my project. Moreover, Jenny Dankelman was, despite of her full agenda, always interested in my project and involved in the relation between Philips and TU Delft. She always knows to ask a critical question, which helps to look with a critical view to your own work.

Further on, I would like to thank my supervisors from Philips Research, Alex Kolen and Fei Zuo, for giving me the opportunity and the confidence to complete this project successfully. Their continuous feedback and their critical view have helped me to get adhesion on the completion of this graduation project. I really appreciate that they were always willing to help me and to discuss about possible solutions. Besides, it was really interesting for me to see how a research department operates within a commercial company. Moreover, they have learned me how every little research contributes to a greater research scope.

Thanks to Jurgen Rusch for giving me, with a lot of patient, the best tips & tricks how to use Matlab in a more efficient way, which have made my simulation model significantly faster. I also would like to thank Erwin Engelsma for converting all my data to cam-files. Moreover, I want to thank Steven Fokkenrood and Ton Rademakers for their contribution to this project. Thanks are also directed to Cees Taal for helping me in the really beginning with the first idea of a simulation model.

I want to thank my friends, Tanne and Steije for their help and required distraction from my graduation project. In special I want to thank the best 'kabouter' who I ever met. Eric, thanks for your enormous mental support, your advices from a different perspective and just for creating wonderful moments. I really had needed you to achieve this result. Finally, many thanks to my lovely parents for giving me the perfect basis, faith, opportunities and for still giving me inspiration every day.

B. Structure of Article and Appendices

Contents

C. Nomenclature

C.1. Terms

A-mode	Amplitude-mode visualizes an envelope signal by presenting the amplitude of this signal in a shade of grey, where white represents maximum reflection and black represents no reflection
Absorption	The intensity of the acoustic wave will decrease caused by conversion of acoustic energy to other forms of energy
Acoustic impedance	Indicates how much sound pressure is generated based on the vibration of a particular tissue and frequency
Atrial fibrillation	Cardiac arrhythmia disease: the atria of a patient contract irregularly or too fast
Attenuation	Loss of intensity of US signal caused by absorption or scattering
Attenuation coefficient	Indicates how strongly the intensity of the US signal decreases as a function of the material where it passes through and of the frequency of the US wave
Cameleo	Name of ablation catheter with integrated US transducers and the acquisition software that is developed and manufactured by Philips Research
Carrier wave	A high frequency signal that is used to transmit information
Envelope signal	A smooth curved line that outlines the extreme amplitudes of a RF signal, but which excludes the high frequency carrier wave
M-mode	The A-mode of each time sample is displayed next to each other, which makes it possible to monitor tissue changes or movements in relation to the transducer of the scanned tissue
Movie-generator	Simulation output that simulates an M-mode image for all the integrated transducers in the catheter for a set time period
Pulmonary Veins	Large blood vessels that connect the atria with the lungs
Radiofrequency Ablation	Transformation of living tissue to dead tissue with a heated catheter, which is generated with a high alternating current
Reflection coefficient	Determines the amplitude of a reflected wave
Refraction	Change in the direction of a wave caused by a change in the observed medium
RF data	Multiple RF signals of multiple time samples
RF signal	The RF signal is the unprocessed electrical signal generated with the piezoelectric element in an US transducer that is brought in movement by a reflected ultrasound wave. This RF signal contains all the information of the propagation of the acoustic waves and the interaction with the observed tissue
RF-generator	Simulation output that simulates RF data for all the integrated transducers in the catheter for a set time period
Scattering	A reflection wave that not propagates back in the direction as where it came from
Sightline	The shades of grey that are observed by the transducer and which are directly displayed
Speckle	The result of interference of different reflections
Transmural lesion	A lesion that is formed through the entire cardiac wall
TSM	Algorithm that is used to calculate a velocity profile of the observed tissue, based on the phase shifts between the RF data of two time samples
Velocity profile	Displays the velocities that occur in the observed tissue, where blue represents tissue particles that move away from the transducer, and red represents tissue particles that move towards the transducer

C.2. Abbreviations

A-line	Amplitude line
A-mode	Amplitude mode
AF	Atrial Fibrillation
AV	Atrio ventricular
B-mode	Brightness mode
HF	Heart Failure
M-mode	Motion mode
PRR	Pulse Repetition Rate
PVs	Pulmonary Veins
SA	Sino atrial
TGC	Time gain control
US	Ultrasound

C.3. Symbols

α_1	Angle that catheter makes in relation to tissue surface
α_2	Catheter angle
θ_x	Rotation around X-axis
θ_y	Rotation around Y-axis
θ_z	Rotation around Z-axis
θ	Rotation around X-axis in 3D rotation matrix
κ	Compressibility of tissue
ϕ	Rotation around Y-axis in 3D rotation matrix
ρ	Density of tissue
φ	Rotation around Z-axis in 3D rotation matrix
c	Speed of sound
cos	Cosine
dx	Translation along X-axis
dy	Translation along Y-axis
dz	Translation along Z-axis
f	Frequency
$f_{carrier}$	Frequency of carrier wave
f_D	Doppler frequency
f_R	Frequency received pulse
f_T	Frequency transmitted pulse
i	Iteration
PRR	Pulse repetition rate
R	Reflection coefficient
sin	Sine
t	Time
$\tan^{-1}$	Inverse tangent
v	Tissue velocity
v_{max}	Maximum tissue velocity that can be measured with TSM
x	Spatial coordinate along the X-axis
y	Spatial coordinate along the Y-axis

z	Spatial coordinate along the Z-axis
x'	Spatial coordinate along the X-axis after a replacement of coordinate x
y'	Spatial coordinate along the Y-axis after a replacement of coordinate y
z'	Spatial coordinate along the Z-axis after a replacement of coordinate z
Z	Acoustic impedance
Z_1	Acoustic impedance of material 1
Z_2	Acoustic impedance of material 2

D. Clinical Context

D.1. Heart anatomy & Cardiac Cycle

The human heart is a hollow muscle that is responsible for pumping 4-6 litters of blood per minute all through the body. The heart exists of two atria and two ventricles. The atrium and ventricle that are located at the right side of the heat are separated by the tricuspid valve, which controls the blood flow between the contracting right atrium and the right ventricle. The mitral valve separates the atrium and ventricle located at the left side of the heart.

Figure 33 represents the pathway of the blood flow. Oxygen-poor blood, coming from the entire body, enters the right atrium via the inferior and superior vena cava. Via the tricuspid valve the blood enters the right ventricle. The pulmonary valve regulates the blood flow from the contracting right ventricle into the pulmonary arteries that moves the blood to the lungs where the blood will pick up oxygen. Pulmonary veins (PVs) will transfer the oxygen-rich blood to the left atrium and controlled by the mitral valve it will move to the left ventricle. The oxygen-rich blood will be delivered to the total body after passing the aorta valve. [16].

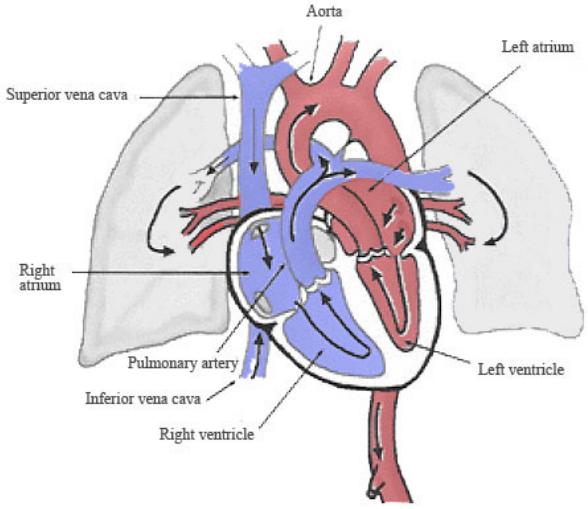

Figure 33: *Pathway of blood flow [16]*

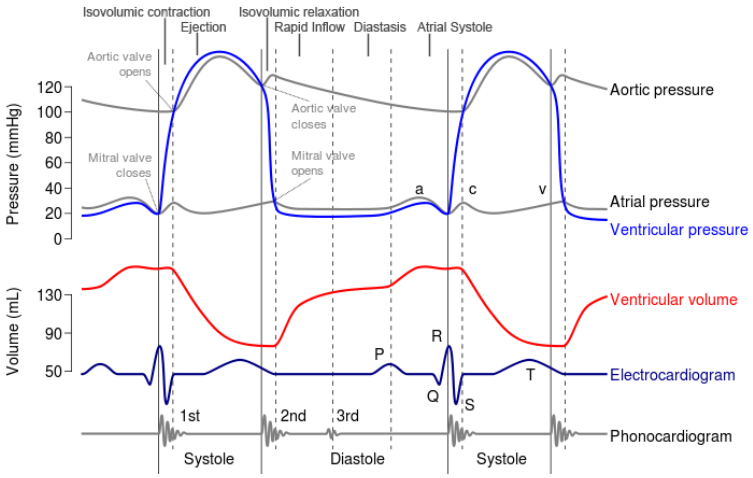

Figure 34: *Cardiac Cycle, subdivided into six stages*

The sequence of these events that regulate the blood flow is called the cardiac cycle, see Figure 34. The cardiac cycle refers to the beginning of a heartbeat till the end of a heartbeat and can be described into two phases. In the diastole phase the heart relaxes and the heart will be filled with blood. In the systole phase the heart contracts and pumps the blood to the rest of the body. These phases can be subdivided into

several stages. During the diastole, the 'Rapid inflow stage' refers to the moment when the pulmonary valve and aorta valve closes and the tricuspid valve and mitral valve open. At that moment the heart is relaxed and blood flows into the right atrium and can flow already to the ventricles. During 'Diastasis' the velocity of the blood flow slows down, which is following by the 'Atrial Systole'. During this stage the atrium gets an electrical trigger from the conduction system, to complete the filling of the ventricles. During the systole, the 'Isovolumic contraction stage' refers to the moment when the ventricles start to contract as a response to a trigger from the conduction system. At this moment all valves are closed. In the 'Ejection' stage the pulmonary and aorta valves are open and the ventricles eject all their blood volume. In the 'Isovolumic relaxtion' the ventricles start to relax and all valves are closed again.

The heart rate is the amount of cardiac cycles that are completed per minute. The heart rate in rest varies between 50 and 100 beats per minutes depending on the condition and activity of a person. Mainly when the heart rate increases, the duration of the systole phase does not change, it is the length of the diastole phase which shortens. [16, 17]

D.2. Heart Conduction System

The heart conduction system takes care for a regular heartbeat and is responsible to generate and propagate an electrical trigger with contraction of the atria and ventricle as results. The main components of the conduction system are the Sino atrial-node (SA-node), Atrioventricular-node (AV-node), bundle of His, bundles of branches and the Purkinje fibers. The SA-node is located at the top of right atrium and serves as a natural pacemaker. The cells situated in the SA-node manifest spontaneous electrical signals and are therefore responsible for a normal heart rhythm. The main components of the conduction systems are responsible for the transmission of the electrical signals throughout the rest of the heart muscle.

When an electrical signal arises in the SA-node, this signal is first propagated to the atria. The electrical signal causes depolarization of these cells; a process is activated that allow calcium to enter these cells, with a muscle contraction as result. The atrial depolarization is transmitted to the AV-node, after a delay the signal is transmitted to the bundle of His, then to the Purkinje fibers with a contraction of the ventricles as result. [16]

D.3. Cardiac dysrhythmia: Atrial Fibrillation

An irregular heartbeat is called an arrhythmia. A heartbeat is called tachycardia if it is too fast and is called bradycardia if it is too slow. Normally, a heart contracts between 50 and 100 beats per minutes and the atria will contract before the ventricles. When a patient suffers from a cardiac dysrhythmia those factors can be disturbed. Atrial fibrillation (AF) is a supraventricular tachyarrhythmia and is characterized by an irregular rhythm of atrial contraction. A result is that mechanical functions deteriorate over time. AF may occur in combination with other arrhythmias. [3] Patients with AF can be classified into different stages.

- A patient gets the diagnosis paroxysmal AF if less than 2 episodes occur within 7 days.
- A patient gets the diagnosis persistent AF if an episode persists for 7 days or even longer.
- A patient gets the diagnoses longstanding persistent if AF is continue or if the duration of paroxysmal AF is longer than one year.
- A patient will have permanent AF if the restoration of sinus rhythm is not possible or would not be performed by any treatment. [3, 9]

D.4. Origin Atrial Fibrillation

In patients who suffer from AF, the electrical signals that cause the heartbeat do not only arise in the SA-node, but also arise in other parts of the atria. Usually these abnormal and undesired action potentials are generated in the PVs. Less common trigger sites for AF are the vein and ligament of Marshall and the posterior left atrium wall. [9] Those undesired action potentials disturb the signals that are generated by the SA-node. The fast and irregular discharges cause an irregular contraction rhythm of the atria, which could lead to 350 atria contractions per minute.

After affecting the atria contraction rhythm, these signals are passed through the rest of the heart muscle. With a delay the signals pass the AV-node. The transmission velocity of the AV-node determines the frequency of ventricle contraction, so the ventricular response to AF is dependent on the electrophysiological

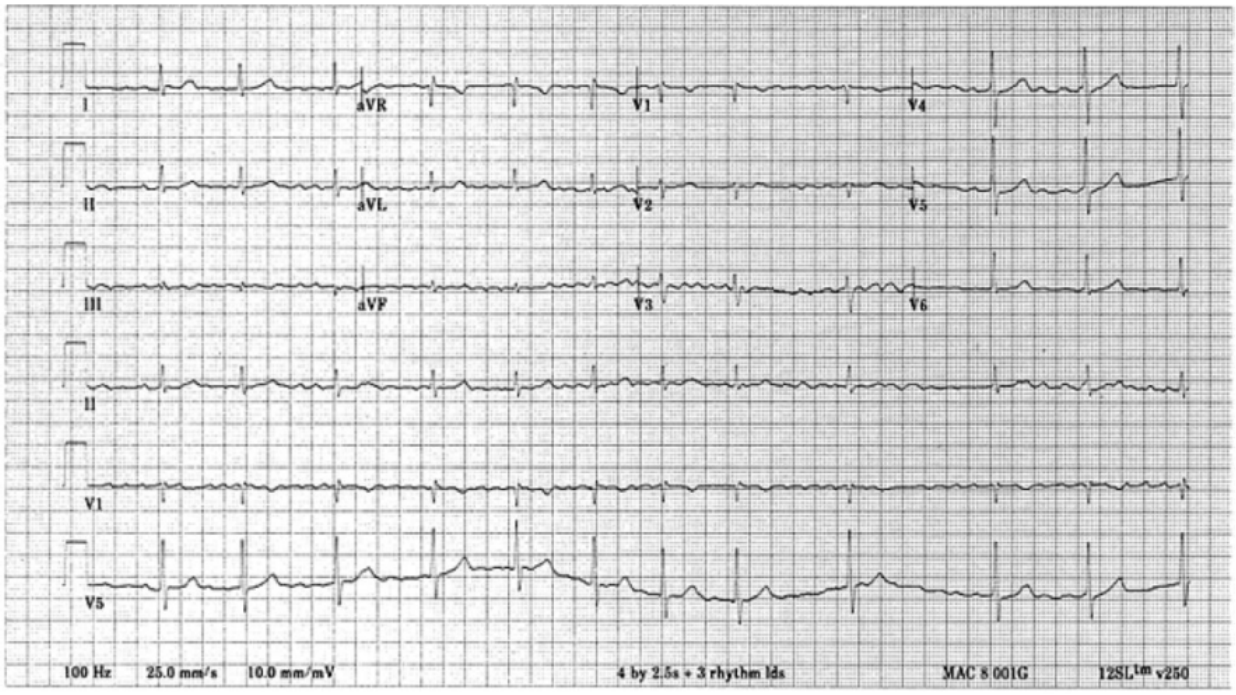

Figure 35: *ECG of patient suffering from AF. P-waves are replaced by rapid oscillations or fibrillatory waves. [3]*

properties of the AV-node. In all probability, the AV-node is not able to pass the electrical signals with the same frequency, but will still cause ventricle contraction with an abnormal rapid and irregular rhythm. The result is that the ventricles and atria contract with a different frequency. Thereby the contraction frequency could still be to high to fully fill the ventricles with blood. In that case less blood is pumped into the body caused by AF. [3, 9]

D.5. Diagnosis Atrial Fibrillation

As discussed in section D.2, the transmission of electrical signals that originating from the SA-node are responsible for a normal heartbeat. A normal heartbeat can be visualised by an electrical cardiogram (ECG), see Figure 34. Arrhythmias in a heartbeat can also be notices on an ECG. When a patient suffers from AF the characteristic P waves in an ECG are replaced by rapid oscillations or fibrillatory waves that very in amplitude, shape and timing, see Figure 35. Also the characteristic ventricle contraction waves occur irregular when the AV-node still functions properly. To diagnose AF in people who having a pacemaker, it is required to temporary inhibit the pacemaker to expose AF activity.

As already mentioned, a patient could have a permanent type of AF or an intermittent type of AF. When it is suspected that a patient has the intermittent type of AF, then a patient can get an ECG for 24 hours. Another option is to wear an event-recorder for 1 or 4 weeks. In that case the patient should press the recording button when irregular heartbeat are sensed.

Furthermore, blood tests are performed to detect abnormalities in blood values and medical imaging techniques like US or X-ray can be used to observe abnormalities in the anatomy of the heart, which may indicate AF. [3, 9, 16]

D.6. Prevalence Atrial Fibrillation

AF is the most common cardiac arrhythmia disease worldwide with an adverse prognosis. [2] Besides, AF is accounting for one third of hospitalizations for cardiac rhythm disturbances. Atrial fibrillation is a disease affecting about 40 million people worldwide. The prevalence is depending of age. In patients aged 60 through 69 the estimated prevalence ranging from 1.2% to 2.8%, in patients older than 80 years it ranging from 7.3% to 13.7%. [3, 4]. The coming fifty years the prevalence will increase significantly considering the

aging population. The estimated growing factor in the coming fifty years lies between 2-fold and 5-fold. [4,18] Even after adjustment for age the prevalence and incidence have substantially increased over time. [2]. In the last 20 years the hospital admissions has been increased with 66% due to a combination of factors including the growth in prevalence and more frequent diagnosis since the upcoming use of ambulatory monitoring devices. AF has become an extremely costly health problem due to hospitalizations (52%), drugs (23%), consultations (9%), investigations (8%), loss of work (6%) and paramedical procedures (2%). This costly health problem will become even more costly as a result of the increasing prevalence. [3]

D.7. Cause Atrial Fibrillation

The most common causes of AF are atrial fibrosis and loss of atrial muscle mass. [3] This remark is in line with the fact that the prevalence of AF in elderly is significant higher. Also lifestyle has a large influence on the cause of AF.

Given the high prevalence of high blood pressure worldwide, high blood pressure has become the most common risk factor for developing AF. Some studies even show that slightly elevated blood pressure already increases the risk of AF. Blood pressure could be linked to an unhealthy and stressed lifestyle.

Obesity is also an important risk factor in the development of AF. People who are obese have a body mass index more than $30kg/m^2$. Obesity could even be the cause of the increasing incidence of AF since also the incidence people who suffer from obesity are increasing. Some studies have found an increased risk factor of 45% of incident AF among obese people compared to people with a normal body mass index. The incidence of AF has also a strong relationship to sleep apnoea patients. However, also this relation can be linked to obesity, since obesity lead to apnoea.

Furthermore, evidence has been found about men who drink excessive amounts of alcohol, which can be defined as 35 alcohol consumptions per week on a regular basis, have an increased risk in the development of AF. Women, who drink more than 14 alcoholic consumptions per week on a regular basis, have 60% increased risk of development of AF compared with non-drinking women. [2, 3]

All these noncardiovascular lifestyle factors have a cardiovascular cause as result, which are actually the direct cause of AF. For example, obesity could lead to a heart failure, alcoholism could lead to coronary artery disease and high blood pressure to hypertension. [19]

D.8. Complications and Prognoses Atrial Fibrillation patients

Patients who suffer from AF have a less coordinated heartbeat as a healthy person. A result is that the blood is not effectively pumped to the rest of the body. If the heart is not able to pump effectively, the body will start to compensate for that. This can lead to a heart failure (HF). HF results in accumulation of fluid in the longs that will cause difficulties in the exchange of oxygen and carbon dioxide from the blood. This is a life-threatening complication.

Another complication that could occur is a stroke. Because of AF blood cloths can be formed in the atria where the blood may stagnate. If these blood cloths enter the bloodstream it is possible that they block certain blood pathways. In less severe cases this could lead to cold feet or hands because of a lack of blood. In more severe cases, when important blood pathways to the brains are blocked, this could lead to a stroke with disability or even death as a consequence. Besides the risks of stroke, HF and death, AF could lead to cognitive dysfunction and a reduced quality of life. [2]

Patients suffering from Atrial fibrillation have a 5-fold increased risk of stroke, increased risk of HF, and all-cause mortality rate is almost double in comparison to people with a normal sine heart rhythm. Moreover, women have an increased risk on these effects in comparison to men. [2, 3]

E. Radiofrequency Ablation

E.1. Radiofrequency catheter ablation

In the past decade radiofrequency (RF) catheter ablation has evolved in a short period of time from an unproven procedure to the golden ablation standard in many major hospitals all over the world. [9]

The goal of RF catheter ablation is to eliminate the abnormal and undesired electrical signals that initiate the abnormal heartbeat in AF. The PVs are the areas where in most patient the undesired electrical signals originate. Nowadays the most common procedure is to ablate circumferential transmural lesions that create total electrical isolation of the PVs, see Figure 36. The conventional approach to reach the goal of ablation is by applying RF energy on the target with a transvenous electrode catheter.

RF catheter ablation is a minimal invasive procedure. A catheter is placed via the groin or the neck into the body. Via the aorta or coronary artery is the catheter placed into the heart. The tip of the catheter is targeted toward the tissue where the undesired electrical signals originate, see Figure 37. A surgeon can activate RF energy in the tip of the catheter, commonly by using a pedal. Applying a high alternating electrical current in the tip of the catheter generates RF energy. When this high frequency energy conducts to high resistant myocardial tissue, the tissue resistivity results in dissipation of RF-energy as heat. When myocardial tissue is exposed for several seconds to a temperature of 50°, irreversible coagulation necrosis will exist, also called lesions. These formed lesions are kind of scars in the tissue and are unable to conduct electrical signals. Good tissue contact and high power delivery improves the efficiency of this procedure. [9] During ablation the surgeon will apply a force on the catheter tip with as goal that the catheter tip has continuous contact with the tissue that needs to be ablated.

E.2. Assessment Lesion forming

The assessment of a lesion formation is currently based on the temperature of the catheter tip, a decreasing amplitude of a local electrogram, duration of ablation, contact force between tip and tissue, electrical impedance, intracardiac echocardiography and delivered power. Only when all the lesions are formed can be demonstrate if all the lesions indeed block electrical signals as was intended. Moreover, this way of assessment is not suitable to assess if the lesion is transmural. Accurate lesion size prediction is limited since the required impedance, temperature and power for a transmural lesion could differ per patient or even per location in a patient. [6]

E.3. Succes rate

More experience, greater knowledge about RF catheter ablation and technical developments have contributed in an increase of the success rate of this treatment.

A success rate of 60% after the first treatment is reported for paroxysmal AF patients a success rate of 30% for persistent AF patients. In 20% till 40% of the cases where AF reoccurred, a re-ablation procedure was performed. For these multiple procedures a success rate of 70% is reported for paroxysmal AF and a success rate of 50% for persistent AF patients. [9]

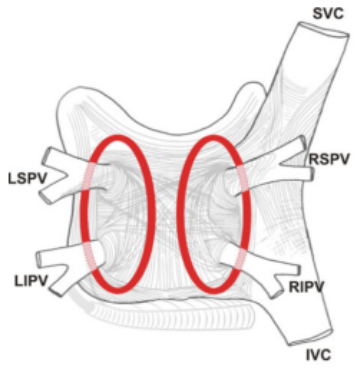

Figure 36: *Circumferential lesions that are created around the left and right PVs, which totally isolate the PVs. [9]*

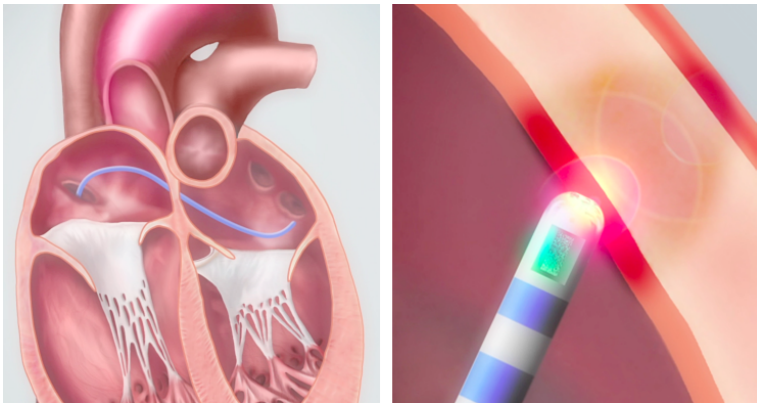

Figure 37: *Left: Insertion of catheter into the heart. Right: Lesion forming by means of radiofrequency catheter ablation*

A study from Cappatto et al. [20, 21] shows a more common percentage about the success rate of RF catheter ablation. In their study they show a success rate of 80% after 1.3 procedures per AF patient. 10% of these patients still need drugs to control the AF. Comparing these numbers with a comparable study they did before shows improvement of catheter ablation over time. In that study they concluded an overall success rate of 75.5% and a percentage of 23.9% of patients who still needed to use drugs to control their AF. [20,21]

E.4. Alternative for radiofrequency ablation

Radiofrequency is the most common and effective treatment for AF. Nevertheless, symptoms or complications of AF can also be controlled in a different way. [3]

Drugs

The types of drugs can be categorized in three categories: medication to control the heart rate, medication to control the heart rhythm and medication to control blood clotting. Still, there is no consensus about which drug is the best to treat AF.

Drugs that control the heart rate slows the heart rate by blocking electrical signals around the atria and counter the transmission of these signals to the ventricles. Beta-blockers are drugs that slow down the heart rate and relax the blood vessels. Calcium channel blockers reduce the heart workload and also relax the blood vessels. Cardiac Glycosides improve the cardiac output, but these drugs can also be toxic, which is one of the disadvantages of these drugs. Even more disadvantages are that it could lead to fatigue, dizziness, shortness of breath or even could introduce other arrhythmia.

Drugs that control the heart rhythm are also called chemical cardio version, this is because the drugs have the aim to restore the normal sinus rhythm of the heart. The drugs can be risky since they associated with serious side effects. Besides, in some cases the patient needs to be monitored when starting with this drugs therapy. [3, 19]

Blood thinners are used to decrease the risk of a stroke in patients with AF. These drugs are called anticoagulants and reduce the possibility to form blood cloths. A disadvantage is that long-term use of anticoagulants may decreases quality of life since it involves multiple drugs interactions and frequent blood testing. Besides, the risk of bleeding increases since a wound would not heal easily.

Especially in patients where the stroke risk is low and where only the sinus rhythm needs to be maintained, drugs are the first choice of treatment. An exception can be made in young patients, when an ablation treatment may be preferred over years of drugs therapy. [3]

Electrical Cardioversion

During an electrical cardioversion a patient gets a shock with a defibrillator with as goal to convert the irregular an abnormal heartbeat back into the regular sinus rhythm. This treatment is performed under anaesthesia. The electrical shock is synchronized with the R wave of the ECG to be sure that the shock does not take place during a sensitive phase of the cardiac cycle. Electrical cardioversion helps the heart to get back in a normal rhythm, but the long-term success rate is low. [3]

F. Philips Cameleo Catheter

F.1. Cameleo Catheter

Philips has designed the Cameleo Catheter, see Figure 38, in order to improve the assessment of a lesion formation. The Cameleo catheter consists of an ablation electrode, an irrigation system to cool down the temperature of the catheter and a 30 MHz single element piezoelectric US transducer. [6] This forward-looking US transducer is fully integrated in the tip of the catheter and transmits US pulses with a frequency of 2 KHz. Between these transmitted pulses a reflected signal is received, which means that A-lines are also generated with a frequency of 2 kHz. The acquired M-mode (A-line observed over time) makes it possible to monitor the lesion formation *in vivo* in real-time. See Figure 39.

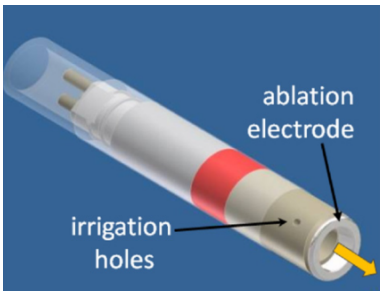

Figure 38: *Cameleo ablation catheter with integrated ultrasound transducers [6]*

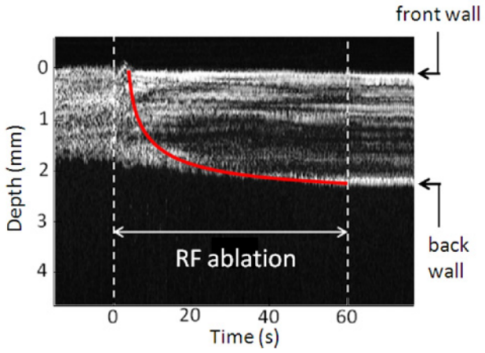

Figure 39: *Real time M-mode image of lesion formation, represented with the red line. [6]*

Meanwhile, the newest prototype is equipped with four 30 MHz single element piezoelectric US transducers. In addition to the transducer located in the tip, three transducers are located at the side of the catheter tip, with a perpendicular orientation in relation to the catheter. The side transducers are orientated with an angle variance of 120°, see Figure 1 and 40. In this study the MUVIC 444-H catheter prototype has been used.

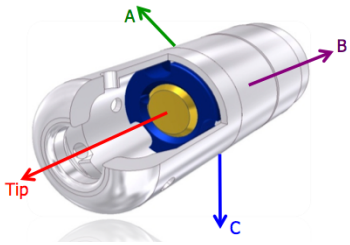

Figure 40: *The MUVIC 444-H Cameleo ablation catheter integrated with four ultrasound transducers*

F.2. Output Cameleo catheter

The US output of the Cameleo Catheter could be visualised as an M-mode image, as a TSM image, or as a Strain Rate image, which will all be explained in more detail. These different visualisations methods give information about different characteristics and properties of the observed tissue, see Figure 41. Furthermore, to obtain information about different properties at the same time it is possible to show the TSM or the Strain Rate as an overlay of the M-mode image.

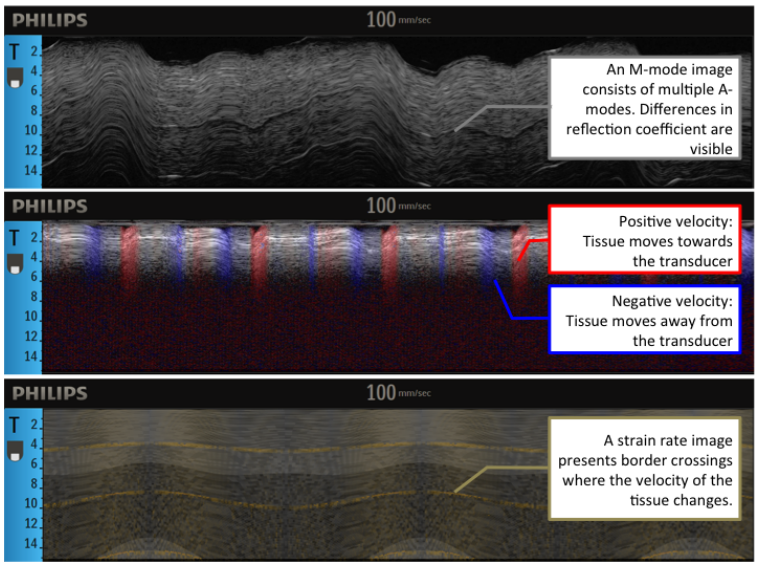

Figure 41: *Example of M-mode image (top), TSM/velocity profile (middle), Strain Rate image (bottom)*

M-mode image
An M-mode image is a brightness mode (B-mode) of one scan line (A-mode) displayed over time, see the upper image in Figure 41. The brightness of the image is in relation to the reflection coefficient of the material. So an M-mode image is obtained by displaying an A-mode continuously over time. Changes in tissue composition or changes in catheter orientation can be seen on the M-mode image.

TSM
The 'Temporal-Spectral-Mean algorithm, developed by Philips research, can be used to calculate the velocities in the tissue and to produce a velocity profile. A TSM shows if the tissue moves towards or away from the transducers, represented with the colours red and blue, see the middle image in Figure 41. The intensity of the colour represents how fast the tissue moves. The velocities are calculated based on the phase shifts that can be measured from the RF data.

The maximum velocity that can be measured can be calculated based on Equation 5. If velocities above this threshold occur in the tissue, then aliasing will occur.

$$v_{max} = \frac{\text{PRR} \cdot c}{4 \cdot f_{carrier}} \tag{4}$$

$$v_{max} = \frac{2\,\text{kHz} \cdot 1540\,m/s}{4 \cdot 30\,\text{MHz}} = 25.6\,mm/s \tag{5}$$

The TSM algorithm is implemented in the Cameleo software. This algorithm works in real time on the acquired US data. During this study a less complicated version of this TSM algorithm has been used in Matlab. With this Matlab version it is not possible to calculate the velocities in real time, but this Matlab script can be used to calculate the velocities of an entire simulation time period. To control the intensity of

the colours in these TSM images, the colormap scale needs to be set according to the maximum measurable velocity, as calculated with Equation 5, which is evaluated in more detail in the manual described in Appendix M.2.6.

Strain rate
A strain rate image shows the boundary of two tissues where the strain of the tissue differs. For example, when a tissue exist of two tissue layers that deform with different velocities, as result of a difference in stiffness, than the boundary between these tissue layers will be visualised on the Strain Rate image, see the lower image in Figure 41. The Strain Rate algorithm is implemented in the Cameleo software.

F.3. Ultrasound physics in Cameleo catheter

Ultrasound is sound with a higher frequency than can be heard by human beings. This means that any sound above 20MHz can be considered as ultrasound. When choosing an operating frequency of an US signal that will be send into a tissue, a trade-off need to be made between the desired resolution of the US image and the penetration depth into the tissue. The higher the frequency of the US wave, the less an US wave can penetrate into the object, so tissue that is located deep in the body cannot be observed. On the other hand, a higher frequency relates to higher image resolution, since higher frequency US waves have smaller wavelengths, which lead to more detailed information. High frequency US is used with the Cameleo catheter, namely 30MHz, because a high resolution of US images is desired to get detailed geographically information and to accurately assess a lesion. The limitation of penetration depth is not a problem, since the transducer is placed exactly on the object of interest.

The transducer in the Cameleo Catheter is both the receiver and the transmitter of the US wave. The main component of a transducer is the piezoelectric element, which is able to convert an electrical signal into an US wave and vice-versa. When the piezoelectric element functions as transmitter, a high alternating current is applied on this element by a pulse generator. A characteristic response of the piezoelectric element is that it will deform with a certain frequency, which generates an US wave. When the piezoelectric element functions as a receiver another useful property of this piezoelectric material is used. When piezoelectric crystals are compressed as a result of a receiving US wave, a voltage is generated, which results in an electrical signal. This signal is processed by the US imaging system, converted with a sampling frequency of 100MHz to a 16-bit digital signal.

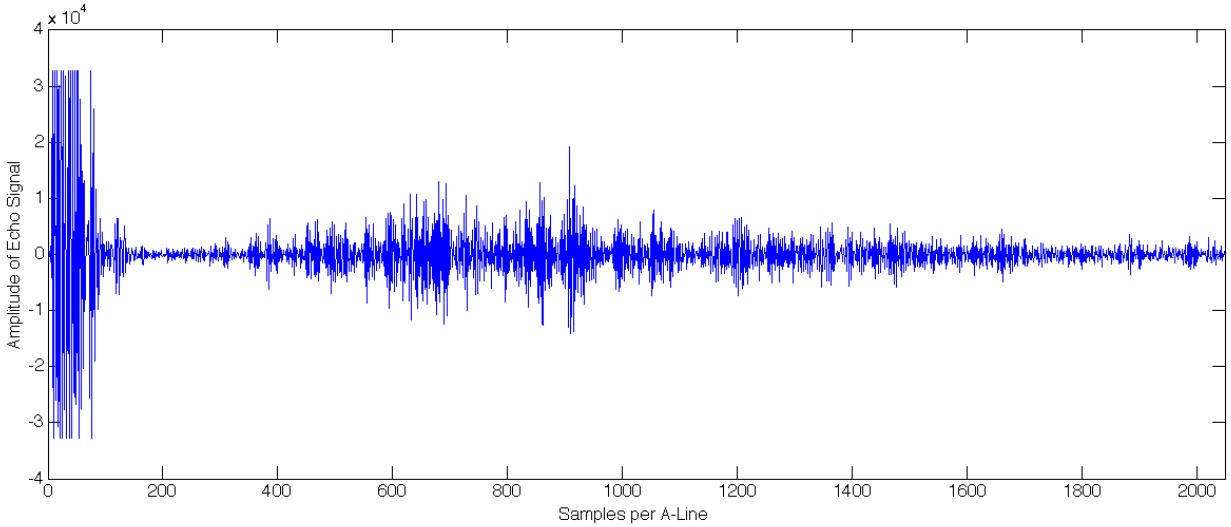

Figure 42: *Received RF-signal. Envelope detection of this signal gives an A-line, which is one time sample of an M-mode image*

Immediately after transmitting an US pulse into the observed tissue, the transducer will be switched to the receiving mode. The speed at which US pulses are transmitted is called the Pulse Repetition Rate (PRR), and is 2kHz in this case. As an US signal is transmitted into the observed tissue, this US pulse is

partially reflected when it meets a boundary of tissues with different acoustic properties. This is called an echo. This echo contains information about the location and the acoustic properties of the reflection point. In an US image the location of a pixel corresponds to the depth of the observed tissue. The brightness of the grayscaled pixel corresponds to the amount of reflection and therefore to the difference in acoustic properties. Since a lot of these reflection boundaries are present in a tissue, the transducer receives a lot of those echoes. In practise, all these echoes will be received as one RF-signal, see Figure 42. This RF signal is not suitable for interpretation, therefore the envelope of this signal is extracted. The envelope of a RF-signal is called an Amplitude line (A-line). This A-line can be displayed in a grayscaled Amplitude mode (A-mode) image, of which the brightness of the grey scale represents the amplitude. All these different amplitudes create a so-called speckle pattern in an US image.

As can be seen in Figure 42, the RF-line consists of 2048 samples. Since the sample frequency is known, 100MHz, it could be calculated what the travel time was of the 2048^{th} sample. With a speed of sound of $1540\,m/s$ can be calculated what the maximum observation depth is. Hereby have to be taken into account that US pulse has to travel the distance back and forth, which means that the echo travel time can be divided by two.

$$1540m/s \cdot \frac{2048 \cdot 100MHz}{2} = 15.8mm \tag{6}$$

The maximum observation depth is thus $15.8\,mm$. This example shows that the amplitudes are plotted as a function of depth and show that the A-line relates to the brightness and physical location of every observed point. Repeating the process of displaying an A-mode is called a Motion Mode (M-mode) as already have been showed in Figure 39. When displaying continuously A-modes over time, differences that occur in tissue can be observed. In this study a sample frequency of 2kHz is used to acquire the M-mode.

G. Problem

The integrated high-frequency single ultrasound transducer and ablation catheter makes it possible to assess tissue-depth and lesion formation real-time. Therefore, the catheter is placed via the aorta or coronary artery into the heart. See Figure 43. During ablation the surgeon will apply a force on the catheter tip with as goal that the catheter tip has continuous contact with the tissue that needs to be ablated. Although this force is applied on the catheter tip, the catheter is still able to wiggle as a result of cardiac motion. This undesired, but also unknown motion, has effect on the M-mode images and corresponding velocity profiles because not the same tissue will be observed over time, see Figure43. Since not the same tissue is observed over time, the interpretation of the acquired M-mode images is difficult, see Figure 44.

In conclusion, the problem statement reads: *'Interpretation of acquired M-mode images and corresponding velocity profiles is difficult since it is unknown how motion patterns in the M-mode images and corresponding velocity profiles relates to cardiac and catheter motion*

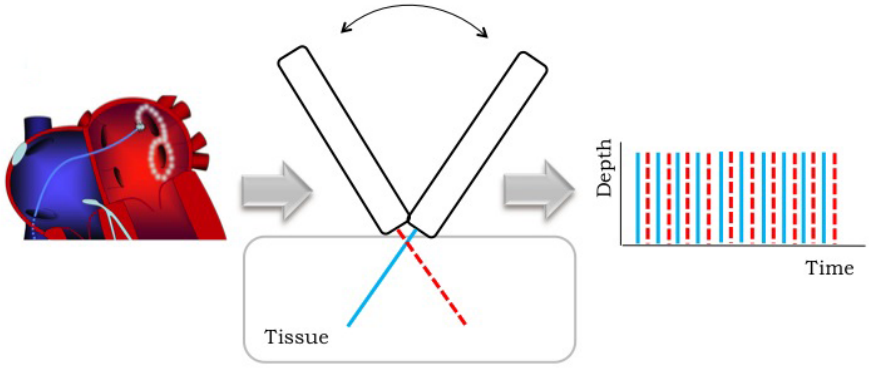

Figure 43: *Problem sketch of M-mode acquisition with a moving integrated ultrasound ablation catheter*

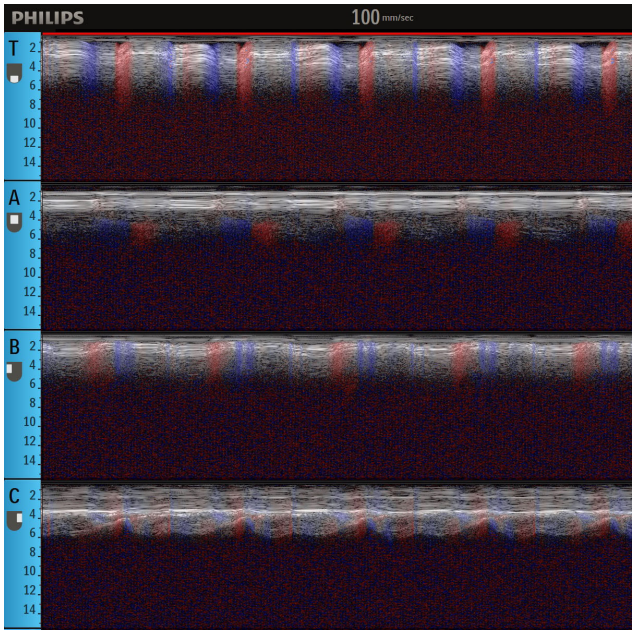

Figure 44: *Example of pre-clinical data, which show that the interpretation of the M-mode images is difficult*

H. Research Goal

The M-mode images can be used to assess lesion formation real time. It is a fact that the M-mode images are effected when the catheter moves during acquisition, but the detailed consequences of catheter motion on M-mode images and corresponding velocity profile are unknown. To make sure that correct observations are taken from the M-mode images during its application, more knowledge is required about which motions patterns are caused by cardiac motion and which patterns by catheter motions. Therefore, it is valuable to gain more insight about how catheter and cardiac motion relates to characteristic patterns in the M-mode images and corresponding velocity profiles. These motion patterns in the M-mode image are also in direct relation to the other visualization methods, shown in Figure 41. Information from these images can also be used to gain more insight about the effect of catheter motion.

From the above, the main goal of this study can be formulated as: *' Gain insight in the relation between catheter motion and characteristic patterns in M-mode images and corresponding velocity profiles*

To reach this goal the focus of this study is twofold. Firstly, develop and validate a novel 2D simulation model of a catheter, including simulated US transducers, that moves during M-mode acquisition of contracting cardiac tissue. This simulation must be a representative model of real US data that is generated with a moving catheter. Therefore, predefined requirements of the model are essential. Secondly, this simulation model can be used to generate a large variety of different output data with different settings for cardiac and catheter motion. Analysis of these datasets should gain insights about how cardiac and catheter motion relates to characteristic M-mode patterns and changes in corresponding velocity profiles.

I. General Design Approach

From the beginning of this study the general approach, shown in Figure 45, was used to achieve the research goal. The thinking behind this approach is to start with a simplified 2D model with only catheter motion. This simplified model helps to keep observations organised instead of making it too complicated in the beginning. If a model is too complicated from the beginning, there is a risk to lose the overview both in the development process as in observing the output data. So, once a version is working properly, the simulation could be extended.

The ideal model is a model that mimics the acquisition of real US data the most representative. That means that a lesion will be formed over time using a catheter with four ultrasound transducers in a 3D space. As already mentioned, the overview will be lost if the development of a simulation model was immediately started with these challenging requirements. Therefore, a distinction have been made in four extensions of the model; 2D simulation model with only catheter motion, a 2D simulation model with catheter and cardiac motion, a 3D simulation model with catheter and cardiac motion and finally a 3D simulation model with catheter motion, cardiac motion and lesion forming over time. All these extensions can be subdivided in the ability of producing the simulated sightline over time or producing RF-data (Figure 11), respectively Movie generator and RF-data generator.

In the time schedule of this study it was not possible to develop all of these extensions. Nevertheless this general approach was created and reported to always keep in mind the extension possibilities of the simulation model during the design process.

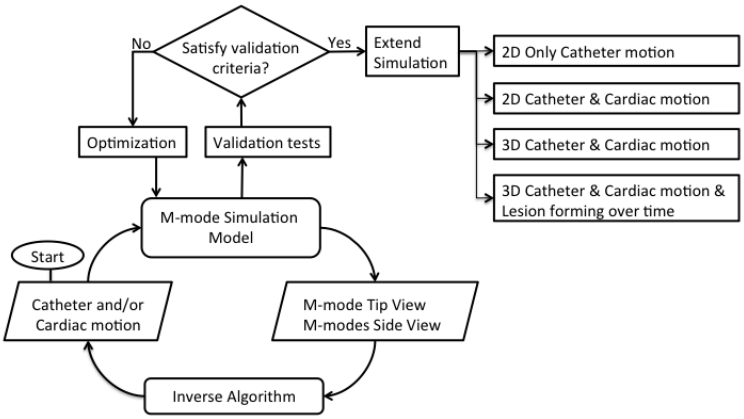

Figure 45: *General approach to achieve research goal*

The first step in the general approach is defining the motion input signals of the simulation model. It should be considered in which dimensions the cardiac and catheter motions are modelled and assumptions should be made about which motions could be excluded from the simulation model.

Next, if the input of the model is determined the simulation model need to be designed (or extended) based on these input parameters, which creates a single M-mode per transducer as result.

Analysis of these M-modes can generate more insights about how cardiac motion and catheter motion relates to characteristic M-mode patterns. Optionally, there could be even determined if it would be possible to write an inverse algorithm based on these M-modes. In that case the M-modes would be the input of this algorithm and the input signals would be the output, which immediately validate the inverse algorithm since these motion signals are self-determined. If desired in the future, such an inverse algorithm could be used for any motion compensation.

Furthermore, the simulation model needs to be validated based on set validation criteria and requirements. When these validation criteria are not satisfied, then the simulation model needs to be optimized. When the validation criteria are satisfied, then the simulation model can be further extended.

J. Requirements

In this Appendix all the requirements are explained in more detail.

1. *Motion of the modelled cardiac tissue, which represents a beating heart, should at least contain motion in the axial direction, which is defined as perpendicular direction in relation to the tissue surface, in other words, the Y direction of the 2D space, see Figure 4 and 5*
   To simplify the model the choice has been made to only model the cardiac motion in the orientation direction of the tip transducer when the catheter is placed perpendicular to the tissue surface, in other words, Y direction of the 2D space. The main deformation of a cardiac wall is that the wall becomes thicker and thinner. The observations that are done with the tip transducer will be most influenced by motions that occur along the axis of the observation direction. Also the velocities measurements are measured along this axis. Furthermore, to programming the cardiac motion in multiple directions would be a hard job, therefore it is useful to first investigate what the effect of motion in one direction is on the M-mode images. In the future, an option is to extend the simulation model by modelling the cardiac motion in multiple dimensions.
   The cardiac motion can be distinguished in the time period that the tissue becomes thicker and the time period when the tissue becomes thinner. In Figure 46 it can be seen that the wall becomes thicker when the heart contracts and that the heart wall becomes thinner when the heart is in relaxation phase. It is important, since these terms are used in this article that these terms are not confused with each other.

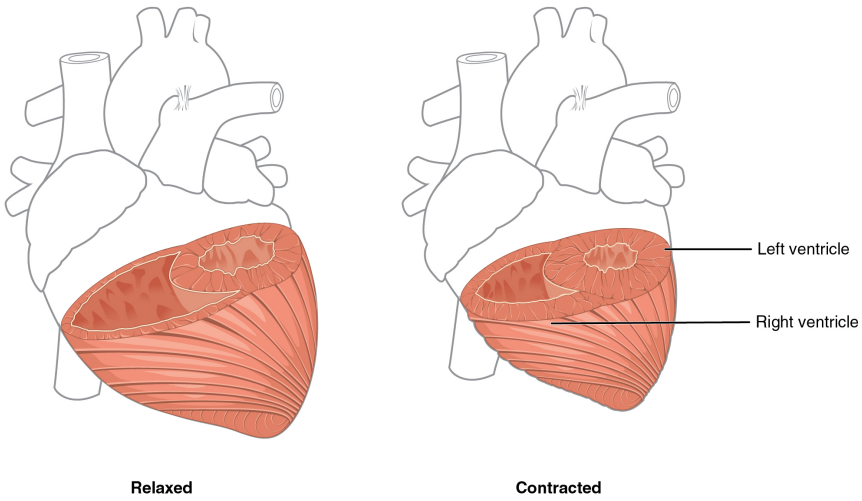

Figure 46: *When the heart contracts, the cardiac wall becomes thicker. When the heart relaxes, the cardiac wall becomes thinner [22]*

2. *At least three catheter motions should be modelled, representing translation in axial and lateral direction, X and Y direction of the 2D space respectively, see Figure 4, and rotation along the Z-axis, see Figure 5*
   In 2D space the catheter can move from left to right, which indicates X-motion, the catheter can move up and down, which indicates Y motion. Furthermore, the catheter can wiggle, which is a rotational motion around the Z-axis with the catheter tip as pivot point.

3. *Every transducer integrated in the catheter tip should provide a single M-mode image*
   Per transducer an A-line should be generated for every time sample. These A-lines should be displayed over time, which resembles an M-mode per transducer.

4. *If identical catheter and cardiac motion is used to generate data, then the simulation model output should generate the same patterns compared to real M-mode images, which can be quantified by comparing the frequency, amplitude and slope that can be derived from the geometry of the M-mode patterns*

This requirement needs to be fulfilled to be sure that the simulated data is a representative alternative for real US data.

5. *The simulation model should display directly the observed moving tissue as result of a changing catheter orientation that can be compared with a real M-mode image or should generate a received RF signal that contains information about the reflections and motions in the observed tissue, see Figure 4*
   The simulation model will be used for several purposes. When the simulation model shows the observed tissue directly, then the model can be used to get new physicians more familiar with an integrated US ablation catheter that displays several M-modes of moving tissue. Also more knowledge can be gained about motion patterns in the M-mode as a result of catheter and cardiac motion. When the simulation model generated RF data from the observed tissue as output, then the data can be used to use for other calculations, like a velocity profile of the observed tissue. It would also be possible to use the RF data as input for the Cameleo system, which is also used to display real US data.

6. *The velocities that occur in the tissue as result of cardiac or catheter motion should be able to be measured from the simulated RF data with an accuracy of 98% using the TSM algorithm*
   In practise, if a tissue particle moves over time, the echo of this particle will also shift on the A-line (Figure 42) because the echo of this particle changes as a function of depth. In Figure 47 are two echoes shown of one single tissue particle at $t = i$ and $t = i + 1$. As can be seen, the frequency stays equal, but the echo has translated in relation to the time, which in turn is in relation to the depth of the tissue. This translation can be measured by looking to the phaseshift of a certain point of these echoes. This phenomenon should also occur in the simulated data when motion takes place.

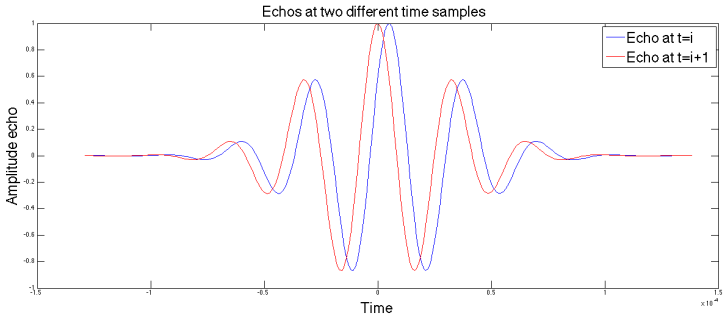

Figure 47: *Echo from a tissue particle that has been moved between iterations at $t = i$ and $t = i + 1$*

As already mentioned, the 'Temporal-Spectral-Mean algorithm, developed by Philips research, can be used to calculate the velocities in the tissue and to produce a velocity profile. These velocities are calculated based on the phase shifts in the RF-data and can be estimated with an accuracy of 2%. The velocities can also be calculated based on the predefined input signals. If the RF data is correctly generated, than these velocities correspond.

7. *If identical catheter and cardiac motion are used to generate data, the TSM of the simulated RF data should be similar to the TSM of real RF data, which can be quantified by comparing if identical velocity directions are determined*
   The TSM algorithm is able to obtain a velocity profile of RF data. The velocity direction is indicated with the colours red and blue. Red means that the tissue moves towards the transducer, and blue means that the tissue moves away from the transducer. The TSM of the simulated data and US data should determine the same velocity directions when applying identical motion during acquisition.

8. *The simulated RF data should be generated in 16-bit integers, which is required to be able to use the simulated data as input for the visualisation Cameleo software (Philips, Version 904, Eindhoven The Netherlands) that is used to process and display the real US data acquired with the Cameleo catheter, shown in Figure 1*
   This is a requirement that is defined by the operator of the Cameleo software.

9. *The values of all parameters in the simulation model should be adjustable*
   To be able to gain insights about different motion patterns all the motion should be able to set as desired. It would also be interesting to test new transducer compositions with the simulation model, so also these parameters should be adjustable. Furthermore, variations in time settings and sample frequencies makes it possible to use the simulation model for different purposes and to improve the calculation time by decreasing these factors if possible.

K. Specifications

In this Appendix the specifications for the 2D simulation model are explained in more detail.

10. *The tip of the catheter should contain one single element transducer*
11. *Two single element transducers should be placed at the side of the catheter tip, orientated with a fixed angle of* 90° *in relation to the orientation of the tip transducer*
    As already have been shown in figure 1 and 40, the MUVIC 444-H catheter consists of 4 transducers. One single element transducer is placed in the tip of the catheter and three single element transducers are placed on the side of the catheter. These side transducers have an angle of 90° in relation to the tip transducer and have an orientation difference of 120° in relation to each other. This simulation model is a 2D model. For that reason, the specifications are deviated from the MUVIC 444-H catheter, but are definitely related to these dimensions. In the future, if a 3D model will be developed, these specifications can be adapted as above-mentioned.

12. *Distance between the side transducers and tip transducer should be* 2.5 *mm*
    According to the MUVIC 444-H catheter, these dimensions are set.

13. *The carrier wave of the received RF signal should be modelled with a frequency of 30 MHz and a sample frequency of 100 MHz*
    In the current used real US system pulses are generated with a 30MHz signal and a received signal is sampled with a frequency of 100MHz.

14. *The observation depth of the transducers should be* 15.8 *mm, which relates to a RF signal consisting of 2048 samples*
    As already mentioned in section F, the acquired real US data exist of 2048 pixels per A-line, which is in relation to 15.8 *mm*.

15. *The frequency for both catheter and cardiac motion should be comparable to an average heart rate of 60 beats per second, which relates to a frequency of 1 Hz of the motion signals*
    When a frequency of 1Hz is used, the cardiac tissue contracts once in a second, which relates to 60 beats per second.

16. *The tissue should consist of at least a two layer structure with different reflection coefficients*
    At least a two layer structure is useful to follow motion patterns in the M-mode image. When only one tissue layer is used, then only changes in the tissue can be based on a speckle pattern, which is less easily to observe.

17. *To be able to measure velocities in the tissue with an accuracy of 98% based on phase shifts in the RF signals with the TSM algorithm, a sample frequency of 2 KHz of the generated RF data is required*
    In 1 *sec* 2000 A-modes are created, which relates to a sample frequency of 2KHz of the M-mode image.

L. Assumptions

In this Appendix all the assumptions that are taken for the development of the 2D simulation model are elaborated in more detail.

- *The density and compressibility of the tissue are not determined, but assumed to be equal in the entire tissue*
- *The speed of sound is assumed to be equal in the entire tissue, since the speed of sound is a function of density and compressibility*
  An US wave propagates through matter via compression and expansion of a material. The density, ρ, and compressibility, κ of a material determine the propagation speed at which the acoustic wave travels through the material [11].

$$c = \sqrt{\frac{1}{\kappa\rho}} \tag{7}$$

  The density and compressibility of the tissue will not influence any behaviour of the catheter motion, but especially the speed of sound. Consequently, these characteristics will not contribute to the research goal of this study, since the focus of this study is to investigate how catheter motion relates to M-mode images. Besides, the complexity of the simulation model will be increased when these properties are taken into account. For that reason, the assumption has been made that the density and compressibility would not influence the US wave propagation. In this simulation model changes in the received US signal are only dependent of catheter motion and the translation of tissue particles, in other words, cardiac motion.

- *The acoustic impedance is assumed to be equal in the entire tissue, since the acoustic impedance is a function of density and speed of sound*
  Equation 8 shows that all the parameters that are assumed to be equal over the entire tissue determine the acoustic impedance. Consequently, the acoustic impedance is also be assumed to be equal and unknown in the entire tissue.

$$Z = \rho c \tag{8}$$

- *In practise, the reflection coefficient is determined by the differences in acoustic impedance between tissue structures. In a real US image, these differences in reflection coefficients are displayed with different shades of grey. Since for this simulation model is assumed that the acoustic impedance is equal in the entire tissue, the reflection coefficients are determined, independent of any physical properties, by a value in the range of 16-bit for every tissue layer. The value 0 relates to no reflection and the value 2^{16} relates to maximal reflection, visualised as respectively black and white in the M-mode image*
- *Differences in reflection coefficients within one tissue layer, a speckle pattern, are introduced in the simulation for detailed visual purposes, but are also not in relation with any physical properties of the tissue*
  In practise, the reflection coefficient is determined by the differences in acoustic impedance between tissue particles as shown in equation 9. Where Z_1 and Z_2 are two tissue layers with a different acoustic impedance and where R is the reflection coefficient.

$$R = \frac{(Z_2 Z_1)}{(Z_2 + Z_1)}^2 \tag{9}$$

  A result of the previous assumptions is that the acoustic impedance is equal and unknown in the entire tissue, which means that there would be now reflection coefficient in the entire tissue. Therefore, to each pixel (or group of pixels) a value is assigned, which represents the reflection coefficient in that point. Logically, these reflection coefficients have not any relationship with physical properties of the tissue. Moreover, the simulation would look more realistic and motion patterns are better visible when little deviations in the reflection coefficients are visualised, indicated as a so-called speckle pattern.

- *The received RF signal does only contain information about the tissue on which the transducer is oriented*
  Normally if an US wave hits an object the wave will be partially transmitted, partially scattered and partially reflected. The angle of the transmitted signal can change when it hits an object, this phenomenon is called refraction. When such refracted signal reflects, theoretically it could be that information is received with the transducer from tissue that is not lying in the sightline of the transducer. In this simulation model is assumed that all the received signals only originates from a tissue particle that is lying in the sightline of the transducer. In the future, an option is to add also refractions or scattering of signals.
  Furthermore, this assumption can be grounded with the maximum time that is needed to travel to the deepest observable tissue particle ($15.8\,mm$ deep, pixel 2048). Because, when the 2048 samples are taken with a sample frequency of 100MHz, then the US wave travels $\frac{2048}{100 \cdot 10^6} = 20.48\,\mu s$. When taken into account that the wave travels back and forth then the time will be $40.96\,\mu s$. The pulse repetition rate is 2kHz, which means that 2000 samples are taken in 1 sec and consequently a wave has $50\,\mu s$ to be transmitted and received.

- *There is no reduction of the amplitude and intensity of the received RF signal as a function of depth*
  In real US data the echoes from deeper located tissue loose intensity. The amplitude of a signal decreases as the wave propagates through material. The term attenuation indicates this loss of signal intensity. Attenuation is caused by absorption and scattering. When a signal is partially absorbed, the signal intensity is converted to thermal energy. When the signal scatters secondary waves are generated as the wave propagates. In this simulation model the reflection coefficients that are defined per tissue particle will determine the amplitude of the RF signal without any loose of intensity. So, in this model the intensity of the signal does not change as a function of depth.
  In practise, Time Gain Compensation (TGC) is applied on the received RF signal to compensate for tissue attenuation. This actually means that the inverse operation of attenuation is applied, because the TGC increases the intensity of the received signal as function of the depth. Since attenuation does not take place in this simulation model, also TGC is not required.

- *No frequency shift of the carrier wave occurs as a result of interaction with a moving tissue particle*
  In the simulation model a carrier wave of 30MHz is used and the velocities in the tissue are in the order of $10mm/s$, see Figure 23. The Doppler frequency shift formula can be used to calculate the frequency shift as result of a moving observed object, see Equation 10, with f_D the Doppler frequency, f_R and f_T the frequency of the received and the transmitted pulse, $|\vec{v}|$ the velocity vector, θ the angle between the velocity vector and the sound beam and c the velocity of sound.
  When using equation 10 it can be calculated that the measurable frequency shift would be 389 Hz in case of the velocities and carrier frequency that are used in this study, see equation 11. A frequency shift of 389 Hz over 30MHz is not an accurate measurable shift. For that reason the assumption has made that no frequency shift occurs when a wave meets a moving object.

$$f_D = f_R - f_T = -\frac{2|\vec{v}|\cos(\theta)}{c} f_T \tag{10}$$

$$389.61 = -\frac{2 \cdot 0.01 \cos(0)}{1540} 30 \cdot 10^6 \tag{11}$$

- *No translation motion of the catheter occurs during ablation*
  A surgeon applies a force on the catheter tip during ablation. This force will keep the catheter tip located at the same place.

M. Development Process of Simulation Model

The development process of the simulation model that has been completed will be discussed in this appendix section. Considerations that have been made are evaluated and some of the programming solutions that did not work properly are discussed in order to also document the knowledge about unsuccessful solutions, which perhaps could contribute during further research.

The development process was started with a really simple model where only catheter motion was modelled. As mentioned in section I the simulation model was extended step by step. In this section the development process is explained by describing different phases where phase 1 indicates a 2D simulation model with only catheter motion, phase 2 the 2D simulation with catheter and cardiac motion as has been evaluated in this article and phase 3 is the start that have been made with the 3D model.

M.1. Phase 1: 2D simulation model with only catheter motion

The simulation as shown in Figure 48 and 49 was the first prototype. At the top of these images the tissue is displayed, where also the motions of the catheter are shown. In the middle, the motion signals of the catheter can be seen. The three lower images display the observed tissue by the catheter. In this simulation model it is possible to add a desired amount of blocks to the tissue composition to obtain extra irregularities in the tissue.

This simulation model has been used to gain the first insights about the effect of catheter motion on the motion patterns that can be seen in the M-mode images.

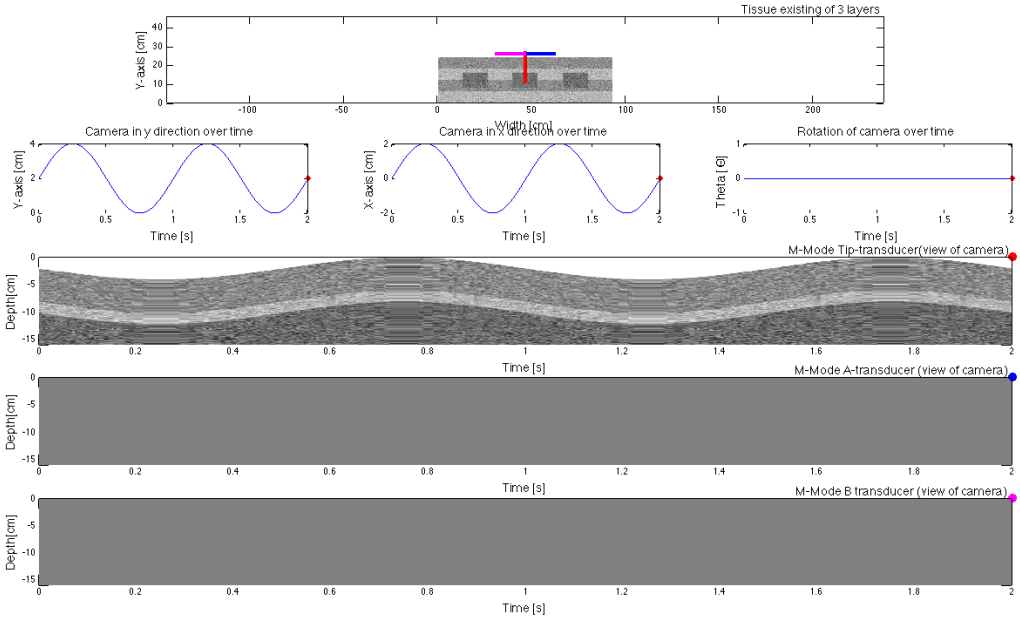

Figure 48: *First prototype of simulation model with only catheter motion (in this example only translation)*

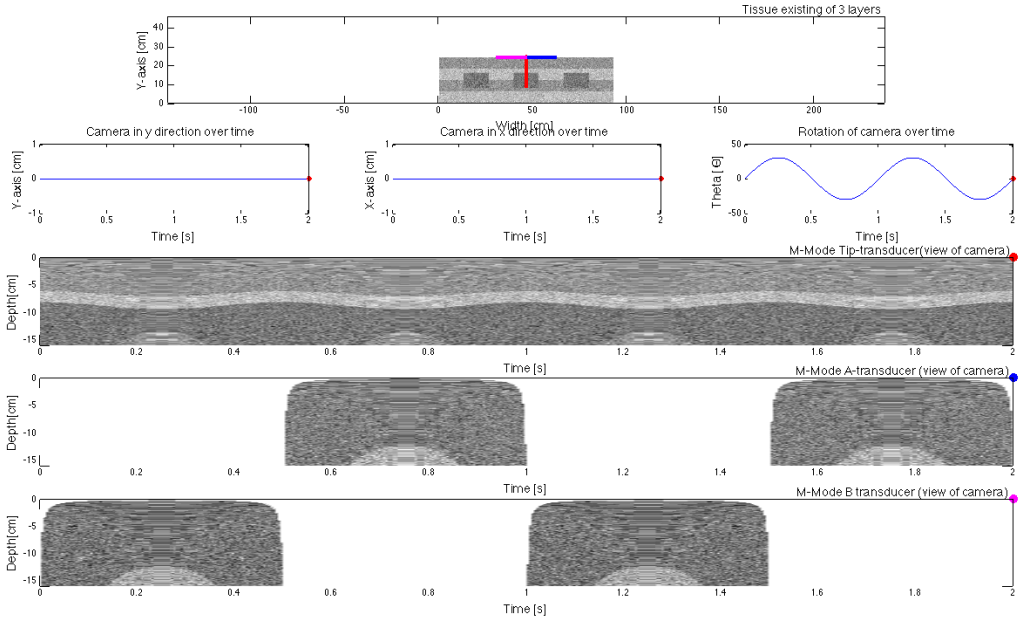

Figure 49: *First prototype of simulation model with only catheter motion (in this example only rotation)*

M.2. Phase 2: 2D simulation model with cardiac & catheter motion

The model as shown in Figure 48 and 49 has been extended to the model described in this article. The simulation model obtained in phase 1 has obtained a lot of useful information in order to determine the requirements and specifications for the 2D simulation model with cardiac & catheter motion.

The Movie generator and RF data generator shown in Figure 6 and 7 are edited in order to show only the most important axis information. In Figure 50 and 51 an unedited screenshot is shown with the actual displayed axis when running the simulation model.

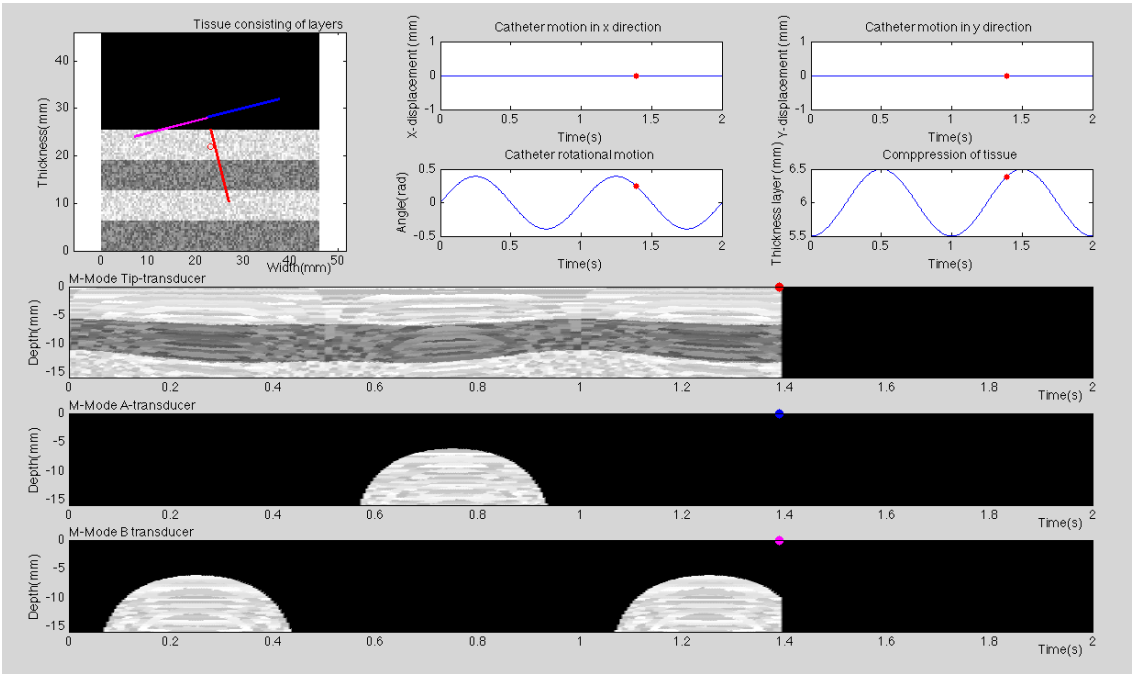

Figure 50: *Unedited screenshot of the output of the Movie generator*

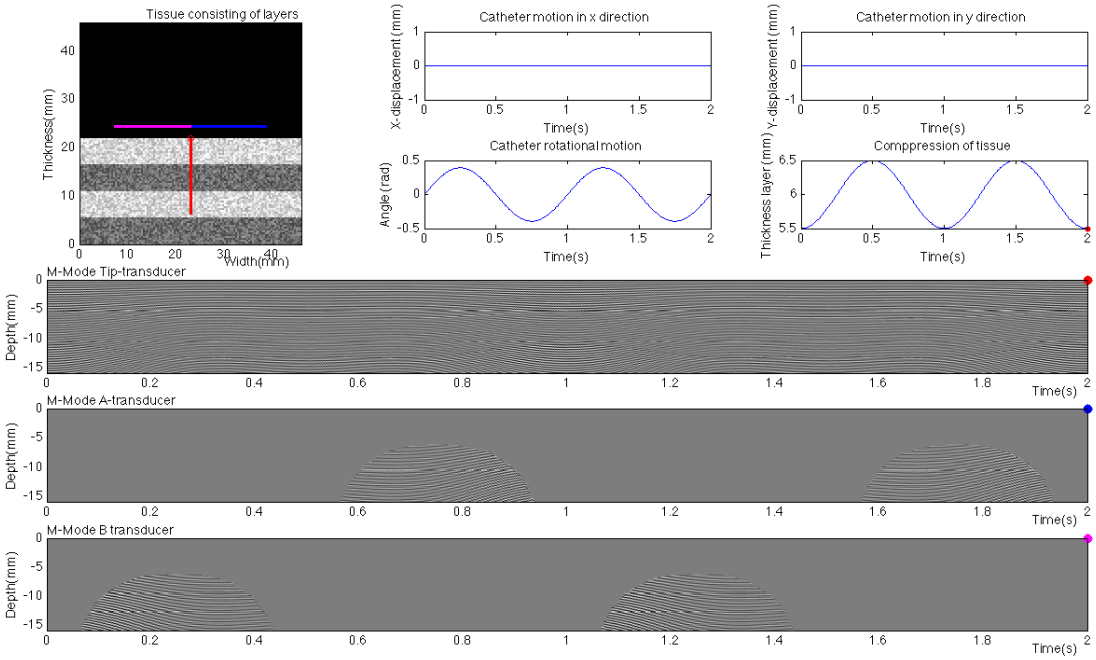

Figure 51: *Unedited screenshot of the output of the RF data generator*

With this simulation model it is possible to use a large variety of signals as motion input signal. Figure 52 shows an example where an ECG signal is used as motion input signal for cardiac and catheter motion with as effect that the contraction of the tissue and the motion of the catheter moves with a representative contracting rhythm of a heart.

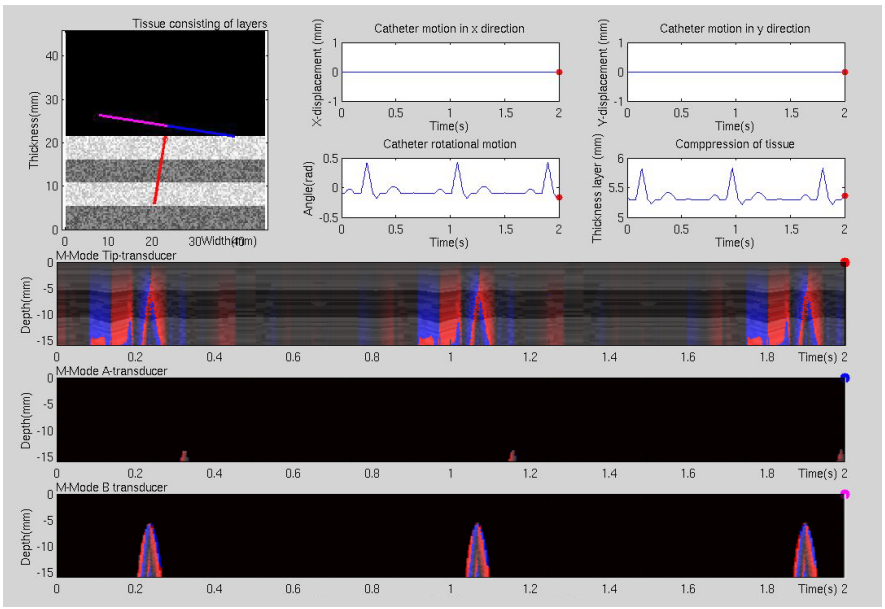

Figure 52: *Output of 2D simulation model where the cardiac & catheter motion signal is simulated with an representative ECG signal with a phaseshift between cardiac and catheter motion. The TSM is an overlay image, which is generated with the output of the RF generator.*

The main difference between the output of the Movie generator and the RF generator is shown in Figure 53. In this Figure two A-modes are displayed; one presents a time sample acquired with the Movie generator and one presents a time sample acquired with the RF generator. The A-mode of the Movie generator shows

only the grey values that are directly copied from the observed tissue, while the A-mode of the RF data generator shows different amplitudes, but modulated with a carrier wave.

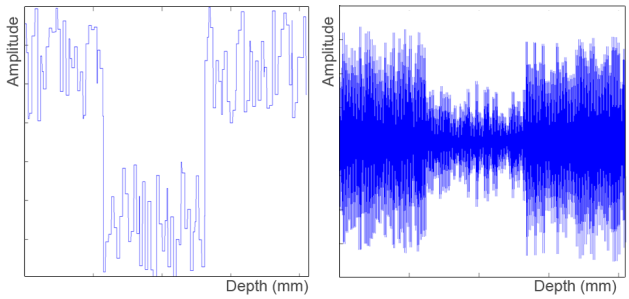

Figure 53: *Left: A-mode obtained with Movie generator. Right: A-mode obtained RF data generator*

M.2.1. Design process of transducer orientation

The manner in which the transducer orientation is modelled has been improved during the design process. The most major changes in how this is modelled will be discussed.

1. First Concept
   For each iteration the position of the transducers was recalculated for every transducer based on the translations, see Figure 54. Then, the orientation of each transducer was calculated separately based on the rotational motion. This means that a lot of calculations needed to be done, which is an expensive job, but which also increases the chance of a modelling error. Furthermore, if the model would be extended with more transducers, then even more calculations are required. For that reason, this way of modelling the orientation of the transducers was improved to another concept.

```
for i = 1:N;
...
    ct = camera;                          % Copy the camera parameters
    ct.loc(1) = ct.loc(1)+xT(i);          % The x location of the camera is changing by the sinus
    ct.loc(2) = ct.loc(2)+yT(i);          % The y location of the camera is changing by the sinus

    ct.xdeltaTip = ct.d * sind(thetaT(i));          % Define the angle of the tip transducer in x indexes
    ct.ydeltaTip = abs(ct.d * cosd(thetaT(i)));     % Define the angle of the tip transducer in y indexes

    ct.xdeltaAB = abs(ct.d * cosd(thetaT(i)));      % Define the angle of the A & B transducer in x indexes
    ct.ydeltaAB = ct.d * sind(thetaT(i));           % Define the angle of the A & B transducer in y indexes

    [mmodeTip, yCamTip] = getCamViewTip(ct, tissue);
    [mmodeA  , yCamA  ] = getCamViewA  (ct, tissue);
    [mmodeB  , yCamB  ] = getCamViewB  (ct, tissue);
...
end
```

Figure 54: *First concept of modelling transducer orientation*

2. Second Concept
   All the transducers move as one object since the transducers are al fixated in one catheter. This means that the orientation of each transducer changes with the same ratio. Therefore, one rotation matrix was used to determine the changes of the transducer orientation per time sample. The only problem with this method was that the contraction of the tissue and the translation of the transducers did not take place at the same time, with as result the saw tooth effect shown in Figure 55.

```
for i = 1:N;
...
tissue = tissuelayer(tissue, yg, height, minheightlayer, resox, Carrier, carriersignal, Noisy, Noise);

    followtissue=thickness-minheighttissue;
    tranYY = tranY(i)+followtissue+0.1;

    rotmat  = makehgtform('translate',[tranX(i) tranYY 0],'zrotate',rotZ(i));
    rotmat1 = makehgtform('translate',origin);% coordinaten van de camera position
    rotmat2 = makehgtform('translate',origin_min);%-x coordinate start punt %-y coordinate startpunt - z
coordinaat startpunt
    rotationmatrix = rotmat1*rotmat*rotmat2;
...
 end
```

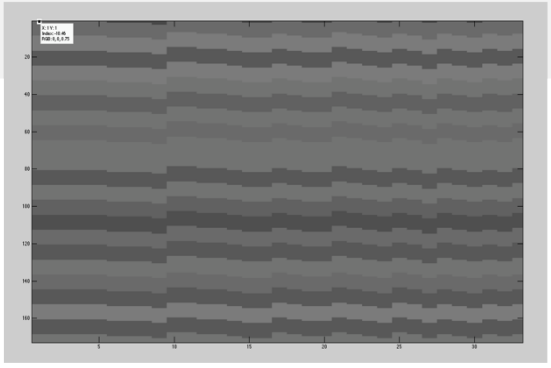

Figure 55: *Second concept of modelling transducer orientation. A saw tooth shaped pattern in the M-mode image was caused by catheter translation and tissue contraction that did not take place at the same time*

3. Final design
   The problem that occurred in the previous concept is in this final concept solved by making the rotation matrix dependent of the exact height of the contracted tissue. In Figure 56 it can be seen that observed tissue does not contains the undesired saw tooth effect anymore.

```
for i = 1:N;
…
   % Recalculate the composition of the deformed tissue
    tissue.plot  = imresize(tissue.dat, [resoy*factor_speckle resox],'nearest');
    tissue.plot  = tissue.plot(1:resoy, 1:resox);
    tissue.data  = tissue.plot;

    [rowzero,~]  = find(tissue.plot(:,1) == 0);                    % Find where tissue starts
    followtissue = (rowzero(1) * heighty / resoy)-transd.Tiploc(2); % Calculate the amount of mm that tissue
grows
    tranYY       = tranY(i)+followtissue;                          % Add those mm to translation in Y
direction

    % Define the catheter orientation dependent of the x translation, y translation and rotation around z-axis
    % With the origin used as pivot point
    rotmat  = makehgtform('translate',[tranX(i) tranYY 0],'zrotate',rotZ(i));
    rotmat1 = makehgtform('translate',origin);     % + Pivot point
    rotmat2 = makehgtform('translate',origin_min); % - Pivot point
    rotationmatrix = rotmat1*rotmat*rotmat2;
…
end
```

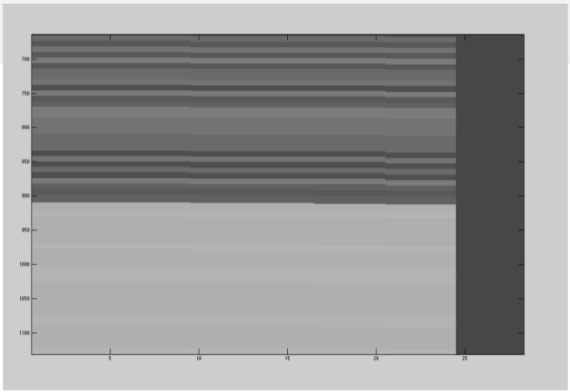

Figure 56: *Final design of modelling transducer orientation, that results in a smooth M-mode image*

M.2.2. Design process of speckle pattern

The manner in which the speckle pattern is modelled has been improved during the design process. The most major changes in how this is modelled will be discussed.

1. First Concept
   In this first concept a random value was added to each pixel of the generated tissue, which created a speckle pattern. A disadvantage was that when a large resolution for the tissue was used, the deviations in reflection coefficients were nearly visible. Furthermore, this concept proved that it was not suitable when the simulation model was extended with cardiac motion. To simulate cardiac motion, it was required that the speckle pattern could contract and extend without changing in reflection coefficient, which was not possible with this concept.

```
noise=0.2;                                    % define the weighting factor for the noise
tissue.data   = dat    ;                      % Save the layers in tissue.data
tissue.data(tissue.data~=0)=tissue.data(tissue.data~=0)+(randn(size(tissue.data(tissue.data~=0)))*noise); % add
random noise to numbers which are not equal to zero, because that represents the environment
tissue.data(tissue.data>0)=-0.1;              % Because of the noise, some data will become larger then zero,
which is not desired, because the zero values represents the environment
tissue.x      = x;                            % Save the width (indexes) of space as width of tissue
tissue.y      = y;                            % Save the height (indexes) of space as height of tissue
```

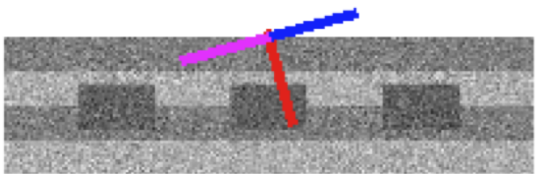

Figure 57: *First concept of modelling speckle pattern: Adding randomized values to the generated tissue.*

2. Second Concept
   In this second concept the speckle pattern was modelled as a combination of multi sinuses. The benefit of using these multi sinuses is that generated signal can be resized, while the values remained intact, which represents cardiac motion. This property was valuable, since that could represent contracting tissue. The problem was that the generated RF data with these multi sinuses caused artefacts in the TSM, because the speckle pattern was too artificial.

```
%% Generate noise in tissue

if Noisy
    Noise1=zeros(resoy,resox);
    Noise2=zeros(resoy,resox);
    Noise3=zeros(resoy,resox);
    Noise4=zeros(resoy,resox);
    time = linspace(0,10,resoy);
    time3 = linspace(0,10,resox);

        for i=1:resox
            phaseshift=rand*pi;
            freq=0.5 + (rand(1) * 0.6);
            ampli=0.2 + (rand(1) * 0.5);
            Noise1(:,i)=ampli*sin(2*pi*freq*time+ phaseshift);

        end

        for i=1:resox
            phaseshift=rand*pi;
            freq=0.5 + (rand(1) * 0.6);
            ampli=0.2 + (rand(1) * 0.5);
            Noise2(:,i)=ampli*sin(2*pi*freq*time+ phaseshift);
        end

        for i=1:resox
            phaseshift=rand*pi;
            freq=0.5 + (rand(1) * 0.6);
            ampli=0.2 + (rand(1) * 0.5);
            Noise3(:,i)=ampli*sin(2*pi*freq*time+ phaseshift);
        end

        for i=1:resox
            phaseshift=rand*pi;
            freq=0.5 + (rand(1) * 0.6);
            ampli=0.2 + (rand(1) * 0.5);
            Noise4(:,i)=ampli*sin(2*pi*freq*time+ phaseshift);
        end

Noise=Noise1+Noise2+Noise3+Noise4;

else
    Noise = 0;
end
```

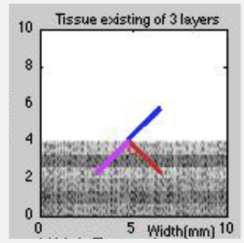

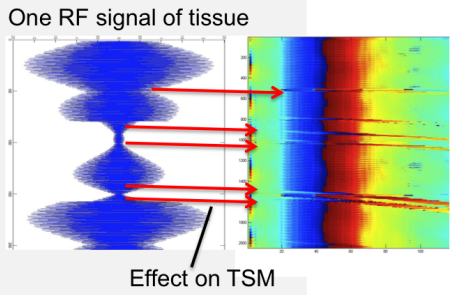

Figure 58: *Second concept of modelling speckle pattern: Adding randomized values determined with multi sinuses*

3. Final design
   A speckle pattern was created of which the size of a speckle can be set as desired. At $t = 1$ a speckle pattern is created for the tissue that has the minimal tissue height. For each time sample this speckle pattern is extended with the function imresize that copies the value of the nearest neighbour, with as result that the determined reflection coefficients are use to extend the cardiac tissue. This change in expansion of the tissue represents contracting cardiac motion.

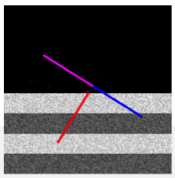

```
if Speckle

Specklesize=80;
Noisecolumn=rand(resoy/Specklesize,resox/Specklesize);
Noise=kron(Noisecolumn,ones(Specklesize,Specklesize)); % Multiplies the Noisecolumn in x and y direction

[row,~] = find(tissue.data(:,1) == 0);
tissue.data((row(1)-1):-1:1,:) = tissue.data((row(1)-1):-1:1,:) - abs(Noise(1:(row(1)-1),:));

end
```

```
for i = 1:N;
...
% Recalculate the composition of the deformed tissue
    tissue.plot  = imresize(tissue.dat, [resoy*factor_speckle resox],'nearest');
    tissue.plot  = tissue.plot(1:resoy, 1:resox);
    tissue.data  = tissue.plot;

...
end
```

Figure 59: *Final design of modelling speckle pattern: Adding a predefined randomized speckle pattern to the generated tissue*

M.2.3. Design process of Carrier wave

The theory of how the RF signal depends on the cardiac and catheter motion is shown in Figure 60. In this Figure it can be seen that a phase shift can be measured between the RF data of different time samples as result of cardiac or catheter motion. In this example the tissue particles move away from the transducer as a result of an expanding cardiac wall or an increasing catheter angle. This theory is supported by the measurements that have been made of real US, see Figure 85 and 87, used for validation test 6.

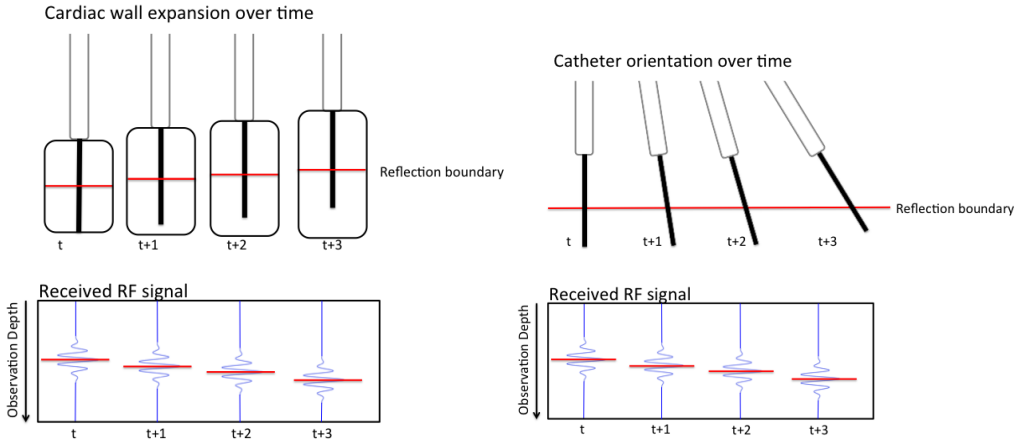

(a) Change of RF signal as result of cardiac motion (b) Change of RF signal as result of cardiac motion

Figure 60: *Change of RF signal as result of cardiac or catheter motion*

The manner in which the carrier wave of the RF signal is modelled has been improved during the design process. The most major changes in how this carrier is modelled will be discussed.

1. First Concept
   The carrier signal was modelled with a sine function, which was multiplied once with the modelled tissue at $t = 1$. For each time sample the tissue was deformed and the catheter orientation was changed, the observed tissue that was multiplied with the carrier wave was used as RF data. These RF data did not give the expected result when using the TSM algorithm, since no phaseshift could be detected between the RF signals of the different time samples.

```
if Carrier
    Acarrier = 4; fcarrier =round(resoy/4); phaseshift = 0;   % Amplitude, Frequency and Phase Shift for
Carrier Signal
    time = linspace(0,1,resoy);                    % Time Line of carriersignal with the same amount of numbers
as resolution in y direction
    carriersignal = Acarrier*sin(2*pi*fcarrier*time + phaseshift);

    tissue.data = tissue.data .* ( carriersignal' * ones([1,size(tissue.data,2)]))
end
```

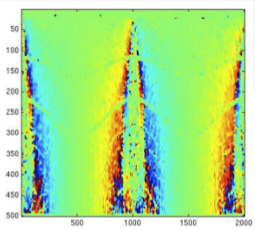

Figure 61: *First concept of modelling carrier wave signal: Multiply generated tissue with carriersignal before running simulation model*

2. Second Concept
   Instead of multiplying the tissue with a carrier wave only at $t = 1$, the deformed tissue was multiplied with a carrier wave for each time sample. Because the tissue deformed over time, a measurable phase shift occurred. The problem with this approach was that the phaseshift was equal for the entire thickness of the tissue, because for every time sample the same carrier wave was used. In the TSM of Figure 62 it can be seen that velocities are estimated equally in the entire tissue, while the velocities of the tissue particles that are located deeper in the tissue should be estimated higher. Consequently, the phase shift should be nearly zero nearby the transducer and should increase as function of depth when the entire tissue moves with the same velocity.

```
if Carrier
    Acarrier = 4; fcarrier =round(resoy/4); phaseshift = 0
    time = linspace(0,1,resoy); % Time of carriersignal
    carriersignal = Acarrier*sin(2*pi*fcarrier*time + phaseshift);
 end
```

```
for i = 1:N;
…
 if Carrier
    mmodeTip=mmodeTip*carriersignal;
 end
…
end
```

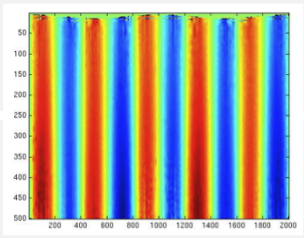

Figure 62: *Second concept of modelling carrier wave signal: Multiply each time sample with carriersignal*

3. Third Concept
   At $t = 1$ a carrier wave was modelled that for each time sample was resampled, in other words, stretched as function of cardiac or catheter motion. This approach only worked properly when a carrier wave was modelled with a frequency of 20 MHz. Figure 63 shows the undesired effect of resampling a 30 MHz signal with a sample frequency of 100 MHz; two subsequent data points can get the same value after resampling. As result the phaseshift between the RF signals of two time samples can not be measured anymore.

```
…
if Carrier
    Acarrier = 4; fcarrier =30e6;   % Amplitude, Frequency for Carrier Signal
    time = linspace(0,1,resoy); % Time of carriersignal with the same amount of numbers as resoy
    carriersignal = Acarrier*sin(2*pi*fcarrier*time);
end
```

```
for i = 1:N;…

 if Carrier
              carrier=resample(carrier,Nom,Denom);
              mmodeTip=mmodeTip*carriersignal;
 end
…
end
```

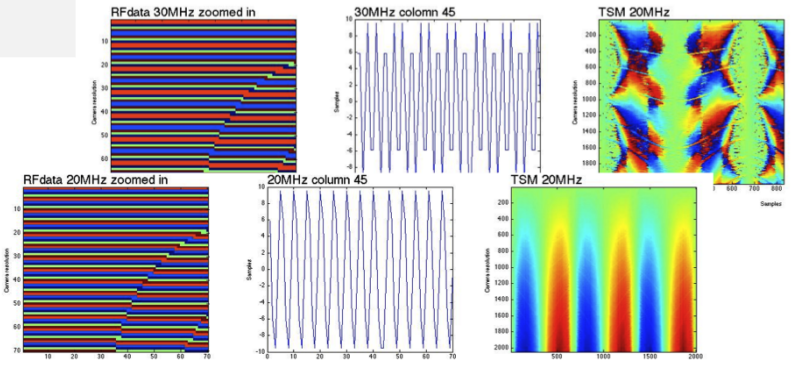

Figure 63: *Third concept of modelling carrier wave signal: Multiply each time sample with a carrier signal that is stretched or compressed as function of cardiac or catheter motion*

4. Fourth Concept
   The idea was to use Gaussian pulses instead of a continuous sine function. For each time sample the carrier wave was upsampled with a factor 100, the carrier signal was then deformed as function of cardiac and catheter motion, and then downsampled again. Unfortunately, this method caused artefacts as result of the 'empty' spaces between these pulses. In Figure 64 it can be seen that for tissue that is located deeper in the tissue the velocities are estimated higher, which is correct, but probably as result of the used pulses the result is not optimal. Furthermore, the frequency of the RF signals of different time samples did change, which should not be the case.

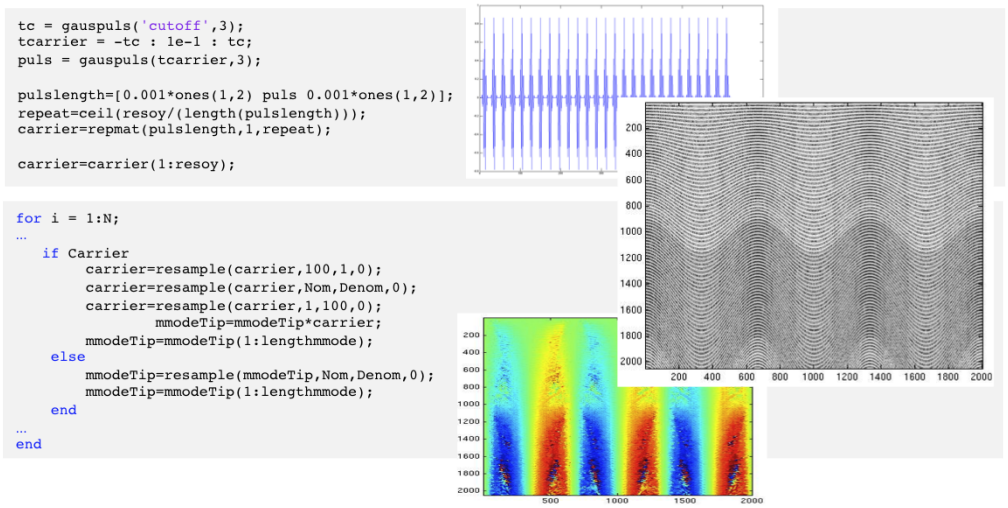

Figure 64: *Fourth concept of modelling carrier wave signal: Multiply each time sample with a pulsed carrier signal that is adapted as function of catheter or cardiac motion*

5. Fifth Concept
   For each time sample a sine function was created of which the phase of this signal changes as function of cardiac and catheter motion and the observation depth. In Figure 65 it can be seen that a desired phase shift occurs between the RF signals of two time samples. Unfortunately, this concept did not work out properly for extreme motions. If the phaseshift became too large, a frequency shift was caused instead of a phase shift. The TSM will be able to estimate velocities from these data, but Figure 65 shows that these velocities are way to high to measure, and as a result aliasing occurs.

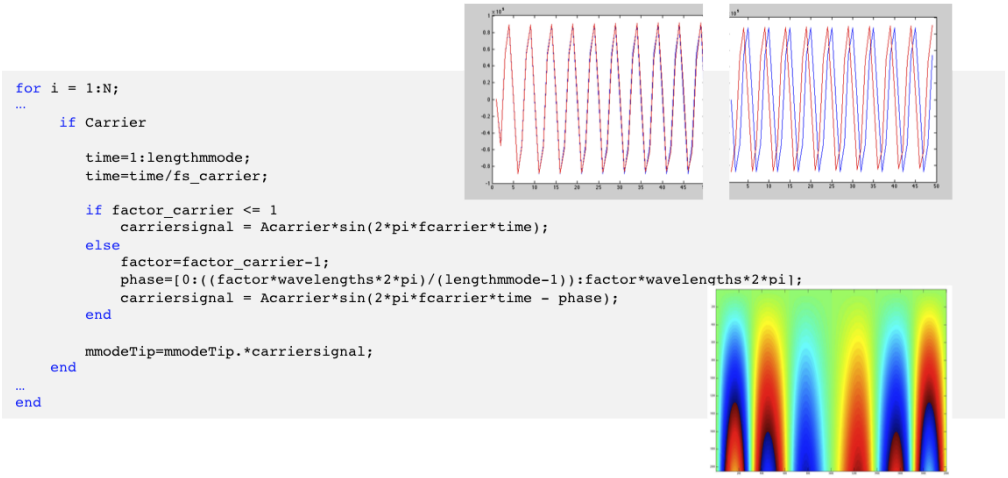

Figure 65: *Fifth concept of modelling carrier wave signal: Multiply each time sample with a carrier wave of which the phase differs as function of observation depth and catheter and cardiac motion*

6. Final design
   For each time sample a carrier wave was modelled that consists of multiple Gaussian pulses with a fixed frequency. This means that the frequency would not change, since this signal is not stretched. Only the distance between these pulses is determined as a function of cardiac and catheter motion and is recalculated for each time sample. By using a really small distance between the Gaussian pulses it seems that the carrier wave is a continuous wave, while this is a result of interfering Gaussian pulses. If there is no cardiac or catheter motion the distance between these Gaussian pulses is $10e^{-6}$, which means that approximately 205 pulses are generated for 2048 pixels. Consequently, every pulse covers 10 pixels. In practise, the created pulses covers more than 10 pixels, with as result that the pulses interfere with each other. This solves the problem of 'empty spaces between pulses' as discussed in the fourth concept. Moreover, no frequency of the signal occurs and the phaseshift changes in relation to the observation depth.

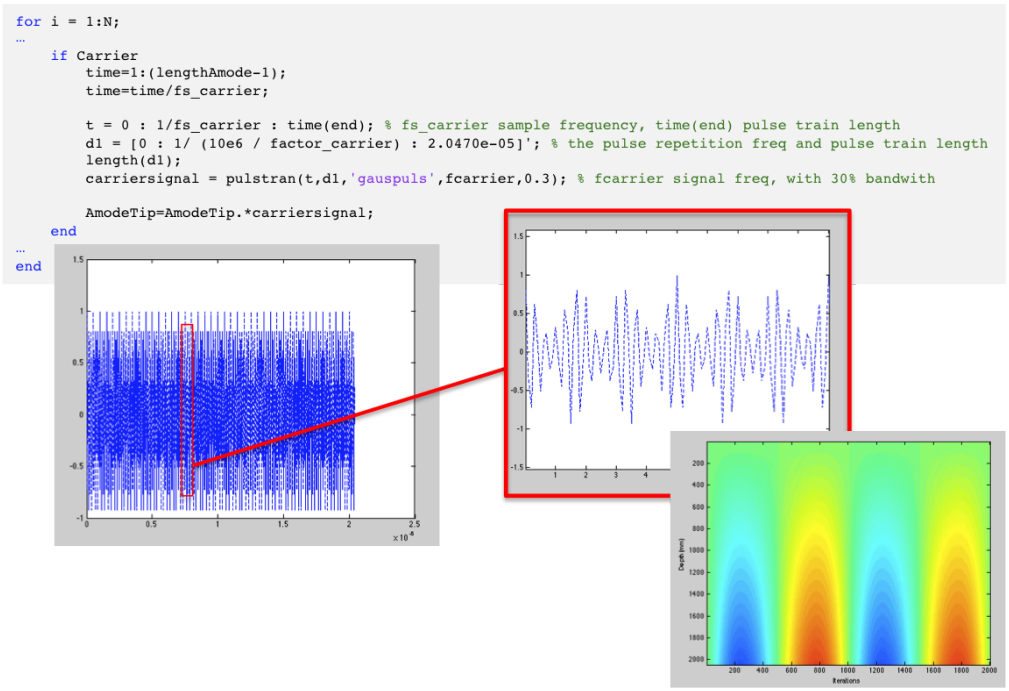

Figure 66: *Final design of modelling carrier wave signal: Multiply each time sample with a carrier signal that consists of multiple Gaussian pulses of which the distance between these pulses differ as function of cardiac or catheter motion*

M.2.4. Detailed Workflow

A more detailed workflow of the simulation model in comparison to Figure 8 is shown in Figure 67. This workflow shows all the steps that are performed when running the simulation model.

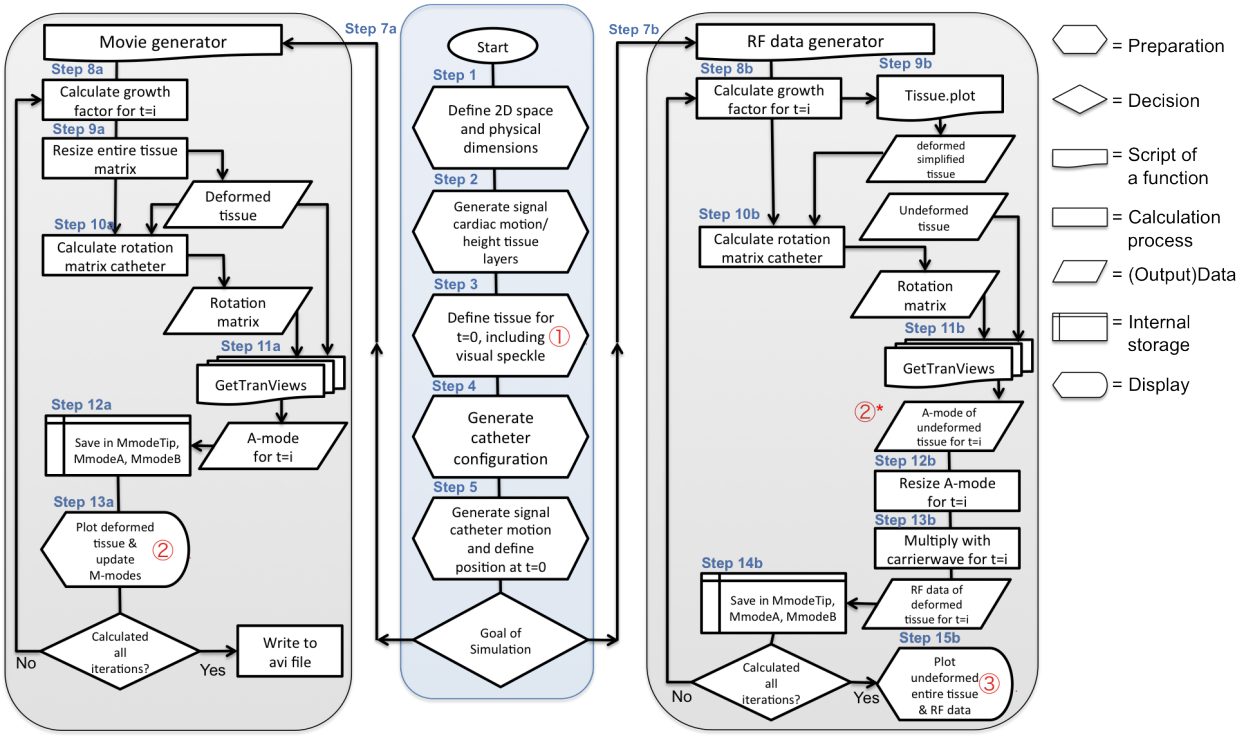

Figure 67: *Detailed workflow of the Movie generator and RF data generator*

User Manual Movie generator

Introduction

The aim of the Movie generator is to produce a movie that shows the effect of a change in cardiac tissue or catheter orientation on M-mode images. The catheter is equipped with multiple single element transducers that all result in a single data matrix. In this manual the script of the Movie generator simulation will be explained in detail. A short explanation is given about every section of the script. The green coloured comments in the script itself give even more specific information per command.

Output Movie generator

The movie generator generates a movie of the tissue changes, catheter orientation and the corresponding sightlines of the different transducers over time. The motion input signals of the cardiac motion and catheter motion are displayed in the upper right corner. The moving tissue and changes in catheter orientation can be seen in the upper left corner. The red line in this image represents the sightline of the tip transducer. The simulated sightline is plotted in the three plots at the bottom of Figure 1. As can be noticed the first plot displays a red dot at the top of the plot, which symbolises the sightline of the tip transducer. The blue and purple lines represent the sightlines of the side transducers. The corresponding plots are indicated with a same coloured dot.

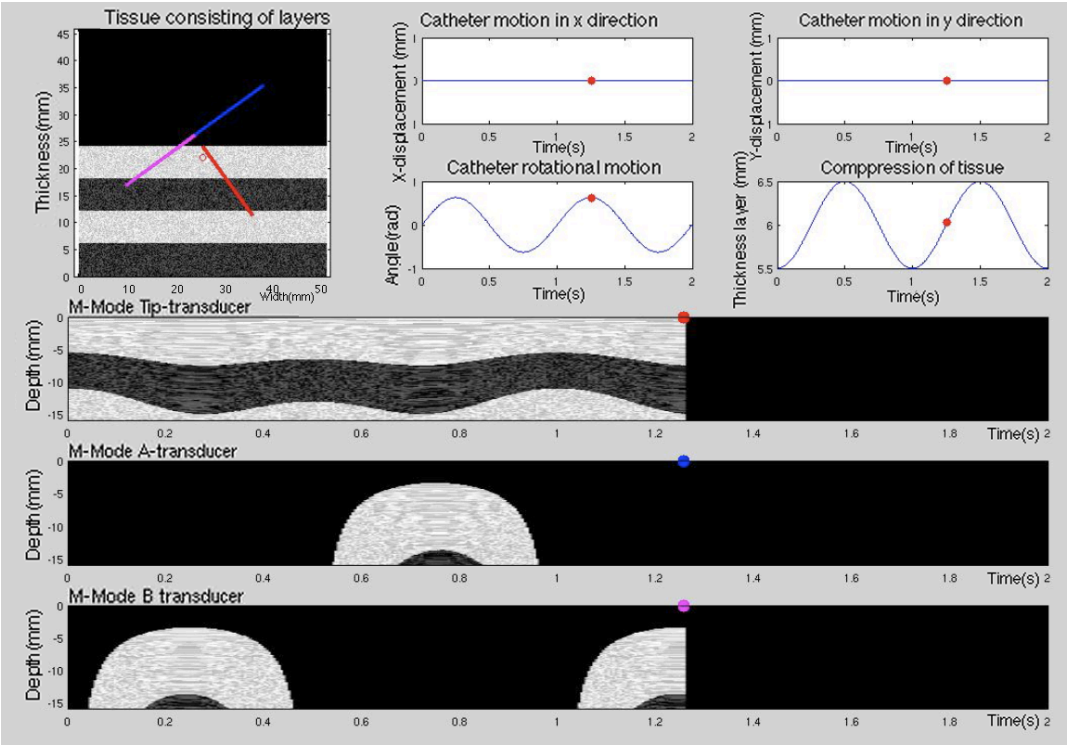

Figure 1 Output Movie generator

Input Movie generator

All the parameters can be adjusted as desired. The parameters that are most interesting for adjustment are the following:
- The cardiac tissue consists of an adjustable amount of layers, which differ from each other by a difference in reflection coefficient.
- The cardiac contracting motion can be set with any signal. The signals that are implemented in current script are (multi) sinusoids and an ECG signal.
- The composition and orientation of the transducers in the catheter can be adapted. In this current script the composition and orientation of the catheter is set as the dimensions of the MUVIC 444-H catheter, developed and manufactured by Philips research.
- The catheter motion is determined by three signals: translation in X-direction, translation in Y direction and rotation around the Z-axis. These signals can be set with any signal. The signals that are implemented in current script are (multi) sinusoids and an ECG signal.

Implementation in Matlab

Generate Workspace and Physical Size (Simulation2D_Movie_Generator.m)

First, an empty workspace is generated. This operation can be seen as pre-allocation of data. The resolution of the physical size is adjustable, in this case the resolution is based on the MUVIC 444-H catheter that has a ratio of 2048 data points per 15.8 mm. For the movie generator the resolution is divided by a factor ten with as result that the simulation becomes way faster. Furthermore, in this section some features of the simulation can be activated by means of the command 'true' or 'false'. For example, if it is desired to save the movie as an avi-file, then the command *Movie* should be activated.

```
%% Generate workspace and physical size

resox   = 600; % number of points in which [0,widthx ] is discretized
resoy   = 600; % number of points in which [0,heighty] is discretized
widthx  = round(resox * 15.8 / 204.8); % real width  of the observed tissue part
heighty = round(resoy * 15.8 / 204.8); % real height of the observed tissue part

x       = linspace(0, widthx , resox); % Create the width of space
y       = linspace(0, heighty, resoy); % Create the height of space
[xg,yg] = meshgrid(x,y);               % Derive handy arrays for computing

doPlot   = true;  % indicates whether plotting is done or not
Simulate = true;  % indicates whether every iteration is plotted or if data is plotted after all iterations
Movie    = true;  % indicates whether a movie of the simulation is saved
ECGtissue= false; % indicates whether a ecg signal is used as contraction signal
ECGtransd= false; % indicates whether a ecg signal is used as wiggling signal
Speckle  = true;  % indicates whether speckle will be added to the tissue layers

% At this point the tissue of physical size widhtx x heighty is represented by (resox-1) by (resoy-1) cells.
```

Set Time and Sample Frequency (Simulation2D_Movie_Generator.m)

In this section the simulation time and sample frequency parameters are defined, which determine automatically the amount of iterations that each simulation run should complete. Real ultrasound data generated with the MUVIC 444-H catheter is normally acquired with a sample frequency of 2000Hz. Such a high frequency is required if subsequent calculations are performed with the generated data. The data output from the Movie generator is not meant to use for further calculations, for that reason it is possible to divide also the sample frequency by a factor ten, which decreases the calculation time.

```
%% Set time and sample frequency

T  = 2;               % Observation time in seconds
fs = 200;             % Sampling frequency
N  = T*fs;            % Same as T/dt, represents total amount of time samples
t  = linspace (0,T,N); % Time axis
```

Generate Signal for Tissue Compression (Simulation2D_ Movie _Generator.m)

In this section the input motion signal for 'cardiac' tissue compression is defined. The tissue consists of several tissue layers, determined in the next section. This signal determines the height of one tissue layer. A simple sinusoid can be extended by using the parameters *tissue.fmulti* and *tissue.amulti*, which results in a multisine. Another option is to make use of the *ECGtissue*, which generates an ECG signal as tissue motion signal. In that case the function *complete_cardiac* is called. This function has been downloaded from the internet and a manual can be found in the *Philips_Bente_de_Lat/3. Matlab Scripts/4. Remaining/1. ECG/ECGmanual*.

```
%% Generate signal for tissue compression

tissue.f=1;            % Define frequency of compression
tissue.a=0.5;          % Define the difference in height
tissue.equil=6;        % Define equillibrium height of the tissue layers
tissue.height=cos(tissue.f*2*pi*t-pi)*tissue.a+tissue.equil;           % Define final signal for compression

tissue.fmulti=0;       % Frequency for introducing irregularities in signal
tissue.amulti=0;       % Determine how much the multisingle should dominate
tissue.height=tissue.height+(sin(tissue.fmulti*2*pi*t)*tissue.amulti); % Add multisin to compression signal
figure;plot(t,tissue.height);

if ECGtissue
    multiply=10;                                % Determine a multiplication factor
    delaytis=0.7;
    [ecg]=complete_cardiac(t+delaytis,multiply); % Call function complete
    tissue.height=ecg;                          % Put ECG signal in theta
    tissue.height=tissue.height/30+tissue.equil; % An alternating motion is achieving by substraction
    figure(1);plot(t,tissue.height); hold on     % Plot the created ECG signal
end
```

Define Tissue Layers and Tissue Height (Simulation2D_ Movie _Generator.m)
In this section the composition of the cardiac tissue is defined. During an US acquisition, the reflection coefficient is determined by the differences in acoustic impedance between tissue structures. In a real US image, these differences in reflection coefficients are displayed with different shades of grey. For this simulation model is assumed that the acoustic impedance is equal in the entire tissue, the reflection coefficients are determined, independent of any physical properties. The value 0 relates to no reflection and the largest value relates to maximal reflection, visualised as respectively black and white in the M-mode image

The number of tissue layers is determined by using a vector, with the vector length defining the number of layers. The value of every layer represents the reflection coefficient. In this case the choice have been made to take reflection coefficients in the range of 16-bit, since the data need to be converted to 16-bit data, to make it compatible with the Cameleo software, but the values can be set with any value.

```
%% Define amount of tissue layers and total tissue height

tissue.layers  = [18000 30000 18000 30000];% Layers will get these values
minheightlayer = min(tissue.height);       % Determine minimal height of one tissue layer
minheighttissue= min(tissue.height)*length(tissue.layers); % Determine minimal total height of tissue
maxheightlayer = max(tissue.height);

tissue.x       = x; % Save the width  (indexes) of space as width of tissue
tissue.y       = y; % Save the height (indexes) of space as height of tissue
```

Generate Tissue (Simulation2D_ Movie _Generator.m)
In this section the cardiac tissue was generated in the pre-allocated empty workspace on the basis of the previously defined minimal tissue height of one layer.

```
%% Generate a tissue

% Calculate the layers for one column (so 1D) and then copy this layer to every column (to save memory)
yg1D = yg(:,1);                  % Determine size prealocation
dat1D = zeros(size(yg1D));       % Prealocate data

for i = 1:length(tissue.layers)
    yLo = (i-1)*minheightlayer ; % Define the lower border for the layer (so the height of the previous layer)
    yHi =  i   *minheightlayer ; % Define the upper border for the layer (so the height of the current layer)
    dat1D( yg1D >= yLo & yg1D < yHi ) = tissue.layers(i); % Give predefined value to tissue layer
end

tissue.dat = dat1D * ones([1,resox]); % Save the layers for every column in tissue.dat
```

Generate Speckle Pattern in Tissue (Simulation2D_ Movie _Generator.m)
A characteristic appearance of US is that structures in a tissue do not seem to be totally equal, but a so-called speckle pattern can be recognized. A speckle pattern occurs because of little deviations in the reflection coefficients within a tissue. This appearance was also added to the simulation model by subtracting randomized smaller values from the main tissue layer value. This results in different reflection coefficients in the entire tissue with as effect a more realistic M-mode image. These speckle patterns have just been added for visual purposes, but are not in relation with any physical properties of the tissue.
This option can be activated or de-activated. The size of the speckles can be adjusted according to the desired effect of the speckle.

```
%% Generate a speckle pattern in tissue

if Speckle

Specklesize=5;
Noisecolumn=rand(resoy/Specklesize,resox/Specklesize)*10000; % Define a random speckle pattern
Noise=kron(Noisecolumn,ones(Specklesize,Specklesize));       % Multiplies the Noisecolumn in x and y direction

% Only add speckle pattern to the tissue, not to the 'air'.
% So, first determine till which row this is the case.
% Then add the speckle pattern to the tissue.dat.
[row,~] = find(tissue.dat(:,1) == 0);
tissue.dat((row(1)-1):-1:1,:) = tissue.dat((row(1)-1):-1:1,:) - abs(Noise(1:(row(1)-1),:));

end
```

Generate Signal for Catheter Motion (Simulation2D_ Movie _Generator.m)
In this section the catheter motion signals are determined in three directions: translation in X-direction, translation in Y-direction and rotation around the Z-axis. First, the frequency and amplitude of these signals are determined. These signals could be generated with a simple sine function or a more complicated multi-sine function by using the *transd.fmulti* and *transd.amulti* parameters. Another option is to use an ECG-signal.

```
%% Generate signal for catheter motion
transd.fx    = 0;        % Frequency of moving catheter in x direction
transd.fy    = 0;        % Frequency of moving catheter in y direction
transd.fsweep= 1;        % Frequency of wiggling catheter
transd.fmulti= 0;        % Frequency for irregularities (by 0 freq no irregularities)

transd.ax    = 0;        % Amplitude of moving catheter in x direction
transd.ay    = 0;        % Amplitude of moving catheter in y direction
transd.asweep= 0.125*pi; % Amplitude of wiggling catheter in pi
transd.amulti= 0;        % Determine how much the irregularities should dominate

tranX = cos(transd.fx*2*pi*t);                  % Create cosine movement of catheter discretized over N samples
tranX = tranX+(sin(transd.fmulti*2*pi*t)*transd.fmulti);% Influence the periodic behaviour
tranX = tranX * transd.ax;                      % Adapt amplitude of transd

tranY = cos(transd.fy*2*pi*t);                  % Create cosine movement of transd discretized over N samples
tranY = tranY+(sin(transd.fmulti*2*pi*t)*transd.fmulti);% Influence the periodic behaviour
tranY = tranY * transd.ay + transd.ay;          % Adapt amplitude of transd and begin position

phaseshift = 0;                                 % Phaseshift of catheter motion in relation to cardiac motion
rotZ = sin(transd.fsweep*2*pi*t-phaseshift*pi); % Create cosine movement of transd discretized over N samples
rotZ = rotZ+(sin(transd.fmulti*2*pi*t)*transd.amulti);  % Influence the periodic behaviour
rotZ = rotZ * transd.asweep;                    % Adapt amplitude of transd
%rotZ(:)= -transd.asweep;                       % Make active if a constant angle is desired

if ECGtransd
    multiply=10;                                % Determine a multiplication factor
    delaycat=0.6;
    [ecg]=complete_catheter(t+delaycat,multiply);% Call function complete to generate the ECG signal
    rotZ=ecg;                                   % Put ECG signal in catheter rotation signal
    rotZ=(rotZ/30)-0.4;                         % A wiggling motion is achieving by substracting a value
    figure(1);plot(t,rotZ,'r');                 % Plot the created ECG signal
end
```

Transducer Settings and Start Location (Simulation2D_ Movie _Generator.m)
In this sections the orientation parameters of the transducers are defined. The resolution and watching depth of the transducers are in this case based on the MUVIC 444-H catheter, but again divided by a factor ten, to make the simulation faster. The resolution of 204.8 is the same number as used in the first section to determine the resolution of the physical size. When the watching depth is larger than the minimal tissue thickness, an error message will be given. Furthermore, the distance from the side transducers in relation to tip transducer has been determined. This distance is used to determine the starting point of all the used transducers, which is dependent on the minimal tissue thickness, watching depth and the physical space. The parameters *transd.loc* represent the starting point of the transducer. The parameters *transd.view* determine in which direction the transducer is orientated and so actually represent the deepest point that can be seen with the transducer. At this point in the parameter settings, the side transducer have the same watching orientation as the tip transducer, in the next section the orientation of the side transducers will be set in relation to the tip transducer.

```
%% Transducer settings and start location
transd.d     = 15.8;     % Watching Depth
transd.reso  = 204.8;     % Amount of pixels that can be seen with transducer

if transd.d > minheighttissue % error message when transd.d is larger then the smallest height of tissue
   throw(MException([mfilename,':transdDepthIncorrect'],'transd Depth is to big (%d)', transd.d));
end

DistAB = 2.5;            % Distance between the tip transducer and the side transducers in mm

transd.Tiploc = [(widthx/2) minheighttissue 0 1];       % Begin location Tip transducer (2D, so Z=0)
transd.Aloc   = [(widthx/2) minheighttissue+DistAB 0 1];% Begin location A transducer
transd.Bloc   = [(widthx/2) minheighttissue+DistAB 0 1];% Begin location B transducer

transd.Tipview = transd.Tiploc;
transd.Tipview(2)=transd.Tipview(2)-transd.d;           % End point of sightline Tip transducer

transd.Aview = transd.Tipview;                          % Temporary sightline end point of A transducer
transd.Bview = transd.Tipview;                          % Temporary sightline end point of B transducer
```

Create Side Transducer configuration and orientation (Simulation2D_ Movie _Generator.m)
The catheter is made up of three transducers. The starting position and orientation of the tip and side transducer were determined in the previous section. The orientation of the side transducers are determined in this section, by making the orientation of the side transducers dependent to the tip transducer by using a rotation matrix. As result all the transducers will move as one object and will not move independently.

```
%% Create transducer configuration and orientation

angle_a = 0.5*pi;               % Define angle between Tip and A transducer
angle_b = 1.5*pi;               % Define angle between Tip and A transducer
origin  = transd.Tiploc(1:3);   % Define pivot point for rotation matrix
origin_min = origin*-1;         % Define negative pivot point for rotation matrix

% Define the end point of the sightline of the side transducers with a
% rotation matrix, with the Tip trasnsducer as reference point.
rotmatA  = makehgtform('translate',[0 DistAB 0],'zrotate',angle_a);
rotmatA1 = makehgtform('translate',origin);
rotmatA2 = makehgtform('translate',origin_min);
rotmatA  = rotmatA1*rotmatA*rotmatA2;
transd.Aview = (rotmatA*transd.Aview')';

rotmatB  = makehgtform('translate',[0 DistAB 0],'zrotate',angle_b);
rotmatB1 = makehgtform('translate',origin);
rotmatB2 = makehgtform('translate',origin_min);
rotmatB  = rotmatB1*rotmatB*rotmatB2;
transd.Bview = (rotmatB*transd.Bview')';
```

Create Sightline for Tip, A and B Transducer and Plot Sightline Per Iteration (Simulation2D_Movie_Generator.m)
This section will be completed for each iteration. At the beginning of each iteration, the growing factor of the tissue is calculated, represented by *factor_speckle*, which indicates the change in height of one tissue layer, cardiac motion respectively. This factor is used to resize the entire tissue matrix, *tissue.dat.*

The value *followtissue* is added to the translation in the Y-direction signal, with as result that the catheter would always move as much in Y-direction as the tissue does, which makes it impossible that the catheter will be placed into the tissue.

A rotation matrix is calculated based on the catheter motion signals for t=i. Hereby is the tip transducer used as pivot point. Because all the transducers are linked to each other, one rotation matrix is used for all the transducers. As a consequence, all the transducers will move as one object.

Depending on the cardiac motion and catheter motion, the sightlines of all the transducers are calculated by calling the functions GetTransViewTip, GetTransViewA and GetTransViewB. How these sightlines are performed will be discussed later.

The output per iteration of the GetTransView-functions is actually one array of reflection coefficients per transducer, comparing to an A-mode. Per iteration this array is stored in the pre-allocated matrices MmodeTip, MmodeA and MmodeB. These matrices are all plotted. This whole process is repeated for each iteration. The plots are updated when a new iteration is added, which results in a 'Movie' of the different sightlines over time.

In the upper left corner of the simulation the changes in the entire tissue are plotted. Also the catheter orientation is plotted per iteration. In order to let the catheter move as one object, all the transducers parameters be linked to each other, which makes it impossible to moves these objects separately.

```
%% Create Mmode for Tip, A and B transducer

tAll = tic;                             % record the time it should take to plot everything
dtArray = zeros(1,length(tranY));       % store the time of one loop, so you could compare the differences over
time

if Movie
    answer =input('Name of videofile: ','s');
    writerObj = VideoWriter(answer);
    open(writerObj);
end

for i = 1:N;
    height = tissue.height(i);          % Select the height of the layer for time=i

    % Calculate the growing factor depending on cardiac motion
    factor_speckle = height/minheightlayer;

    % Recalculate the composition of the deformed tissue
    tissue.plot  = imresize(tissue.dat, [resoy*factor_speckle resox],'nearest');
    tissue.plot  = tissue.plot(1:resoy, 1:resox);
    tissue.data  = tissue.plot;

    [rowzero,~]  = find(tissue.plot(:,1) == 0);                     % Find where tissue starts
    followtissue = (rowzero(1) * heighty / resoy)-transd.Tiploc(2); % Calculate the amount of mm that tissue
grows
    tranYY       = tranY(i)+followtissue;                           % Add those mm to translation in Y
direction

    % Define the catheter orientation dependent of the x translation, y translation and rotation around z-axis
    % With the origin used as pivot point
    rotmat  = makehgtform('translate',[tranX(i) tranYY 0],'zrotate',rotZ(i));
    rotmat1 = makehgtform('translate',origin);     % + Pivot point
    rotmat2 = makehgtform('translate',origin_min); % - Pivot point
    rotationmatrix = rotmat1*rotmat*rotmat2;

    % Call the GetTranViews functions to obtain the A-mode per iteration
    [AmodeTip, yTranTip] = getTranViewTip(transd, tissue, rotationmatrix);
    [AmodeA  , yTranA  ] = getTranViewA  (transd, tissue, rotationmatrix, resox, resoy, widthx, heighty);
    [AmodeB  , yTranB  ] = getTranViewB  (transd, tissue, rotationmatrix, resox, resoy, widthx, heighty);

    if i==1 % Preallocate array in the first iteration when final size is known.
        MmodeTip = zeros(length(AmodeTip), N);
        MmodeA = MmodeTip;
        MmodeB = MmodeTip;
    end

    % Store current A-modes of transducers in MmodeTip, MmodeA or MmodeB
    MmodeTip(:,i) = AmodeTip;
    MmodeA  (:,i) = AmodeA  ;
    MmodeB  (:,i) = AmodeB  ;
```

```
    if doPlot
        timerI = tic;

        if i==1
            figure('units','normalized','outerposition',[0 0 1 1],'Renderer','zbuffer'); subplot(5, 3, [1 4]);
                plot1=pcolor(tissue.x, tissue.y, tissue.plot);set(gca,'FontSize',12)
                shading interp; colormap('gray');hold on
                title('Tissue consisting of layers','Units', 'normalized', 'Position', [1 1],
'HorizontalAlignment', 'right','FontSize',12)

                Parent = hgtransform;

                catheter = hggroup();
                tT =
line([transd.Tiploc(1),transd.Tipview(1)],[transd.Tiploc(2),transd.Tipview(2)],[transd.Tiploc(3),
transd.Tipview(3)],'Color', 'r','LineWidth',3, 'Parent', catheter);
                tA = line([transd.Aloc(1),transd.Aview(1)],    [transd.Aloc(2),transd.Aview(2)],
[transd.Aloc(3), transd.Aview(3)],    'Color', 'b','LineWidth',3, 'Parent', catheter);
                tB = line([transd.Bloc(1),transd.Bview(1)],    [transd.Bloc(2),transd.Bview(2)],
[transd.Bloc(3), transd.Bview(3)],    'Color', 'm','LineWidth',3, 'Parent', catheter);
                set(catheter,'Parent',Parent);hold on;
                axis equal; ylim ([0 widthx]);
                xlabel('Width(mm)','Units', 'normalized', 'Position', [0.95 -0.04], 'HorizontalAlignment',
'right','FontSize',12);
                ylabel('Thickness(mm)')

                plotstart=plot(transd.Tiploc(1),transd.Tiploc(2), 'ro','MarkerSize',6);hold on;% Starting point
        else
                set(plot1,'CData',tissue.plot);
                set(Parent,'Matrix',rotationmatrix)
        end


        if i==1
           % Plot cardiac motion signal
           subplot(5, 3, 6);
                plot7b=plot(t, tissue.height); set(gca,'FontSize',12)
                hold on
                title('Comppression of tissue','FontSize',12)
                xlabel('Time(s)','FontSize',12)
                ylabel('Thickness layer (mm)','FontSize',12)
                plot8b=plot(t(i),tissue.height(i),'r.','MarkerSize',20);
        else
                set(plot8b,'XData',t(i),'YData',tissue.height(i));
        end

        if i==1
           % Plot translation in Y direction
           subplot(5, 3, 3);
                plot7=plot(t, tranY);set(gca,'FontSize',12)
                hold on
                title('Catheter motion in y direction','FontSize',12)
                xlabel('Time(s)','FontSize',12)
                ylabel('Y-displacement (mm)','FontSize',12)
                plot8=plot(t(i),tranY(i),'r.','MarkerSize',20);
        else
                set(plot8,'XData',t(i),'YData',tranY(i));
        end

        if i==1
           % plot translation in X direction
           subplot(5, 3, 2)
                plot9 = plot(t, tranX);set(gca,'FontSize',12)
                hold on
                title('Catheter motion in x direction','FontSize',12)
                xlabel('Time(s)','FontSize',12)
                ylabel('X-displacement (mm)','FontSize',12)
                plot9 = plot(t(i),tranX(i),'r.','MarkerSize',20);
        else
                set(plot9,'XData',t(i),'YData',tranX(i));
        end
```

```
        if i==1
           % plot rotation around Z-axis
           subplot(5, 3, 5);
                plot11=plot(t, rotZ);set(gca,'FontSize',12)
                hold on
                title('Catheter rotational motion','FontSize',12)
                xlabel('Time(s)','FontSize',12)
                ylabel('Angle(rad)','FontSize',12)
                plot10=plot(t(i),rotZ(i),'r.','MarkerSize',20);
        else
                set(plot10,'XData',t(i),'YData',rotZ(i));
        end

        if i==1
            subplot(5,3,[7 8 9]);
            % yTran - max(yTran) because otherwise the images are vertically flipped
                plot11=pcolor(t, (yTranTip-max(yTranTip)), MmodeTip);set(gca,'FontSize',12)
                shading interp; colormap('gray');hold on
                Tran=0*t;
                plot12=plot(t(i), Tran(i), 'r.','MarkerSize',30);
                title('M-Mode Tip-transducer','Units', 'normalized', 'Position', [0 1], 'HorizontalAlignment',
'left','FontSize',12);
                xlabel('Time(s)','Units', 'normalized', 'Position', [0.99 -0.1], 'HorizontalAlignment',
'right','FontSize',12);
                ylabel('Depth(mm)','FontSize',12);
        else
                set(plot11,'CData',MmodeTip);
                set(plot12, 'XData',t(i));
        end

        if i==1
            subplot(5,3,[10 11 12]);
            % yTran - max(yTran) because otherwise the images are vertically flipped
                plot13=pcolor(t, (yTranA-max(yTranA)), MmodeA);set(gca,'FontSize',12)
                shading interp; colormap('gray');hold on
                Tran=0*t;
                plot14=plot(t(i), Tran(i), 'b.','MarkerSize',30);
                title('M-Mode A-transducer ','Units', 'normalized', 'Position', [0 1], 'HorizontalAlignment',
'left','FontSize',12);
                xlabel('Time(s)','Units', 'normalized', 'Position', [0.99 -0.1], 'HorizontalAlignment',
'right','FontSize',12);
                ylabel('Depth(mm)','FontSize',12);
        else
                set(plot13,'CData',MmodeA);
                set(plot14, 'XData',t(i));
        end

        if i==1
            subplot(5,3,[13 14 15]);
            % yTran - max(yTran) because otherwise the images are vertically flipped
                plot15=pcolor(t, (yTranB-max(yTranB)), MmodeB);set(gca,'FontSize',12)
                shading interp; colormap('gray');hold on
                Tran=0*t;
                plot16=plot(t(i), Tran(i), 'm.','MarkerSize',30);
                title('M-Mode B transducer ','Units', 'normalized', 'Position', [0 1], 'HorizontalAlignment',
'left','FontSize',12)
                xlabel('Time(s)','Units', 'normalized', 'Position', [0.99 -0.1], 'HorizontalAlignment',
'right','FontSize',12);
                ylabel('Depth(mm)','FontSize',12)
        else
                set(plot15,'CData',MmodeB);
                set(plot16, 'XData',t(i));
        end

        if Simulate
        drawnow % force all plotting stuff to be actually drawn.
        end

        if Movie
        subplotframe=gcf;
        frame = getframe(subplotframe);
        writeVideo(writerObj,frame);
        end

        dtArray(i) = toc(timerI);
%         fprintf(1,'... i=%3d: time to plot was %f seconds;\n', i, dtArray(i));
    end
end
```

Call Function GetTransViewTip, GetTransViewA, GetTransViewB (getTranViewTip.m getTranViewA.m getTranViewB.m)

The functions GetTransView determine the sightlines of the observed tissue for t=i. Therefore, two coordinates are determined with the previous determined rotation matrix. These coordinates are the begin-position and end-position of a sightline, see Figure 2. The intermediate coordinates between the begin and end position are determined based on the set transducer resolution. Subsequently, this series of coordinates, are used to find the corresponding reflection coefficients in the already deformed tissue data, which are later on plotted as the sightline for t=i.

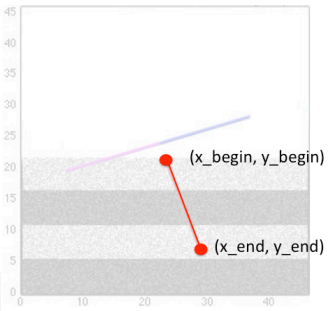

Figure 2 Coordinates sightline

```
function [AmodeTip, yTranTip] = getTranViewTip(transd, tissue, rotationmatrix)

transd.Tiploc  = rotationmatrix * transd.Tiploc';

% Calculate the x-index in the tissue where the transd start (you can do this by substract
% the x-transd-coordinate from the tissue.x values. Where this value is zero it is the same position.
[~, xi_begin]    = min(abs(tissue.x-transd.Tiploc(1)));
% Calculate the y-index in the tissue where the transd start
[~, yi_begin]    = min(abs(tissue.y-transd.Tiploc(2)));

transd.Tipview = rotationmatrix * transd.Tipview';

% Calculate the x-index in the tissue where the transd ends (you can do this by substract
% the x-transd-coordinate from the tissue.x values. Where this value is zero it is the same position.
[~, xi_end]    = min(abs(tissue.x-transd.Tipview(1)));
% Calculate the y-index in the tissue where the transd ends
[~, yi_end]    = min(abs(tissue.y-transd.Tipview(2)));

j_index=round(linspace(xi_begin, xi_end, transd.reso));
i_index=round(linspace(yi_begin, yi_end, transd.reso));

% Define M-mode by using the data from the tissue but now with y-begin with a step -1 to y_end (depending
on the depth)
AmodeTip = tissue.data( sub2ind(size(tissue.data), i_index, j_index) );

AmodeTip   = AmodeTip(end:-1:1); % Flips the image so that you get the view from the top to the bottom
yTranTip   = linspace(0, transd.d, transd.reso);% The y-axis for the Mmode plot (0 : steps : transd.d)
```

Summary in Workflow

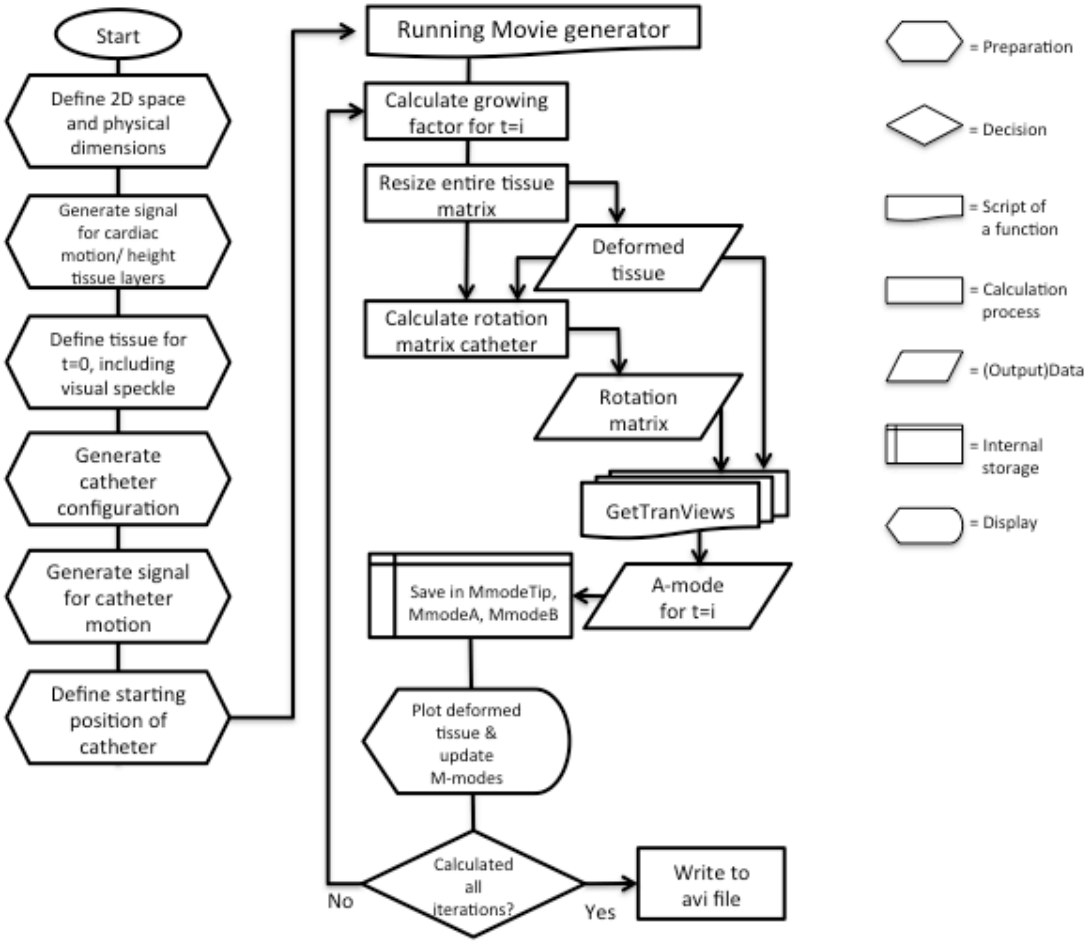

Main difference Movie generator and RF generator

First have to be mentioned that the Movie generator only calculates the so-called simulates sightline, while the RF generator also multiplies this sightline with a carrier wave signal, with an RF data as result, see Figure 3.

The main difference in calculation of this sightline between the Movie generator and RF generator is that in the Movie generator the entire tissue is resized as a result of the cardiac motion signal and the sightline is already determined with the correct elongation, while in the RF data generator the observed sightline is taken from undeformed tissue, and only this observed sightline is resized as result of the cardiac motion signal. Obviously, it saves a lot of time to only resize one column instead of 6000 columns in case of the Movie data generator.

Another main difference is that the acquired sightlines/A-modes are plotted in the Movie generator per iteration, while in the RF data generator all the data is plotted after running all the iterations. That means that only in the Movie generator the entire moving tissue and the moving catheter can be observed over time in the upper left corner. In the RF data generator only the begin position of the entire tissue and catheter is shown in the upper left corner.

Moreover, the resolution and sample frequency of the Movie generator can be decreased with a factor ten, without losing visible result. For the RF data generator a larger sample frequency and resolution is required to be able to use the data as representative US data, which for example can be used to measure velocities in the tissue.

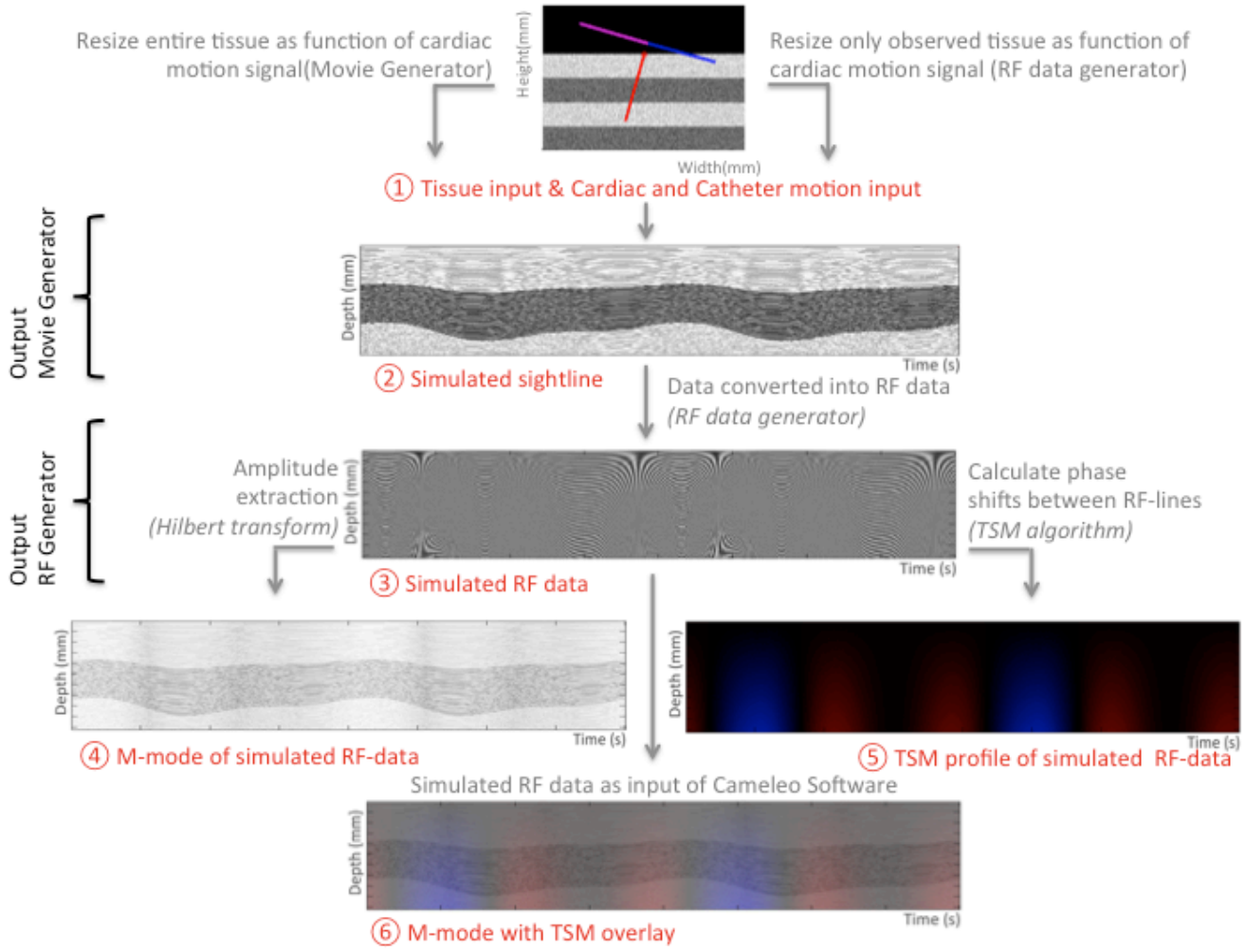

Figure 3 Overview of output of Movie generator and RF data generator

User Manual RF data generator

Introduction

The aim of the RF data generator is to generate representative radiofrequency ultrasound data of contracting 'cardiac' tissue that is acquired with a moving catheter. The catheter is equipped with multiple single element transducers that all result in a single data matrix. In this manual the script of this simulation will be explained in detail. A short explanation is given about every section of the script. The green coloured comments in the script itself give even more specific information per command. Moreover, the simulated RF data can be converted to an M-mode image by means of envelope extraction. The RF data can also be directly used to calculate a velocity profile of the observed tissue with the TSM algorithm, which is also developed by Philips Research. Finally, the data can be converted to a format that can serve as input for the Cameleo Software, which is developed and manufactured by Philips Research. In the end of this manual an additional explanation will be given about the calculations that need to be done for these purposes.

Output RF data generator

The motion input signals of the cardiac motion and catheter motion are displayed in the upper right corner. The observed moving tissue and moving catheter can be seen in the upper left corner. The red line represents the sightline of the tip transducer. The RF data is plotted in the three plots at the bottom of Figure 1. As can be noticed the first plot displays a red dot at the top of the plot, which symbolises the tip transducer. The blue and purple lines represent the sightlines of the side transducers. The corresponding plots are indicated with a same coloured dot.

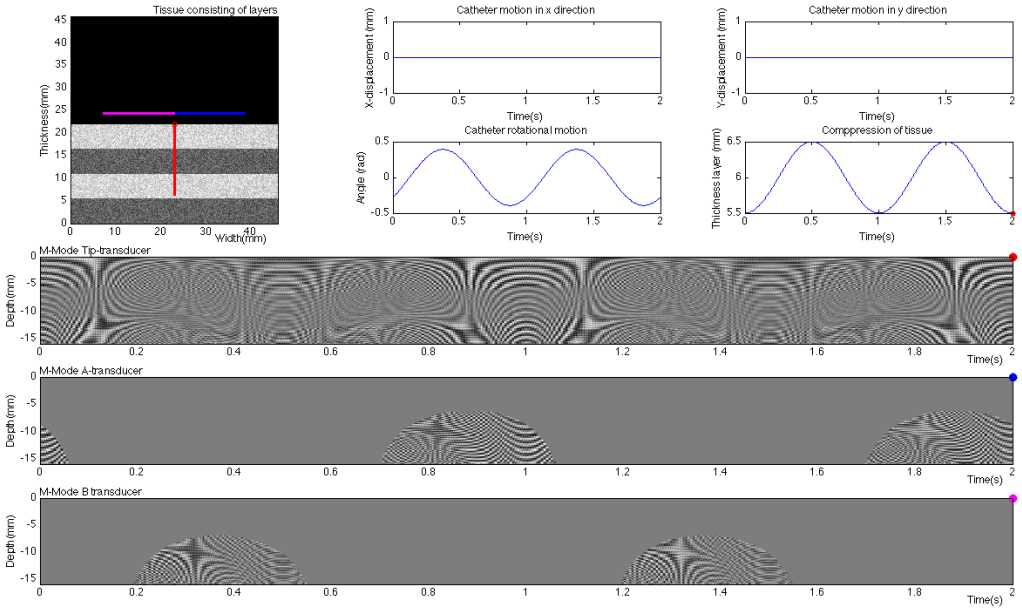

Figure 1 Plotted Output RF data Generator

Input RF data generator

All the parameters can be adjusted as desired. The parameters that are most interesting for adjustment are the following:
- The cardiac tissue consists of an adjustable amount of layers, which differ from each other by a difference in reflection coefficient.
- The cardiac contracting motion can be set with any signal. The signals that are implemented in current script are (multi) sinusoids and an ECG signal.
- The composition and orientation of the transducers in the catheter can be adapted. Currently, in this script the composition and orientation of the catheter are set based on the dimensions of the MUVIC 444-H catheter, developed and manufactured by Philips research.
- The catheter motion is determined by three signals: translation in X-direction, translation in Y direction and rotation around the Z-axis. These signals can be set with any signal. The signals that are implemented in current script are (multi) sinusoids and an ECG signal.

Implementation in Matlab

Generate Workspace and Physical Size (Simulation2D_RFdata_Generator.m)

First, an empty workspace is generated. This operation can be seen as pre-allocation of data. The resolution of the physical size is adjustable, but in this case based on the MUVIC 444-H catheter that has a ratio of 2048 data points per 15.8 mm. Furthermore, in this section some features of the simulation can be activated by means of the command 'true' or 'false'.

```
%% Generate workspace and physical size

resox   = 6000; % number of points in which [0,widthx ] is discretized
resoy   = 6000; % number of points in which [0,heighty] is discretized
widthx  = round(resox * 15.8 / 2048); % real width  of the observed tissue part
heighty = round(resoy * 15.8 / 2048); % real height of the observed tissue part

x       = linspace(0, widthx , resox); % Create the width of space
y       = linspace(0, heighty, resoy); % Create the height of space
[xg,yg] = meshgrid(x,y);               % Derive handy arrays for computing

doPlot   = true; % indicates whether plotting is done or not
ECGtissue= false;% indicates whether a ecg signal is used as contraction signal
ECGtransd= false;% indicates whether a ecg signal is used as wiggling signal
Speckle  = true; % indicates whether speckle will be added to the tissue layers
Carrier  = true; % indicates whether the result will be realistic US RF data

% At this point the tissue of physical size widhtx x heighty is represented by (resox-1) by (resoy-1) cells.
```

Set Time and Sample Frequency (Simulation2D_RFdata_Generator.m)

In this section the simulation time and sample frequency parameters are defined, which determine automatically the amount of iterations that each simulation run should complete. Real ultrasound data generated with the MUVIC 444-H catheter is normally acquired with a sample frequency of 2000Hz. Furthermore, a sample frequency of at least 2000Hz is required to calculate a velocity profile from the RF-data.

```
%% Set time and sample frequency

T  = 2;                % Observation time in seconds
fs = 2000;             % Sampling frequency
N  = T*fs;             % Same as T/dt, represents total amount of time samples
t  = linspace (0,T,N); % Time axis
```

Generate Signal for Tissue Compression (Simulation2D_RFdata_Generator.m)

In this section the input motion signal for 'cardiac' tissue compression is defined. The tissue consists of several tissue layers, determined in the next section. This signal determines the height of one tissue layer. A simple sinusoid can be extended by using the parameters *tissue.fmulti* and *tissue.amulti*, which results in a multisine. Another option is to make use of the *ECGtissue*, which generates an ECG signal as tissue motion signal. In that case the function *complete_cardiac* is called. This function has been downloaded from the internet and a manual can be found in the *Philips_Bente_de_Lat/3. Matlab Scripts/4. Remaining/1. ECG/ECGmanual*.

```
%% Generate signal for tissue compression

tissue.f=1;            % Define frequency of compression
tissue.a=0.5;          % Define the difference in height
tissue.equil=6;        % Define equillibrium height of the tissue layers
tissue.height=cos(tissue.f*2*pi*t-pi)*tissue.a+tissue.equil;          % Define final signal for compression

tissue.fmulti=0;       % Frequency for introducing irregularities in signal
tissue.amulti=0;       % Determine how much the multisingle should dominate
tissue.height=tissue.height+(sin(tissue.fmulti*2*pi*t)*tissue.amulti); % Add multisin to compression signal
figure;plot(t,tissue.height);

if ECGtissue
    multiply=10;                                % Determine a multiplication factor
    delaytis=0.7;
    [ecg]=complete_cardiac(t+delaytis,multiply); % Call function complete
    tissue.height=ecg;                          % Put ECG signal in theta
    tissue.height=tissue.height/30+tissue.equil; % A alternating motion is achieving by
                                                substracting a value
    figure(1);plot(t,tissue.height); hold on     % Plot the created ECG signal
end
```

Define Tissue Layers and Tissue Height (Simulation2D_RFdata_Generator.m)
In this section the composition of the cardiac tissue is defined. During an US acquisition, the reflection coefficient is determined by the differences in acoustic impedance between tissue structures. In a real US image, these differences in reflection coefficients are displayed with different shades of grey. For this simulation model is assumed that the acoustic impedance is equal in the entire tissue, the reflection coefficients are determined, independent of any physical properties. The value 0 relates to no reflection and the largest value relates to maximal reflection, visualised as respectively black and white in the M-mode image

The number of tissue layers is determined by using a vector, with the vector length defining the number of layers. The value of every layer represents the reflection coefficient. In this case the choice have been made to take reflection coefficients in the range of 16-bit, since the data need to be converted to 16-bit data, to make it compatible with the Cameleo software, but the values can be set with any value.

```
%% Define amount of tissue layers and total tissue height

tissue.layers  = [18000 30000 18000 30000];% Layers will get these values
minheightlayer = min(tissue.height);       % Determine minimal height of one tissue layer
minheighttissue= min(tissue.height)*length(tissue.layers); % Determine minimal total height of tissue
maxheightlayer = max(tissue.height);

tissue.x       = x; % Save the width  (indexes) of space as width of tissue
tissue.y       = y; % Save the height (indexes) of space as height of tissue
```

Generate Tissue (Simulation2D_RFdata_Generator.m)
In this section the cardiac tissue was generated in the pre-allocated empty workspace on the basis of the previously defined minimal tissue height of one layer.

```
%% Generate a tissue

% Calculate the layers for one column (so 1D) and then copy this layer to every column (to save memory)
yg1D = yg(:,1);                  % Determine size prealocation
dat1D = zeros(size(yg1D));       % Prealocate data

for i = 1:length(tissue.layers)
    yLo = (i-1)*minheightlayer ; % Define the lower border for the layer (so the height of the previous layer)
    yHi =  i   *minheightlayer ; % Define the upper border for the layer (so the height of the current layer)
    dat1D( yg1D >= yLo & yg1D < yHi ) = tissue.layers(i); % Give predefined value to tissue layer
end

tissue.data = dat1D * ones([1,resox]); % Save the layers for every column in tissue.data
```

Generate Speckle Pattern in Tissue (Simulation2D_RFdata_Generator.m)
A characteristic appearance of US is that structures in a tissue do not seem to be totally equal, but a so-called speckle pattern can be recognized. A speckle pattern occurs because of little deviations in the reflection coefficients within a tissue. This appearance was also added to the simulation model by subtracting randomized smaller values from the main reflection coefficient of one tissue layer. This results in different reflection coefficients in the entire tissue with as result a more realistic M-mode image. These speckle patterns have just been added for visual purposes, but are not in relation with any physical properties of the tissue. This option can be activated or de-activated. The size of the speckles can be adjusted according to the desired effect of the speckle.

```
%% Generate a speckle pattern in tissue

if Speckle

Specklesize=50;
Noisecolumn=rand(resoy/Specklesize,resox/Specklesize)*10000; % Define a random speckle pattern
Noise=kron(Noisecolumn,ones(Specklesize,Specklesize));       % Multiplies the Noisecolumn in x and y direction

% Only add speckle pattern to the tissue, not to the 'air'. So, first determine till which row this is the
case. Then add the speckle pattern to the tissue.data.
[row,~] = find(tissue.data(:,1) == 0);
tissue.data((row(1)-1):-1:1,:) = tissue.data((row(1)-1):-1:1,:) - abs(Noise(1:(row(1)-1),:));

end
```

Generate Signal for Catheter Motion (Simulation2D_RFdata_Generator.m)
In this section the catheter motion signals are determined in three directions: translation in X-direction, translation in Y-direction and rotation around the Z-axis. First, the frequency and amplitude of these signals are determined. These signals could be generated with a simple sine function or a more complicated multi-sine function by using the *transd.fmulti* and *transd.amulti* parameters. Another option is to use an ECG-signal.

```
%% Generate signal for catheter motion

transd.fx    = 0;        % Frequency of moving catheter in x direction
transd.fy    = 0;        % Frequency of moving catheter in y direction
transd.fsweep= 1;        % Frequency of wiggling catheter
transd.fmulti= 0;        % Frequency for irregularities (by 0 freq no irregularities)

transd.ax    = 0;        % Amplitude of moving catheter in x direction
transd.ay    = 0;        % Amplitude of moving catheter in y direction
transd.asweep= 0.125*pi; % Amplitude of wiggling catheter in pi
transd.amulti= 0;        % Determine how much the irregularities should dominate

tranX = cos(transd.fx*2*pi*t);                  % Create cosine movement of catheter discretized over N samples
tranX = tranX+(sin(transd.fmulti*2*pi*t)*transd.fmulti);% Influence the periodic behaviour
tranX = tranX * transd.ax;                      % Adapt amplitude of transd

tranY = cos(transd.fy*2*pi*t);                  % Create cosine movement of transd discretized over N samples
tranY = tranY+(sin(transd.fmulti*2*pi*t)*transd.fmulti);% Influence the periodic behaviour
tranY = tranY * transd.ay + transd.ay;          % Adapt amplitude of transd and begin position

phaseshift = 0;                                 % Phaseshift of catheter motion in relation to cardiac motion
rotZ = sin(transd.fsweep*2*pi*t-phaseshift*pi); % Create cosine movement of transd discretized over N samples
rotZ = rotZ+(sin(transd.fmulti*2*pi*t)*transd.amulti);  % Influence the periodic behaviour
rotZ = rotZ * transd.asweep;                    % Adapt amplitude of transd
%rotZ(:)= -transd.asweep;                       % Make active if a constant angle is desired

if ECGtransd
    multiply=10;                                % Determine a multiplication factor
    delaycat=0.6;
    [ecg]=complete_catheter(t+delaycat,multiply);% Call function complete to generate the ECG signal
    rotZ=ecg;                                   % Put ECG signal in catheter rotation signal
    rotZ=(rotZ/30)-0.4;                         % A wiggling motion is achieving by substracting a value
    figure(1);plot(t,rotZ,'r');                 % Plot the created ECG signal
end
```

Transducer Settings and Start Location (Simulation2D_RFdata_Generator.m)
In this sections the orientation parameters of the transducers are defined. The resolution and watching depth of the transducers are in this case based on the MUVIC 444-H catheter. When the watching depth is larger than the minimal tissue thickness, an error message will be given. Furthermore, the distance from the side transducers in relation to tip transducer has been determined. This distance is used to determine the starting point of all the used transducers, which is dependent on the minimal tissue thickness, watching depth and the physical space. The parameters *transd.loc* represent the starting point of the transducer. The parameters *transd.view* determine in which direction the transducer is orientated and so actually represent the deepest point that can be seen with the transducer. At this point in the parameter settings, the side transducer have the same watching orientation as the tip transducer, in the next section the orientation of the side transducers will be set in relation to the tip transducer.

```
%% Transducer settings and start location
transd.d     = 15.8;     % Watching Depth
transd.reso  = 2048;     % Amount of pixels that can be seen with transducer

if transd.d > minheighttissue % error message when transd.d is larger then the smallest height of tissue
   throw(MException([mfilename,':transdDepthIncorrect'],'transd Depth is to big (%d)', transd.d));
end

DistAB = 2.5;            % Distance between the tip transducer and the side transducers in mm

transd.Tiploc = [(widthx/2) minheighttissue 0 1];       % Begin location Tip transducer (2D, so Z=0)
transd.Aloc   = [(widthx/2) minheighttissue+DistAB 0 1];% Begin location A transducer
transd.Bloc   = [(widthx/2) minheighttissue+DistAB 0 1];% Begin location B transducer

transd.Tipview = transd.Tiploc;
transd.Tipview(2)=transd.Tipview(2)-transd.d;           % End point of sightline Tip transducer

transd.Aview = transd.Tipview;                          % Temporary sightline end point of A transducer
transd.Bview = transd.Tipview;                          % Temporary sightline end point of B transducer
```

Create Side Transducer configuration and orientation (Simulation2D_RFdata_Generator.m)
The catheter is made up of three transducers. The starting position and orientation of the tip and side transducer were determined in the previous section. The orientation of the side transducers are determined in this section, by making the orientation of the side transducers dependent to the tip transducer by using a rotation matrix. As result all the transducers will move as one object and will not move independently.

```
%% Create transducer configuration and orientation

angle_a = 0.5*pi;               % Define angle between Tip and A transducer
angle_b = 1.5*pi;               % Define angle between Tip and A transducer
origin  = transd.Tiploc(1:3);   % Define pivot point for rotation matrix
origin_min = origin*-1;         % Define negative pivot point for rotation matrix

% Define the end point of the sightline of the side transducers with a
% rotation matrix, with the Tip trasnsducer as reference point.
rotmatA  = makehgtform('translate',[0 DistAB 0],'zrotate',angle_a);
rotmatA1 = makehgtform('translate',origin);
rotmatA2 = makehgtform('translate',origin_min);
rotmatA  = rotmatA1*rotmatA*rotmatA2;
transd.Aview = (rotmatA*transd.Aview')';

rotmatB  = makehgtform('translate',[0 DistAB 0],'zrotate',angle_b);
rotmatB1 = makehgtform('translate',origin);
rotmatB2 = makehgtform('translate',origin_min);
rotmatB  = rotmatB1*rotmatB*rotmatB2;
transd.Bview = (rotmatB*transd.Bview')';
```

Define Carrierwave Parameters (Simulation2D_RFdata_Generator.m)
The real ultrasound MUVIC 444-H catheter operates with a carrier frequency of 30MHz and a sampling frequency of 100MHz. These settings are set in this section and used later on in the functions *GetTranView*.

```
%% Define carrierwave parameters

fs_carrier = 100e6;      % Sample frequency Carrier wave
fcarrier   =  30e6;      % Frequency Carrier wave
```

Create RF data for Tip, A and B transducer (Simulation2D_RFdata_Generator.m)
This section will be completed for each iteration. At the beginning of each iteration, the growing factor of the tissue is calculated. A distinction can be made between the change in the tissue height, *factor_speckle,* and the growing factor for the carrier wave, *factor_carrier*. The difference is that the growing factor for the carrier wave is also dependent on the catheter angle, while *factor_speckle* only calculates how the speckle pattern should grow in Y-direction. When the catheter angle becomes larger, it seems that the tissue becomes thicker. This principle is used to calculate the *factor_carrier.* The imaginary increase is assumed in this case as an increase in thickness. Later on will become clear what effect this will have on the simulated US signal.

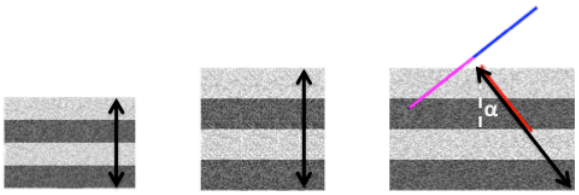

$$\text{Factor\_speckle} = \frac{\text{Height at } t \text{ (only dependent on cardiac motion)}}{\text{Minimal height}}$$

$$\text{Factor\_carrier} = \frac{\text{Height at } t \text{ (including catheter motion)}}{\text{Minimal height}}$$

Then, the function *tissueplot* is called, which is used to follow the tissue growth over time. (If you want to plot every iteration of the RF-data over time, than the tissueplot can be used in the upper left corner in the simulation as representation of the moving

tissue). The value *followtissue* is added to the translation in the Y-direction signal, with as result that the catheter would always move as much in Y-direction as the tissue does, which makes it impossible that the catheter will be placed into the tissue.

A rotation matrix is calculated based on the catheter motion signals for t=i. The tip transducer is then used as pivot point. Because all the transducers are linked to each other, one rotation matrix is used for all the transducers. As a consequence, all the transducers will move as one object.

Depending on the cardiac motion and catheter motion, the A-modes of all the transducers are calculated by calling the functions GetTransViewTip, GetTransViewA and GetTransViewB. How these A-modes are performed will be discussed later, based on the scripts of these functions.

The output per iteration of the GetTransView-functions is actually one A-mode per transducer. Per iteration this A-mode is stored in the pre-allocated matrices MmodeTip, MmodeA and MmodeB. And the whole process is repeated for iteration at t=i+1.

```
%% Create RFdata for Tip, A and B transducer

tAll = tic;                        % record the time it should take to plot everything
dtArray = zeros(1,length(tranY)); % store the time of one loop, so you could compare the differences over time

for i = 1:N;
    height = tissue.height(i);    % Select the height of the layer for time=i

    % Calculate the growing factor depending on cardiac and catheter motion
    factor_carrier = (height/abs(cos(rotZ(i))))/minheightlayer;

    % Calculate the growing factor depending on cardiac motion
    factor_speckle = height/minheightlayer;
    factor_speckle = round(factor_speckle*1000)/1000;
    [Nom, Denom]=rat(factor_speckle);

    % Calculate in a simplified way the new size of the tissue by calling tissueplot
    tissue = tissueplot(tissue, yg, height, resox);

    [rowzero,~]  = find(tissue.plot(:,1) == 0);                    % Find where tissue starts
    followtissue = (rowzero(1) * heighty / resoy)-transd.Tiploc(2); % Calculate the amount that tissue grows
    tranYY       = tranY(i)+followtissue;                          % Add those mm to Y direction

    % Define the catheter orientation dependent of the x translation, y translation and rotation around z-axis
    % With the origin used as pivot point
    rotmat  = makehgtform('translate',[tranX(i) tranYY 0],'zrotate',rotZ(i));
    rotmat1 = makehgtform('translate',origin);     % + Pivot point
    rotmat2 = makehgtform('translate',origin_min); % - Pivot point
    rotationmatrix = rotmat1*rotmat*rotmat2;

    % Call the GetTranViews functions to obtain the A-mode per iteration
    [AmodeTip, yTranTip] = getTranViewTip(...
    [AmodeA  , yTranA  ] = getTranViewA  (...
    [AmodeB  , yTranB  ] = getTranViewB  (...

    if i==1 % Preallocate array in the first iteration when final size is known.
        MmodeTip = zeros(length(AmodeTip), N);
        MmodeA = MmodeTip;
        MmodeB = MmodeTip;
    end

    % Store current A-modes of transducers in AmodeTip, AmodeA or AmodeB
    MmodeTip(:,i) = AmodeTip;
    MmodeA  (:,i) = AmodeA  ;
    MmodeB  (:,i) = AmodeB  ;
```

Call Function Tissueplot (tissueplot.m)
This function calculates the composition of the tissue based on the height per tissue layer at t=i. To make this function faster, the calculation of the composition has been done for just one column of the tissue and is then multiplied in relation to the width of the tissue.

```
function tissue = tissueplot(tissue, yg, height, resox)

% Calculate the layers for one column (so 1D) and then copy this layer configuration to every
column (to save memory)

    yg1D = yg(:,1);
    dat1D = zeros(size(yg1D));

    for i = 1:length(tissue.layers)
        yLo = (i-1)*height ; % Define the lower border for the layer
        yHi =  i   *height ; % Define the upper border for the layer
       dat1D( yg1D >= yLo & yg1D < yHi ) = tissue.layers(i);
    end
    tissue.plot = dat1D * ones([1,resox]);  % Save the layers for every column in tissue.plot
end
```

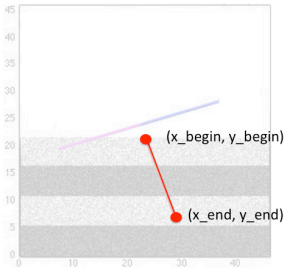

Figure 2 Coordinates sightline

Call Function GetTransViewTip (getTranViewTip.m)
The function GetTransViewTip determines the A-mode of the observed tissue for t=i. First, the sightline of the tip transducer is determined. Therefore, two coordinates are determined with the previous determined rotation matrix. These coordinates are the begin-position and end-position of the sightline of the tip transducer, see Figure 2. The tissue data that is used is the data that is still undeformed (to make a faster calculation). Since the undeformed tissue is used the parameter *followtissue* needs to be subtracted again, do be sure that we start at the top of the tissue. The intermediate coordinates between the begin and end position are determined based on the set transducer resolution. Subsequently, this series of coordinates, are used to find the corresponding reflection coefficients in the tissue data. Next, the observed A-mode is resized with *factor_speckle*, which is here been expressed in *Nom* and *Denom*. After resizing the entire array has become larger than *transd.reso,* which means that the observed tissue is longer than the actual possible observation depth. Therefore, only the data that can be seen with the set depth is used, the rest of the data is excluded. At this point a sightline has been created of the observed deformed tissue.

To make these data comparable to real US data, the data is multiplied with a carrier wave signal. This carrier wave signal is modelled with multiple Gaussian-modulated sine wave pulses. The center frequency and sample frequency is determined with the parameters *fs_carrier* and *fcarrier.* The distance between these pulses was increased depending on the growing factor of the cardiac motion or catheter motion. This factor is the *factor_carrier.* The change in distance between the Gaussian pulses is fully dependent of cardiac and catheter motion, shown in Figure 3 and as discussed in section *'Create RF data for Tip, A and B transducer'*. The change of the distance between these pulses causes a phaseshift of the pulses if you observe the A-modes over time. These phase shifts can be used to derive velocities in the tissue. This generated carrier wave signal is multiplied with the sightline of the observed tissue, *AmodeTip*, which will make the reflection coefficient serve as the amplitude of this signal. Over time these amplitudes move in a same way as the distance between the pulses, so they are completely in relation to each other.

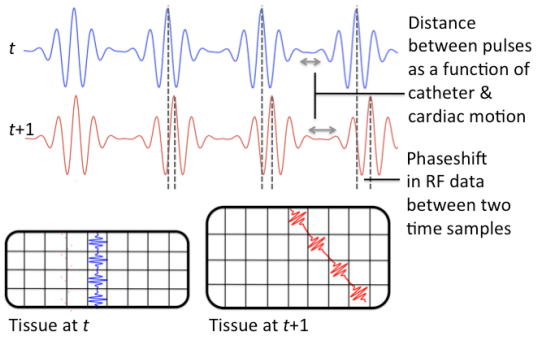

Figure 3 Schematic representation of carrier wave signal of two time samples that differ as a function of cardiac and catheter motion

```
function [AmodeTip, yTranTip] = getTranViewTip(transd, tissue, rotationmatrix, followtissue, Nom, Denom,
Carrier, factor_carrier, fs_carrier, fcarrier)

transd.Tiploc  = rotationmatrix * transd.Tiploc';
transd.Tiploc(2)=transd.Tiploc(2)-followtissue; % Place y_begin at begin of undeformed tissue

% Calculate the x-index in the tissue where the transd start (you can do this by substract
% the x-transd-coordinate from the tissue.x values. Where this value is zero it is the same position.
[~, xi_begin]    = min(abs(tissue.x-transd.Tiploc(1)));
% Calculate the y-index in the tissue where the transd start
[~, yi_begin]    = min(abs(tissue.y-transd.Tiploc(2)));

transd.Tipview = rotationmatrix * transd.Tipview';
transd.Tipview(2)=transd.Tipview(2)-followtissue;

% Calculate the x-index in the tissue where the transd ends (you can do this by substract
% the x-transd-coordinate from the tissue.x values. Where this value is zero it is the same position.
[~, xi_end]    = min(abs(tissue.x-transd.Tipview(1)));
% Calculate the y-index in the tissue where the transd ends
[~, yi_end]    = min(abs(tissue.y-transd.Tipview(2)));

j_index=round(linspace(xi_begin, xi_end, transd.reso));
i_index=round(linspace(yi_begin, yi_end, transd.reso));

%Define M-mode by using the data from the tissue
AmodeTip = tissue.data( sub2ind(size(tissue.data), i_index, j_index) );
lengthAmode = length(AmodeTip);
% Resize the tissue according to the growing factor
AmodeTip=resample(AmodeTip,Nom,Denom,0);
% Give Amode original size of transd.reso
AmodeTip=AmodeTip(1:lengthAmode);

% Add carrier wave to signal
    if Carrier
        time=1:(lengthAmode-1);
        time=time/fs_carrier;

        t = 0 : 1/fs_carrier : time(end); % fs_carrier sample frequency, time(end) pulse train length
        d1=[0 : 1/ (10e6/factor_carrier) : 2.0470e-05]';%the pulse repetition freq and pulse train length
        length(d1);
        carriersignal = pulstran(t,d1,'gauspuls',fcarrier,0.3); % fcarrier signal freq, with 30% bandwith

        AmodeTip=AmodeTip.*carriersignal;
    end
AmodeTip = AmodeTip(end:-1:1);% Turn around the image so that you get the view from the top to the bottom
yTranTip = linspace(0, transd.d, transd.reso); % The y-axis for the Amode plot (0 : steps : transd.d)
```

Call Functions GetTransViewA and GetTransViewB (getTranViewA.m, getTranViewB.m)
The functions for the side transducers are comparable to the GetTranViewTip function of the tip transducer, but there is one main difference. The side transducers are placed with a distance of 2.5mm above the tip transducers, which results in the fact that the side transducers also observe 'air'. In the RF generator the observed tissue, the sightline, is resized according to *factor_speckle* after observation, because of faster calculation purposes. The disadvantage in this case is that you would also 'resize' the observed air, while only the tissue is contracting. For that reason for the side transducers is determined where the tissue starts and only that part of the sightline is resampled with the *factor_speckle*.

```
function [AmodeA, yTranA] = getTranViewA(transd, tissue, rotationmatrix, followtissue, Nom, Denom, Carrier,
factor_carrier, fs_carrier, fcarrier);

transd.Aloc  = rotationmatrix * transd.Aloc';
transd.Aloc(2)=transd.Aloc(2)-followtissue; % Place y_begin at begin of undeformed tissue

% Calculate the x-index in the tissue where the transd start (you can do this by substract
% the x-transd-coordinate from the tissue.x values. Where this value is zero it is the same position.
[~, xi_begin]    = min(abs(tissue.x-transd.Aloc(1)));
% Calculate the y-index in the tissue where the transd start
[~, yi_begin]    = min(abs(tissue.y-transd.Aloc(2)));

transd.Aview = rotationmatrix * transd.Aview';
transd.Aview(2)=transd.Aview(2)-followtissue;

% Calculate the x-index in the tissue where the transd ends (you can do this by substract
% the x-transd-coordinate from the tissue.x values. Where this value is zero it is the same position.
[~, xi_end]    = min(abs(tissue.x-transd.Aview(1)));
% Calculate the y-index in the tissue where the transd ends
[~, yi_end]    = min(abs(tissue.y-transd.Aview(2)));

j_index=round(linspace(xi_begin, xi_end, transd.reso));
i_index=round(linspace(yi_begin, yi_end, transd.reso));

% Define M-mode by using the data from the tissue
AmodeA = tissue.data( sub2ind(size(tissue.data), i_index, j_index) );
lengthAmode = length(AmodeA);

    if isempty(AmodeA(find(AmodeA(:)~=0)));
        % if you only see 'air', which has value 0, then no action is needed
    else
        %Resize only the tissue according to the growing factor, so do not resample the 'air',which has value 0
        AmodeA=[AmodeA(find(AmodeA(:)==0)) resample(AmodeA(find(AmodeA(:)~=0)),Nom,Denom,0)];
    end

% Give Amode original size of transd.reso
AmodeA=AmodeA(1:lengthAmode);

% Add carrier wave to signal
    if Carrier
        time=1:(lengthAmode-1);
        time=time/fs_carrier;

        t = 0 : 1/fs_carrier : time(end); % fs_carrier sample frequency, time(end) pulse train length
        d1 = [0 : 1/ (10e6 * factor_carrier) : 2.0470e-05]'; % the pulse repetition freq and pulse train length
        length(d1);
        carriersignal = pulstran(t,d1,'gauspuls',fcarrier,0.3); % fcarrier signal freq, with 30% bandwith

        AmodeA=AmodeA.*carriersignal;
    end

AmodeA   = AmodeA(end:-1:1);              % Flip the image so that you get the view from the top to the bottom
yTranA   = linspace(0, transd.d, transd.reso); % The y-axis for the Amode plot (0 : steps : transd.d)
```

Plot RF data (Simulation2D_RFdata_Generator.m)
The RF data is plotted in one time.

```
%% Plot RF Data

   if doPlot
        timerI = tic;

        figure('Renderer','zbuffer');
        subplot(5, 3, [1 4]);
            plot1=pcolor(tissue.x, tissue.y, tissue.data);set(gca,'FontSize',12)
            shading interp; colormap('gray');hold on
            title('Tissue consisting of layers','Units', 'normalized', 'Position', [1 1],
            'HorizontalAlignment', 'right','FontSize',12)

            Parent = hgtransform;
            catheter = hggroup();
            tT = line([transd.Tiploc(1),transd.Tipview(1)],  [transd.Tiploc(2),transd.Tipview(2)],
                [transd.Tiploc(3), transd.Tipview(3)], 'Color', 'r','LineWidth',3, 'Parent', catheter);
            tA = line([transd.Aloc(1),transd.Aview(1)],      [transd.Aloc(2),transd.Aview(2)],
                [transd.Aloc(3), transd.Aview(3)],   'Color', 'b','LineWidth',3, 'Parent', catheter);
            tB = line([transd.Bloc(1),transd.Bview(1)],      [transd.Bloc(2),transd.Bview(2)],
                [transd.Bloc(3), transd.Bview(3)],   'Color', 'm','LineWidth',3, 'Parent', catheter);
            set(catheter,'Parent',Parent);hold on;
            axis equal; ylim ([0 widthx]);
            xlabel('Width(mm)','Units', 'normalized', 'Position', [0.95 -0.04], 'HorizontalAlignment',
            'right','FontSize',12);
            ylabel('Thickness(mm)')
            plot(transd.Tiploc(1),transd.Tiploc(2), 'ro','MarkerSize',6);hold on; % Starting point

        % Plot cardiac motion
        subplot(5, 3, 6);
            plot(t, tissue.height); set(gca,'FontSize',12)
            hold on
            title('Comppression of tissue','FontSize',12);xlabel('Time(s)','FontSize',12)
            ylabel('Thickness layer (mm)','FontSize',12)
            plot8b=plot(t(i),tissue.height(i),'r.','MarkerSize',20);

        % Plot translation in Y direction
        subplot(5, 3, 3);
            plot(t, tranY);set(gca,'FontSize',12)
            hold on
            title('Catheter motion in y direction','FontSize',12)
            xlabel('Time(s)','FontSize',12)
            ylabel('Y-displacement (mm)','FontSize',12)

        % Plot translation in X direction
        subplot(5, 3, 2);
            plot(t, tranX);set(gca,'FontSize',12)
            hold on
            title('Catheter motion in x direction','FontSize',12)
            xlabel('Time(s)','FontSize',12)
            ylabel('X-displacement (mm)','FontSize',12)

        % Plot rotation around Z-axis
        subplot(5, 3, 5);
            plot(t, rotZ);set(gca,'FontSize',12)
            hold on
            title('Catheter rotational motion','FontSize',12)
            xlabel('Time(s)','FontSize',12)
            ylabel('Angle (rad)','FontSize',12)

        subplot(5,3,[7 8 9]);
            % yTran - max(yTran) because otherwise the images are vertically flipped
            pcolor(t, (yTranTip-max(yTranTip)), MmodeTip);set(gca,'FontSize',12)
            shading interp; colormap('gray');hold on
            Tran=0*t;
            plot(t(end), Tran(end), 'r.','MarkerSize',30);
            title('M-Mode Tip-transducer','Units', 'normalized', 'Position', [0 1], 'HorizontalAlignment',
            'left','FontSize',12);
            xlabel('Time(s)','Units', 'normalized', 'Position', [0.99 -0.1], 'HorizontalAlignment',
            'right','FontSize',12);
            ylabel('Depth(mm)','FontSize',12);
```

```
        subplot(5,3,[10 11 12]);
            % yTran - max(yTran) because otherwise the images are vertically flipped
            pcolor(t, (yTranA-max(yTranA)), MmodeA);set(gca,'FontSize',12)
            shading interp; colormap('gray');hold on
            Tran=0*t;
            plot(t(end), Tran(end), 'b.','MarkerSize',30);
            title('M-Mode A-transducer ','Units', 'normalized', 'Position', [0 1], 'HorizontalAlignment',
           'left','FontSize',12);
            xlabel('Time(s)','Units', 'normalized', 'Position', [0.99 -0.1], 'HorizontalAlignment',
            'right','FontSize',12);
            ylabel('Depth(mm)','FontSize',12);

        subplot(5,3,[13 14 15]);
            % yTran - max(yTran) because otherwise the images are vertically flipped
            plot15=pcolor(t, (yTranB-max(yTranB)), MmodeB);set(gca,'FontSize',12)
            shading interp; colormap('gray');hold on
            Tran=0*t;
            plot(t(end), Tran(end), 'm.','MarkerSize',30);
            title('M-Mode B transducer ','Units', 'normalized', 'Position', [0 1], 'HorizontalAlignment',
            'left','FontSize',12)
            xlabel('Time(s)','Units', 'normalized', 'Position', [0.99 -0.1], 'HorizontalAlignment',
            'right','FontSize',12);
            ylabel('Depth(mm)','FontSize',12)

        dtArray = toc(timerI);
        %fprintf(1,'... i=%3d: time to plot was %f seconds;\n', i, dtArray(i));
    end

dtAll = toc(tAll);
% figure;plot(t,dtArray)
fprintf(1,'...loop over all %d time-samples took %f seconds;\n', length(tranY), dtAll);
```

Make M-mode image of RF data (envelope.m)

The hilbert function is used in Matlab to extract the envelope of the RF data, which results in an M-mode image. This method is not the most optimal option, but gives an impression of envelope extraction. Especially in case of the side transducers this function has difficulties with the 'air' above the tissue.

```
%% Make M-mode images from RF data

clear all
close all
clc

%%
uiopen % open de RF-data matrices of the Tip transducer, the A transducer, the B transducer

%%
env_Tip = log10(abs(hilbert(flipud(MmodeTip))));
figure;imagesc(env_Tip);

env_A = log10(abs(hilbert(flipud(MmodeA))));
figure;imagesc(env_A);

env_B = log10(abs(hilbert(flipud(MmodeB))));
figure;imagesc(env_B);
```

Make Data Compatible with Cameleo Software (ControlClientCompatible.m)

To be able to use the generated RF data as input for the Cameleo Software, the data first needed to convert to a 16-bit file. Therefore the following script is written. Depending on the height of the chosen reflection coefficients the *MmodeTip, MmodeA,* and *MmodeB* matrices needed to be multiplied or divided by a ten-power factor, with as result that a large range of the 16-bit numbers is used. These 16-bit files are written to a .dat file. This .dat file can be sent to Erwin Engelsma, which could use the .dat file as input data for the Cameleo Software. He is also able to make a 'playback' version of the data, a so-called .cam file. This .cam file can only be displayed in the Cameleo Software.

```
%% Make RF data compatible with Control Client software
load('rfdata.mat')

RF_Tip = int16(flipud(MmodeTip/10));
max(max(RF_Tip))
min(min(RF_Tip))
fid = fopen('case_14B_Tip.dat','w');
fwrite(fid,RF_Tip(:),'int16');
fclose(fid)

RF_A = int16(flipud(MmodeA/10));
max(max(RF_A))
min(min(RF_A))
fid1 = fopen('case_14B_A.dat','w');
fwrite(fid1,RF_A(:),'int16');
fclose(fid1)

RF_B = int16(flipud(MmodeB/10));
max(max(RF_B))
min(min(RF_B))
fid2 = fopen('case_14B_B.dat','w');
fwrite(fid2,RF_B(:),'int16');
fclose(fid2)
```

Use data to calculate velocity profile (test_tsm_simul.m)

The generated data can be used to calculate the velocities in the tissue. These velocities can be calculated with a 'Temporal-Spectral-Mean' algorithm (TSM), developed by Philips research, which calculates the velocities based on phase shifts in the RF-data. Therefore should first the generated data be written to the variable *us_slot*, which serves as input for the TSM algorithm. The data also need to be flipped.

```
us_slot=flipud(MmodeTip);
```

Furthermore, to control the intensity of the colours in the TSM images, the colour map scale needs to be set according to the maximum measurable velocity, which is now set from -25.6 mm/s to 25.6 mm/s (can be changed all at the bottom of the script).

$$v_{max} = \frac{\mathrm{PRR} \cdot c}{4 \cdot f_{carrier}}$$

$$v_{max} = \frac{2\,\mathrm{kHz} \cdot 1540\ m/s}{4 \cdot 30\,\mathrm{MHz}} = 25.6\ mm/s$$

Then, the algorithm can be used. It is recommended to set `all_data_out = rawTsmOut` if simulated data are used and to use `all_data_out = cleanTsmOut` if real US data are used. In that case your result is less infected with noise. Moreover, the colormap of the image can be set with the colours as used in the Cameleo Software and common Doppler Software, namely red represents motion towards the transducer and blue represents motion away from the transducer, see Figure 4. If you not set this colour map, the standard 'jet' colour map will be used.

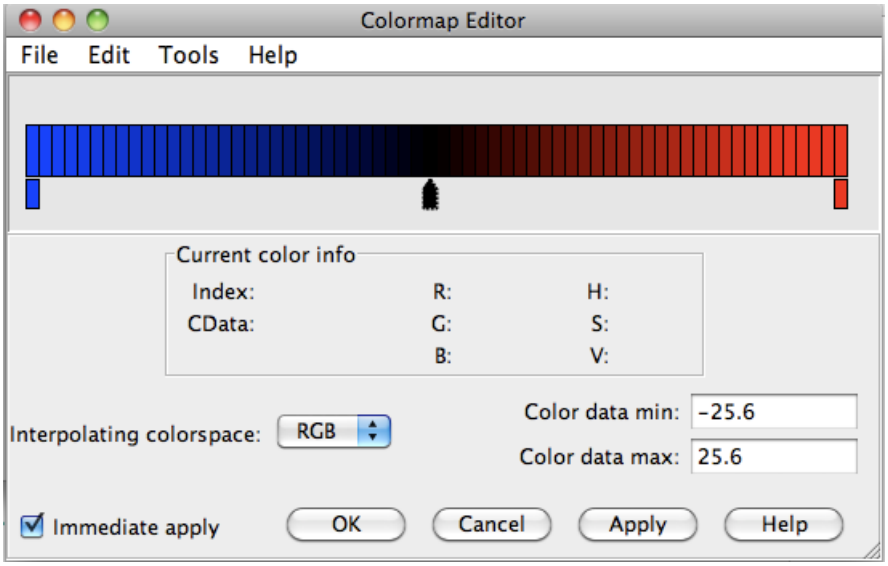

Figure 4 Set colour map of TSM

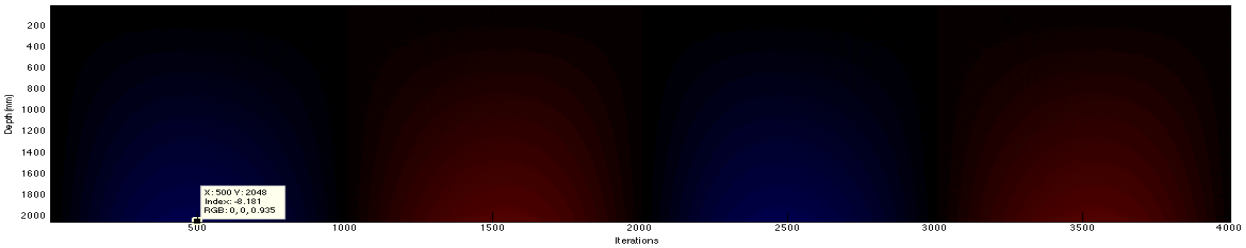

Figure 5 TSM image

```
% MmodeTip should already in the Matlab workspace
noise_threshold = 0.6;
cmap = 'jet';
%-----------------------------------us----------------------------------------
% Read sensor data from one experiment
%-------------------------------------------------------------------------------
[R_us_slot, C_us_slot] = size(us_slot);
%-------------------------------------------------------------------------------
% Create algorithm instances and get their default parameters
%-------------------------------------------------------------------------------
data_header.width = C_us_slot;
data_header.height = R_us_slot;
data_header.Fs_data = 100e6;
data_header.Fs_alines = 2000;
[local.tsm, ~, par.tsm] = tsm('create');
%-------------------------------------------------------------------------------
% Initialize algorithm
%-------------------------------------------------------------------------------
par.tsm.horfilt_enable = 1;
par.tsm.packet_size = 16;
par.tsm.time_step = 1;
par.tsm.depth_step = 4;
par.tsm.bpf_enable = 0;
par.tsm.var_freq_threshold = noise_threshold;
[local.tsm, ~, par.tsm] = ...
    tsm('init', local.tsm, par.tsm, data_header);
tsmFuns = tsm_members; % returns access functions for tsm members
tsmOutDataDynamicRange = tsmFuns.GetTsmOutDataDynamicRange(local.tsm);

%-------------------------------------------------------------------------------
fprintf('tsm packet-size is: %d\n', par.tsm.packet_size);
fprintf('tsm time_step is  : %d\n', par.tsm.time_step);
fprintf('tsm depth_step is : %d\n', par.tsm.depth_step);

%-------------------------------------------------------------------------------
% allocate memory for the algorithm input and output data buffers, and for
% the RGB display window buffer.
%-------------------------------------------------------------------------------
% all_data_out = double(zeros(R_us_slot, C_us_slot));
%-------------------------------------------------------------------------------
% run the algorithm in a block-oriented fashion (like in a real-time appl.)
%-------------------------------------------------------------------------------
% H = figure;
fprintf('computing...')
[local.tsm, status.tsm, par.tsm, ~] = ...
        tsm('run', local.tsm, par.tsm, us_slot(:, 1:data_header.width));
% Retrieve tsm/tsv/tsmraw output from the tsm module at the same
% resolution as the tsm input as defined in the input data_header.
tsmFuns     = tsm_members; % returns access functions for tsm members
dim         = [data_header.height data_header.width];
tsvOut      = tsmFuns.GetTsvOut(local.tsm, dim);
rawTsmOut   = tsmFuns.GetRawTsmOut(local.tsm, dim);
cleanTsmOut = tsmFuns.GetCleanTsmOut(local.tsm, dim);
duration = status.tsm.duration;

%-------------------------------------------------------------------------
% Buffer all output for later full data displaying.
%-------------------------------------------------------------------------
all_data_out = rawTsmOut; % or rawTsmOut or tsvOut
fprintf('done.\n')
%-------------------------------------------------------------------------------
% close the algorithm
%-------------------------------------------------------------------------------
[local.tsm, ~] = tsm('close', local.tsm);
%-------------------------------------------------------------------------------
% Display the data in a sweep, or all data at once.
%-------------------------------------------------------------------------------
fprintf('displaying data...');
data=(all_data_out/pi)*25.6;
figure; imagesc(data,[-25.6 25.6]); % axis image;
xlabel('Iterations')
ylabel('Depth(mm)')
```

Summary in Workflow

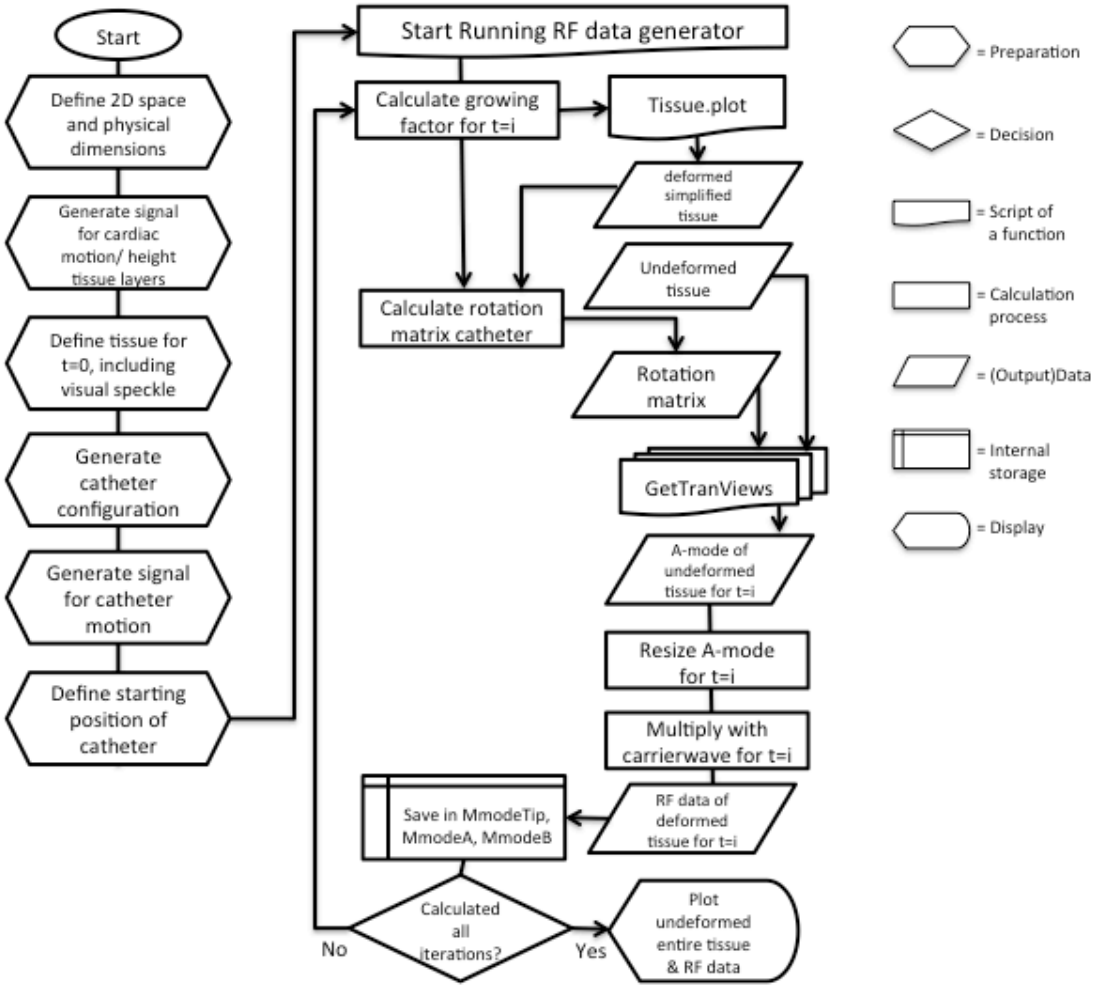

Main difference Movie generator and RF generator

First have to be mentioned that the Movie generator only calculates the so-called simulates sightline, while the RF generator also multiplies this sightline with a carrier wave signal, with an RF data as result, see Figure 5.

The main difference in calculation of this sightline between the Movie generator and RF generator is that in the Movie generator the entire tissue is resized as a result of the cardiac motion signal and the sightline is already determined with the correct elongation, while in the RF data generator the observed sightline is taken from undeformed tissue, and only this observed sightline is resized as result of the cardiac motion signal. Obviously, it saves a lot of time to only resize one column instead of 6000 columns in case of the Movie data generator.

Another main difference is that the acquired sightlines/A-modes are plotted in the Movie generator per iteration, while in the RF data generator all the data is plotted after running all the iterations. That means that only in the Movie generator the entire moving tissue and the moving catheter can be observed over time in the upper left corner. In the RF data generator only the begin position of the entire tissue and catheter is shown in the upper left corner.

Moreover, the resolution and sample frequency of the Movie generator can be decreased with a factor ten, without losing visible result. For the RF data generator a larger sample frequency and resolution is required to be able to use the data as representative US data, which for example can be used to measure velocities in the tissue.

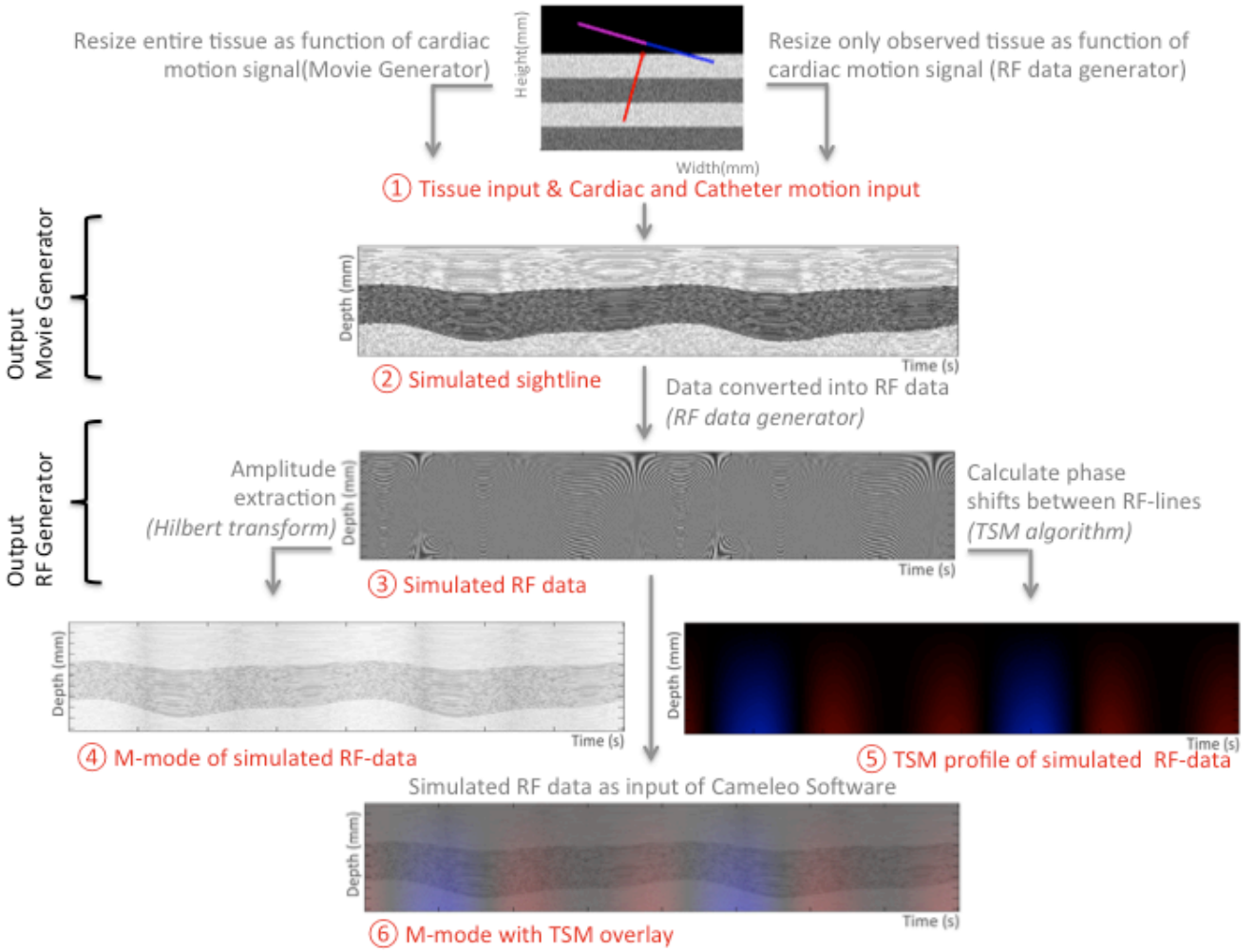

Figure 6 Overview output of Movie generator and RF data generator

M.3. Phase 3: 3D simulation model with catheter motion

The 2D simulation model has been further developed to a 3D simulation model, shown in Figure 68. This model can be compared with the 2D Movie generator.

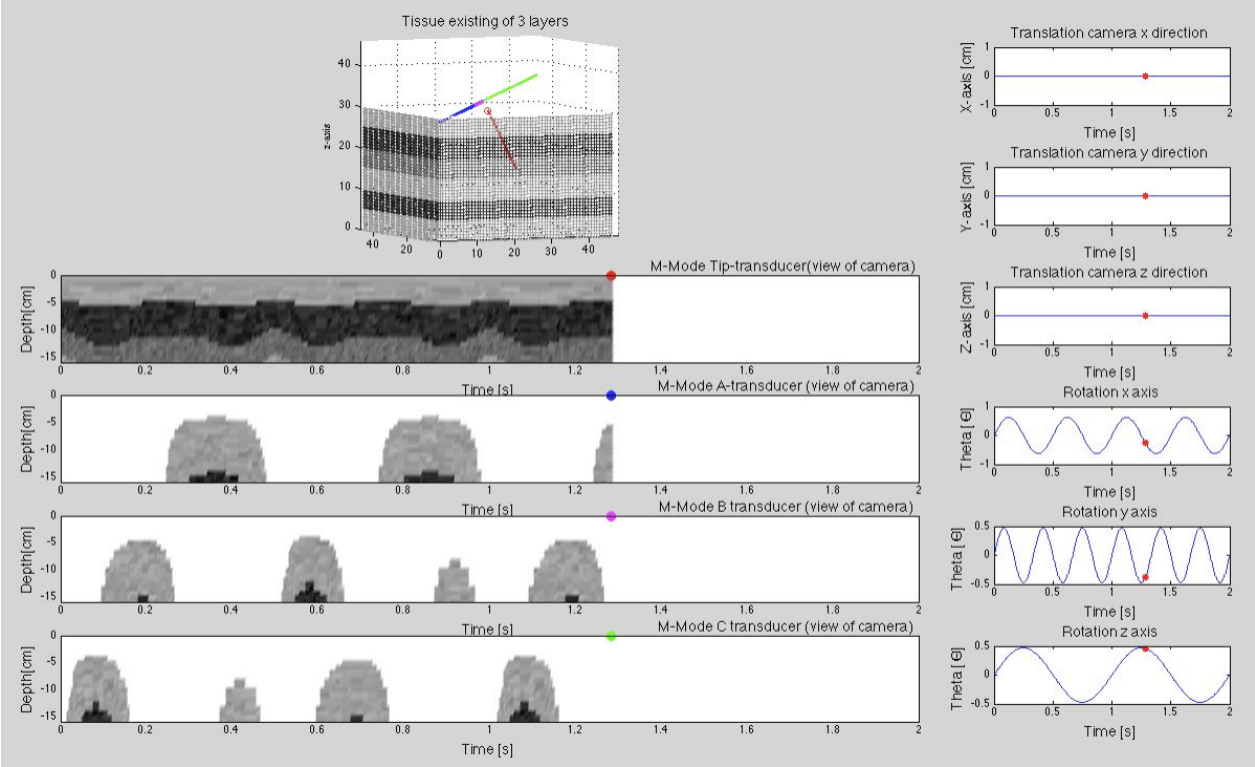

Figure 68: *Output of 3D simulation model, which has more input signals than the 2D model. The catheter consists of one more transducer, which consequently leads to an extra M-mode image*

The catheter orientation has been modelled in a comparable way as has been done in the 2D simulation model. The main difference is that the catheter in this model has more degrees of freedom. The rotation matrix as has been used in the 2D model is adapted to a 3D space. To calculate a rotation matrix for a 3D space, the rotation matrix around the z-axis, shown in equation 1 can be combined with a rotation matrix around the x-axis, equation 12, and with a rotation matrix around the y-axis, equation 13.

$$\begin{bmatrix} x' \\ y' \\ z' \\ 1 \end{bmatrix} = \begin{bmatrix} 1 & 0 & 0 & dx \\ 0 & \cos\theta_x & -\sin\theta_x & dy \\ 0 & \sin\theta_x & \cos\theta_x & dz \\ 0 & 0 & 0 & 1 \end{bmatrix} \begin{bmatrix} x \\ y \\ z \\ 1 \end{bmatrix} \tag{12}$$

$$\begin{bmatrix} x' \\ y' \\ z' \\ 1 \end{bmatrix} = \begin{bmatrix} \cos\theta_y & 0 & \sin\theta_y & dx \\ 0 & 1 & 0 & dy \\ -\sin\theta_y & 0 & \cos\theta_y & dz \\ 0 & 0 & 0 & 1 \end{bmatrix} \begin{bmatrix} x \\ y \\ z \\ 1 \end{bmatrix} \tag{13}$$

The order in which the equations 1, 12 and 13 are multiplied determines the combined 3D rotation matrix. Equation 14 shows the final rotation matrix when first a rotation around the x-axis is applied, then around the y-axis, then around the z-axis, followed by translation given in dx, dy and dz. In this equation the θ represents the rotation around the x-axis, ϕ represents the rotation around the y-axis, and φ represents the rotation around the z axis. These rotations can also be indicated with the terms pitch (rotation around

x-axis), roll (rotation around y-axis) and yaw (rotation around z-axis).

$$\begin{bmatrix} x' \\ y' \\ z' \\ 1 \end{bmatrix} = \begin{bmatrix} \cos\phi \cdot \cos\varphi & -\cos\phi \cdot \sin\varphi & \sin\phi & dx \\ \cos\theta \cdot \sin\varphi + \sin\theta \cdot \sin\phi \cdot \cos\varphi & \cos\theta \cdot \cos\varphi - \sin\theta \cdot \sin\phi \cdot \sin\varphi & -\sin\theta \cdot \cos\phi & dy \\ \sin\theta \cdot \sin\varphi - \cos\theta \cdot \sin\phi \cdot \cos\varphi & \sin\theta \cdot \cos\varphi + \cos\theta \cdot \sin\phi \cdot \sin\varphi & \cos\theta \cdot \cos\phi & dx \\ 0 & 0 & 0 & 1 \end{bmatrix} \begin{bmatrix} x \\ y \\ z \\ 1 \end{bmatrix} \tag{14}$$

Currently, this 3D model can only serve as a Movie generator with catheter motion. The calculation proceedings that are required to generate cardiac motion and RF data still need to be implement in this model, this can be done based on how this in modelled in the 2D simulation model.

A large disadvantage of this 3D model is the computation time. In the Movie-generator this problem can be solved by significantly decrease the resolution of the tissue and the sample frequency. Unfortunately this would not be a solution for the RF data generator since a sample frequency of 2 kHz and 2048 samples for one RF signal are required when the RF data is used as input for the TSM or Cameleo software. Consequently, to run the 3D RF generator, computers are desired that have a lot of computation power.

N. Validation of 2D Simulation Model

N.1. Test set-up

The set-up shown in Figure 69 is a heart phantom that contains different chambers. This phantom is used to show how the Cameleo catheter can be used within a heart. The movements of the heart phantom are motorized controlled with the set-up shown in Figure 12. For this study it was desired to fully control the catheter motion instead of using this heart phantom. The heart phantom was replaced by an additional part that was designed and manufactured for this study, shown in Figure 70.

The parts shown in Figure70 make it possible to place the catheter tip aligned with the pivot point of the motorized controlled motion like is the case in the simulation model, shown in Figure 71.

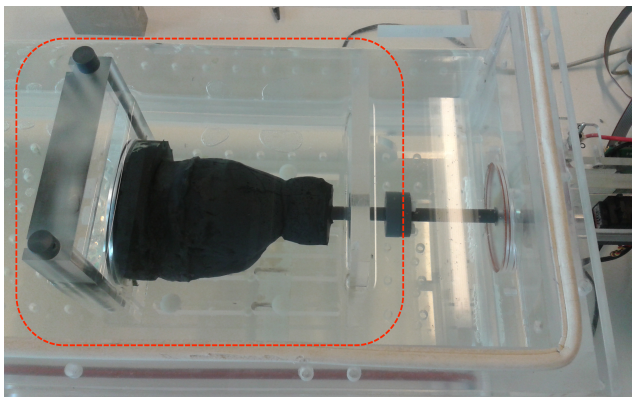

Figure 69: *Orginal test set-up of a heart phantom that is rebuild based on the purpose of this study by replacing the red bordered part with the manufactured parts shown in Figure 70*

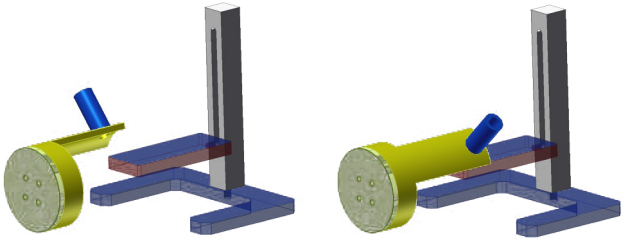

Figure 70: *Designed en manufactured catheter holder (yellow) and tissue holder (blue) that are used to control the catheter motion with the catheter tip aligned at the pivot point*

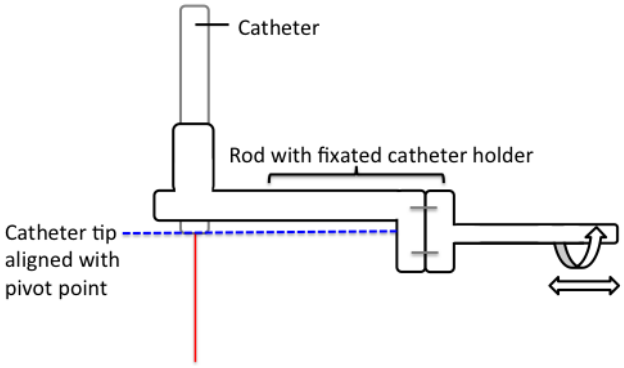

Figure 71: *Side view of set up (shown in Figure 70). The catheter tip is aligned with the pivot point of the motorized controlled motion*

N.2. Test 1: Compare simulated sightline with real US data

During the design process, data were acquired to obtain information how the simulation model should be modelled. These data can be found in the digital appendices. The data that are used for the validation tests and that are used in this article, are small time periods of a longer acquisition. In this appendix the complete time period of these data sets are shown.

N.2.1. Case I Y Motion

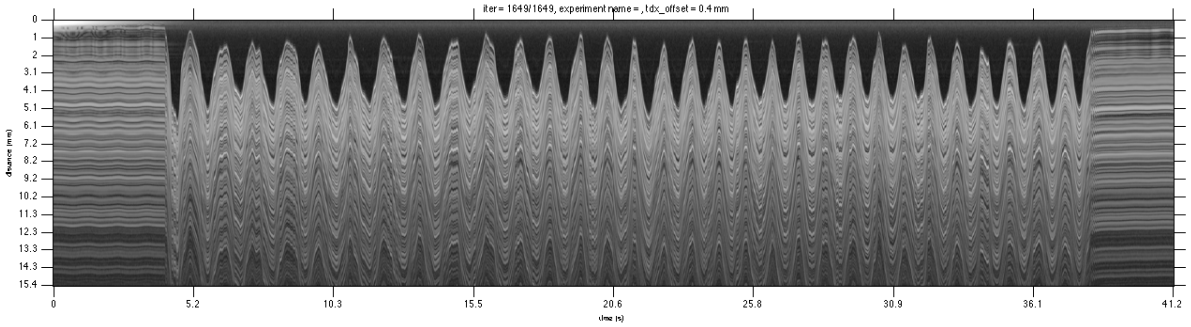

Figure 72: *Full time period of data acquired with tip transducer and only catheter translation in Y-direction*

N.2.2. Case II X Motion

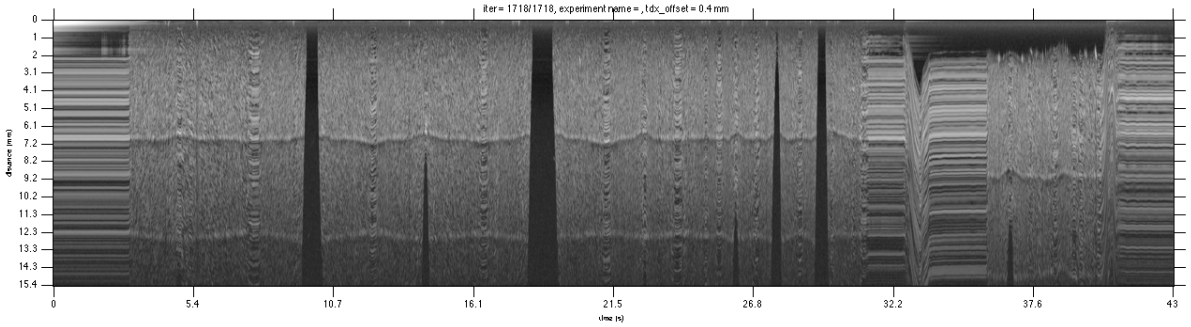

Figure 73: *Full time period of data acquired with tip transducer and only catheter translation in X-direction*

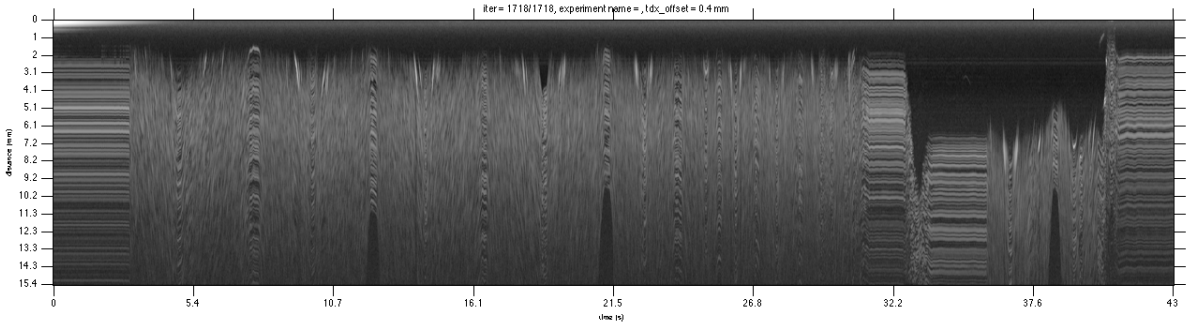

Figure 74: *Full time period of data acquired with side transducer and only catheter translation in X-direction*

In Figure 75 the data of case II from Table 1 is displayed for different constant catheter angles: 0.1π, 0.2π and 0.25π. This Figure shows that the steepness of the slope is not dependent on a constant catheter angle, but is purely caused by the catheter translation in X direction. So, the amplitude of the translation in the X direction could be determined independent of the constant catheter angle.

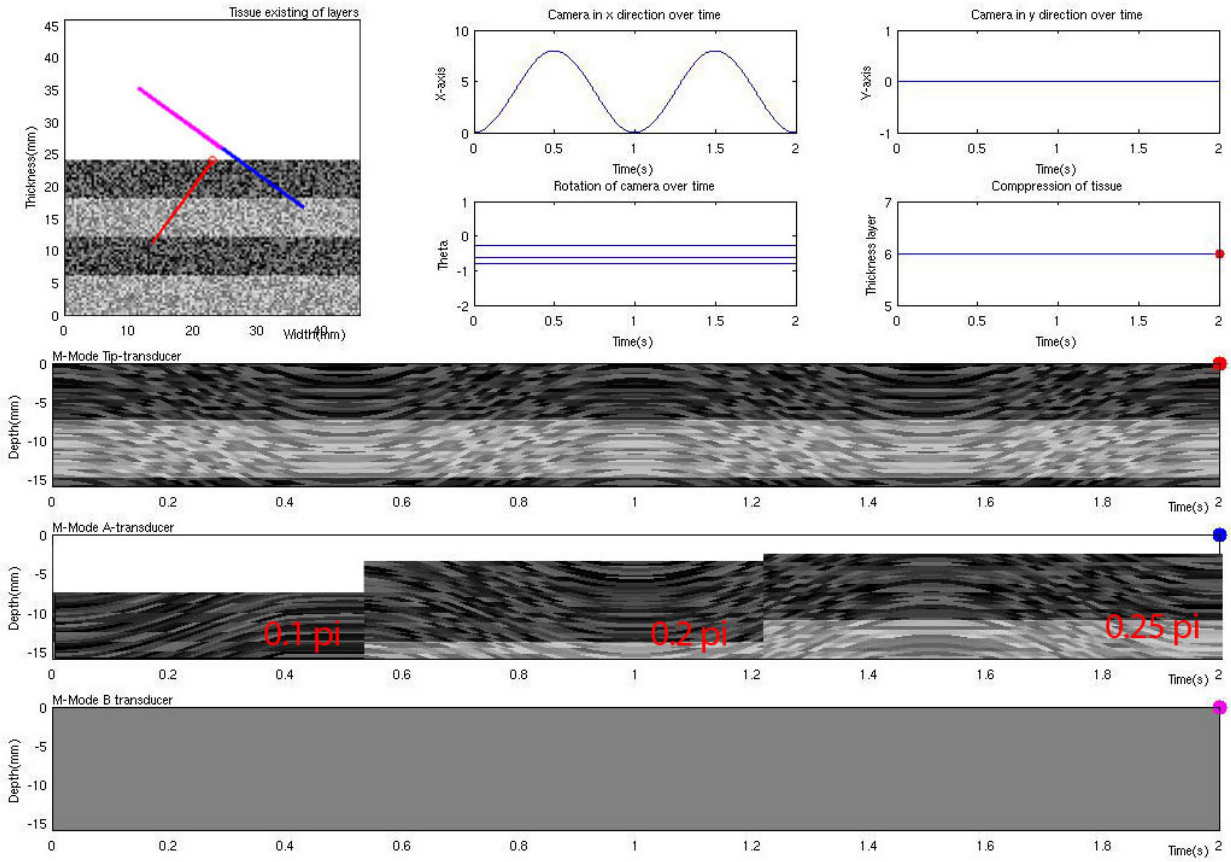

Figure 75: *The steepness of the of the M-mode image as a result of translation in the X-direction is not dependent on the catheter angle, but is purely caused by translational motion*

N.2.3. Case III Cardiac Motion

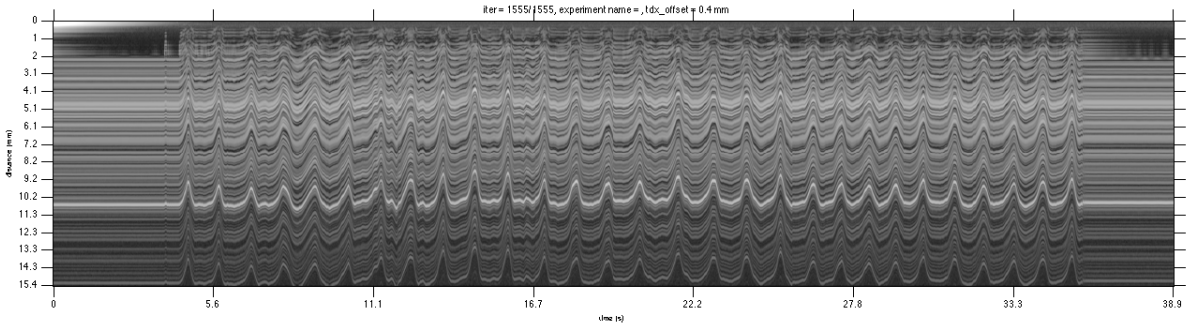

Figure 76: *Full time period of data acquired with only cardiac motion*

N.2.4. Case IV Catheter Motion

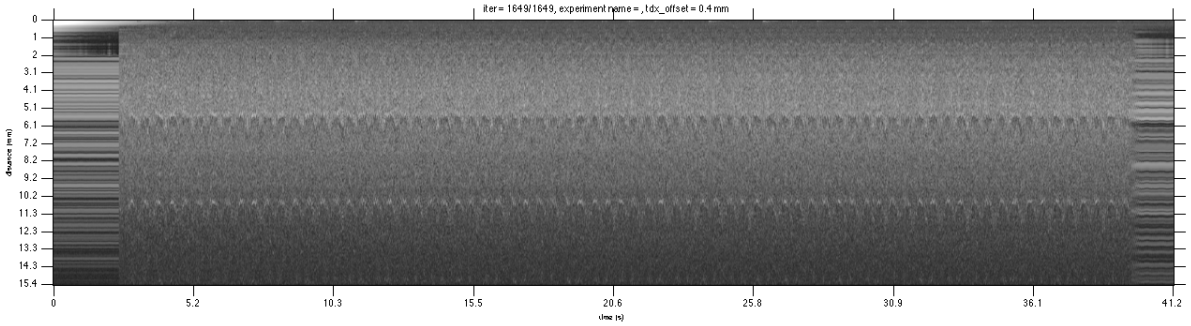

Figure 77: *Full time period of data acquired with tip transducer and only rotational catheter motion*

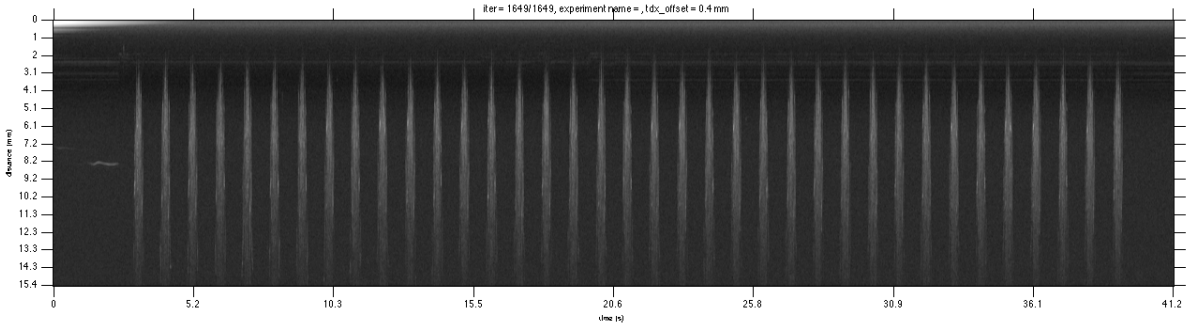

Figure 78: *Full time period of data acquired with side transducer and only rotational catheter motion*

N.2.5. Case V Cardiac and Catheter Motion

Figure 79 shows the data acquired with the settings of case V from Table 1. It can be seen that with the current used set up it was not able to accurately control the cardiac and catheter motion. For that reason, these data were excluded for comparison with simulated data.

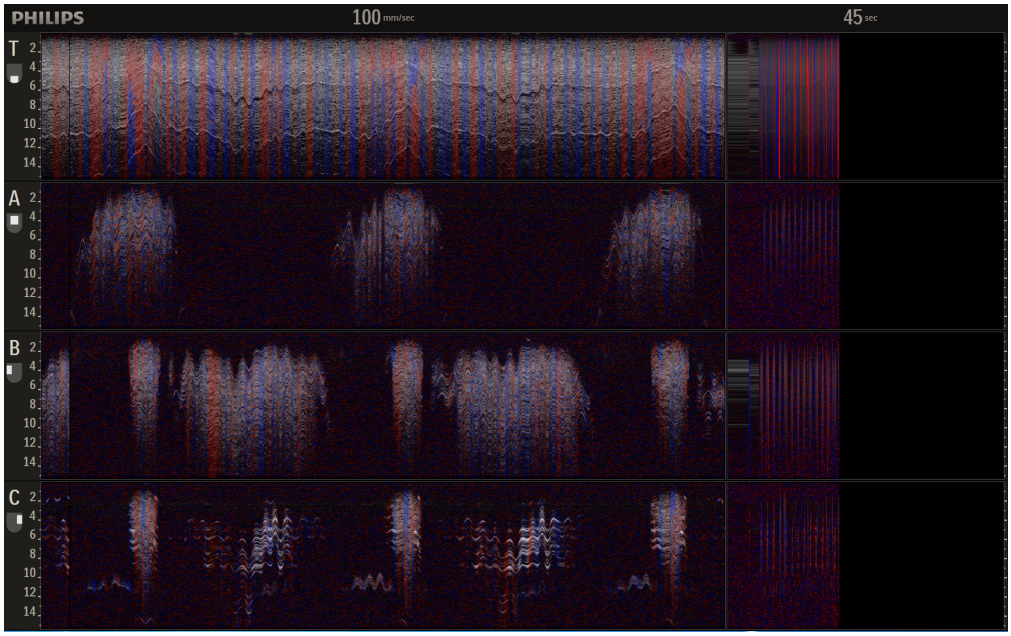

Figure 79: *Real US data where catheter motion is motorized controlled and cardiac motion is controlled by hand*

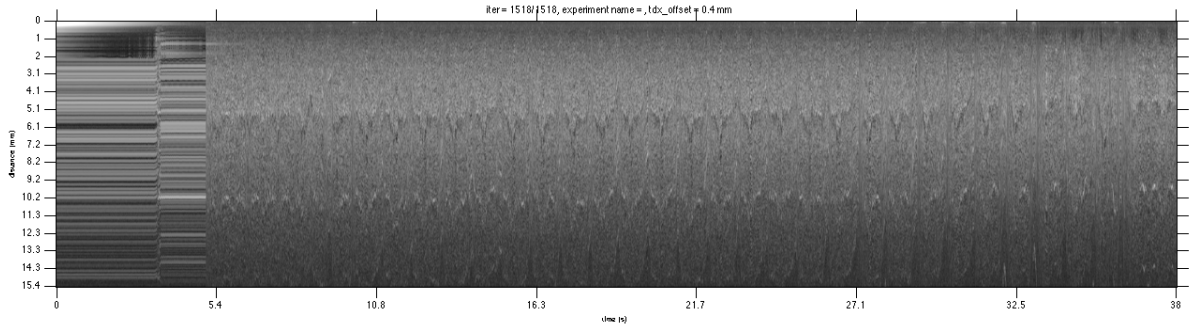

Figure 80: *Full time period of data acquired with cardiac motion controlled by hand and catheter motion motorized controlled*

N.2.6. Case VI Cardiac and Catheter Motion controlled by hand

Figure 81 shows the data acquired with the settings of case VI from Table 1. Also for this example applies that both the cardiac and catheter motion were not accurately controlled and therefore not suitable for comparison with simulated data.

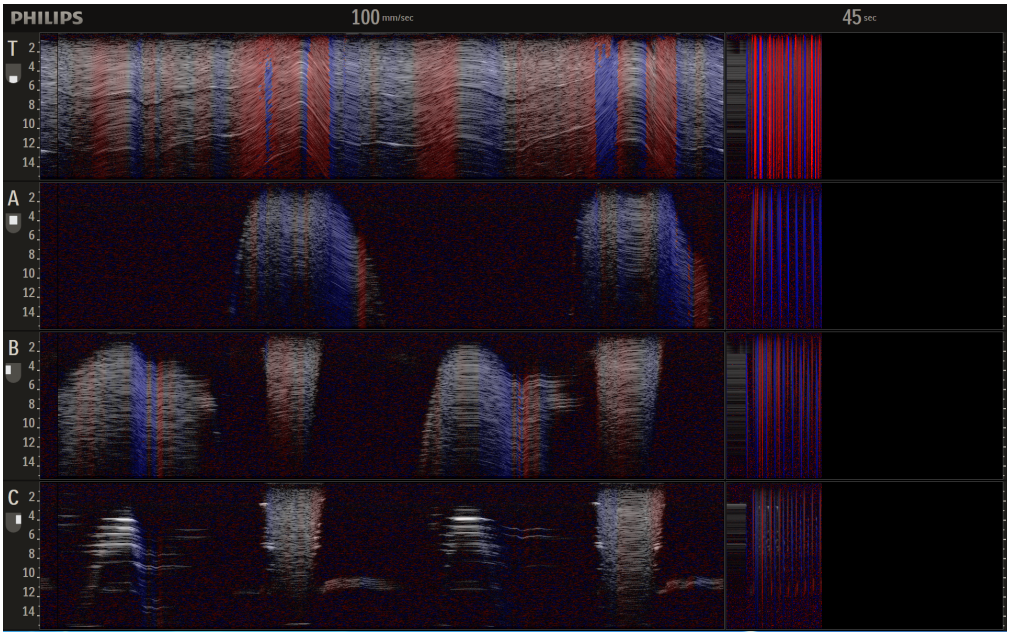

Figure 81: *Real US data where catheter motion and cardiac motion are controlled by hand*

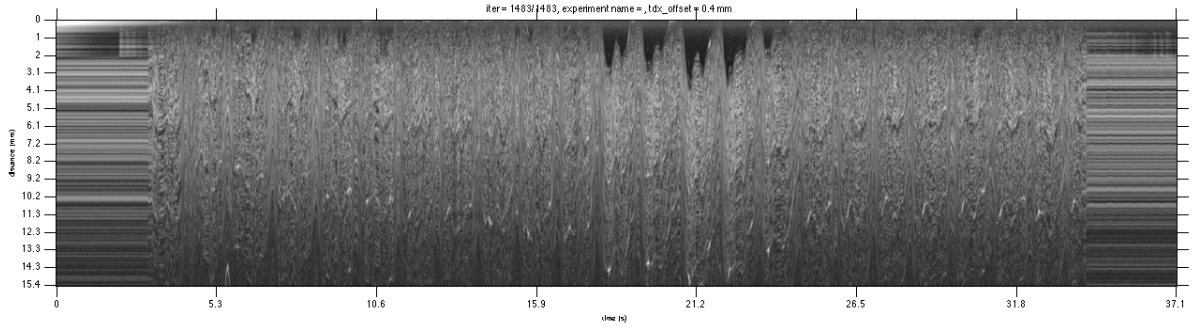

Figure 82: *Full time period of data acquired with cardiac and catheter motion controlled by hand*

N.3. Test 2: Envelope of RF data

In Figure 83 and 84 the results of case III and case IV from the validation test 2 are shown.

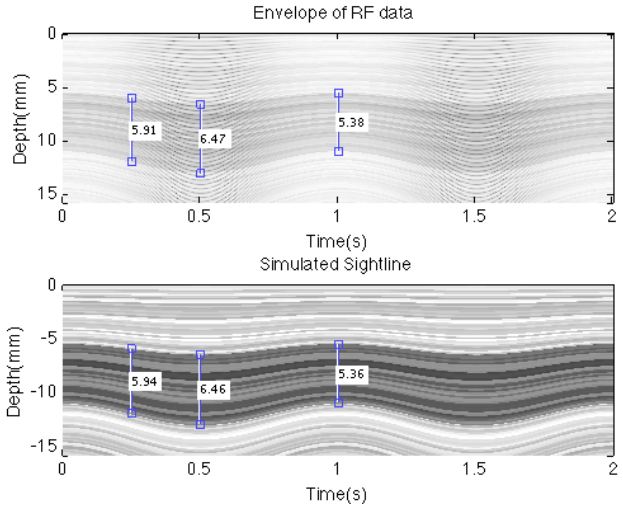

Figure 83: *Top: M-mode image derived from simulated RF data. Bottom: Simulated sightline. Both were acquired by settings of case III from Table 1 that only includes cardiac motion*

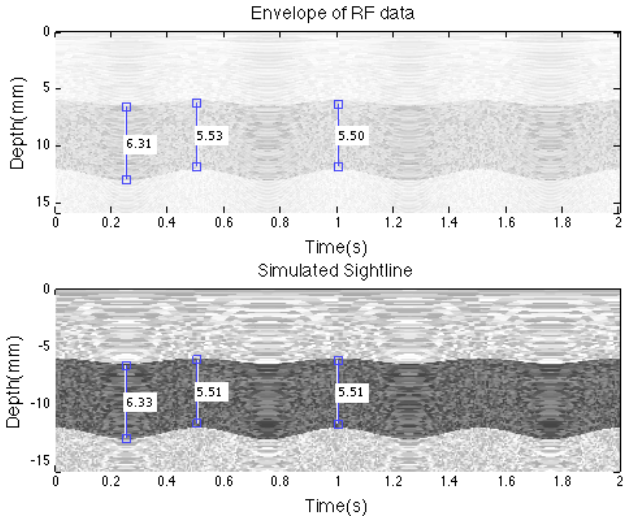

Figure 84: *Top: M-mode image derived from simulated RF data. Bottom: Simulated sightline. Both were acquired by settings of case IV from Table 1 that only includes catheter motion*

N.4. Test 6: Compare TSM of RF data with real US data

Observing simulated data and real US data on more detailed level can support the comparison between the TSM of the simulated data and real US data that has been showed in validation test 6 of this article.

Figure 85 shows real US data acquired with only a palpating motion, which represents cardiac motion. In the close-up of the M-mode image, the motion patterns of the M-mode image are visible. When using plotted RF data as an overlay of the M-mode close-up, then it can be seen that similar motion patterns are visible in the RF data and in the M-mode image. The TSM obtained from these RF data show that a decreasing slope of the patterns in the M-mode image is estimated as a negative velocity and an increasing slope of the patterns in the M-mode image is estimated as a positive velocity. This corresponds to the input signal. Also can be seen that the slope of the motion patterns increases as function of depth, which means that tissue particle located further away from the transducer move with a higher velocity in relation to the transducer compared to particles that are located near to the transducer.

These same patterns can also be seen in Figure 86 for simulated data. The motion patterns that can be seen in the RF data corresponds exactly to the motion patterns of the M-mode image, this suggests that the way in which the RF signal depends on the cardiac motion is modelled correctly. Also a decreasing slope of the patterns in the M-mode image are estimated as a negative velocity and a increasing slope of the patterns in the M-mode image are estimated as a positive velocity.

Figure 87 shows real US data acquired with only catheter motion. Figure 88 shows simulated data acquired with only catheter motion. For both the real US data and the simulated data acquired with only catheter motion can the same conclusions be made as done for acquired data with only cardiac motion. Also for the motion patterns of the simulated RF data applies that these exactly corresponds to the motion patterns that can be seen in the M-mode image, this suggests that the way how the RF signal depends on the catheter motion is also modelled correctly. Moreover, in Figure 87 it can be seen that when the catheter angle increases, in other words, when the tissue seems to become thicker, the M-mode motion pattern and slope of the RF data decreases, estimated with a negative velocity by the TSM. When the catheter angle decreases, in other words, when the tissue becomes thinner, the M-mode pattern and the slope of the RF data increases, estimated with a positive velocity by the TSM.

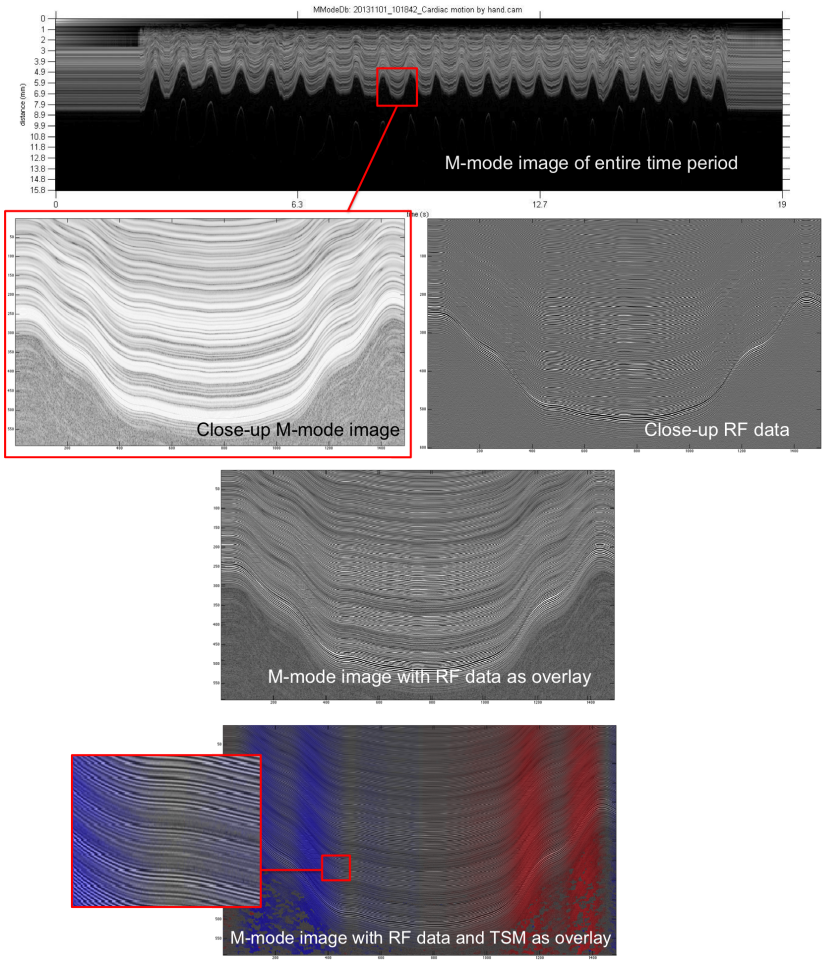

Figure 85: *Schematic overview of how the patterns in M-mode images relate to patterns in RF data and corresponding TSM for real US data acquired with only cardiac motion*

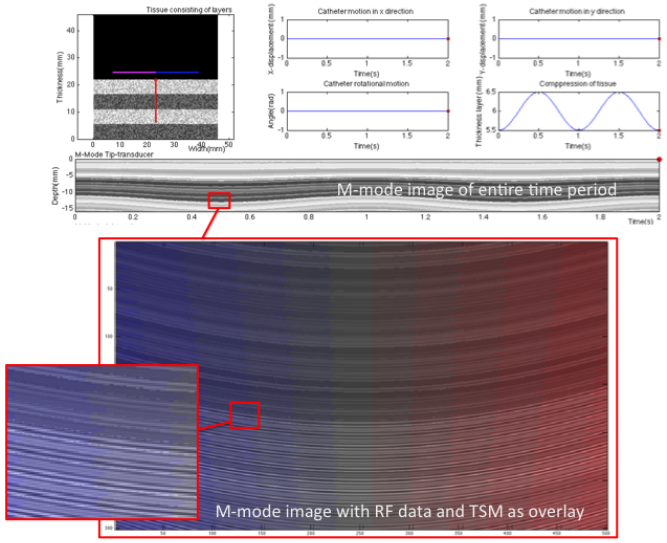

Figure 86: *Schematic overview of how the patterns in M-mode images relate to patterns in RF data and corresponding TSM for simulated data acquired with only cardiac motion*

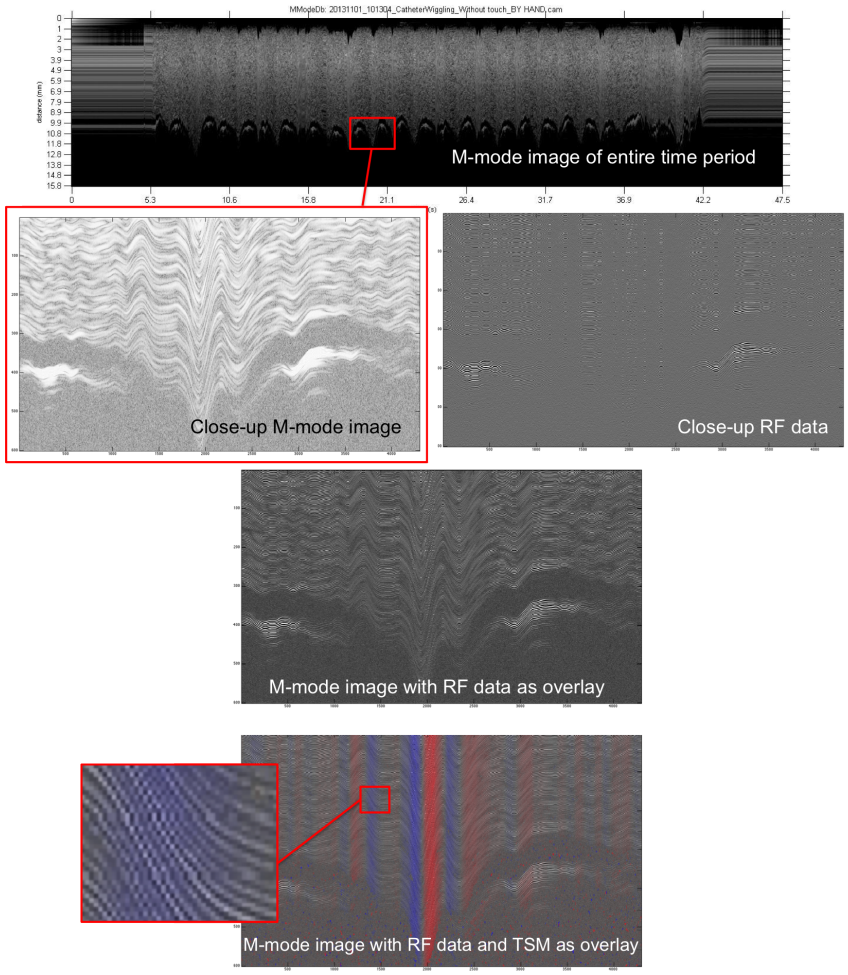

Figure 87: *Schematic overview of how the patterns in M-mode images relate to patterns in RF data and corresponding TSM for real US data acquired with only catheter motion*

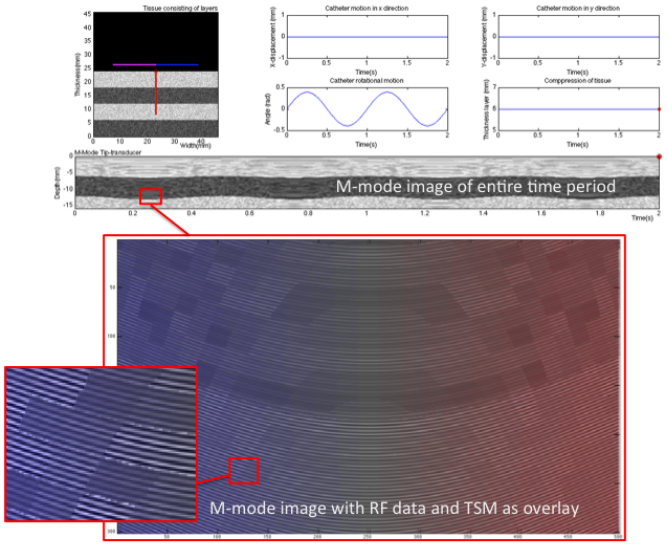

Figure 88: *Schematic overview of how the patterns in M-mode images relate to patterns in RF data and corresponding TSM for simulated data acquired with only catheter motion*

N.5. Test 7: Fast Fourier Transform of two A-modes

As has been discussed in appendix M.2.3, one of the challenges during the development of the RF data was that no frequency shift should occur between the RF signals of two subsequent time samples as result of cardiac or catheter motion, see appendix L for a detailed explanation of this assumption. Validation test 7 was used during the design process to test if a frequency shift was measurable in the generated RF data by making use of the Fast Fourier Transforms (FFT).

Finally this test was also used to test the final design of the simulation model, as will be discussed in this Appendix. Therefore, test 7 was performed for simulated RF data with parameter settings of cases III to V given in Table 1.

In this validation test the FFT of two A-lines were compared where the difference in height of the observed tissue were in maximum and minimum position, so two signals between which any undesired and unexpected frequency shift should be best measurable. This is the case at $t = 0.5sec$ and $t = 1sec$, 1000^{th} and 2000^{th} iteration respectively, for case III shown in Figure 89. The resampled FFT of these two A-lines shows that the centre frequency does not change, but the FFT shows that the distance between the peaks differ. The peaks for the blue line, the 1000^{th} iteration, lie closer to each other, than the peaks of the 2000^{th} iteration. This means that the distance between pulses in the A-mode of the 1000^{th} iteration is larger than the distance between pulses in the A-mode of the 2000^{th} iteration, which is relation to the elongation of the tissue. For case IV and case V, shown in Figure 90 and 91, similar observations can be done.

These results show that now frequency shift occurs. In case of this final concept this result was expected, since the carrier wave is build up with Gaussion pulses with a fixed frequency. Nevertheless, during the design process this method was useful to test the different design concepts.

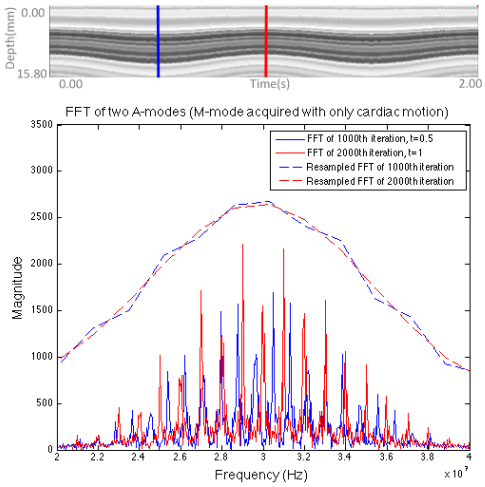

Figure 89: *Top: M-mode of tip transducer acquired with cardiac motion. Bottom: FFT of simulated RF data of A-mode at $t = 0.5$ sec and $t = 1sec$*

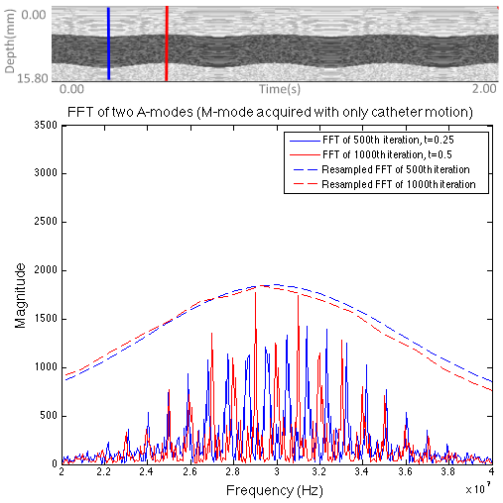

Figure 90: *Top: M-mode of tip transducer acquired with catheter motion. Bottom: FFT of simulated RF data of A-mode at* $t = 0.25$ *sec and* $t = 0.5sec$

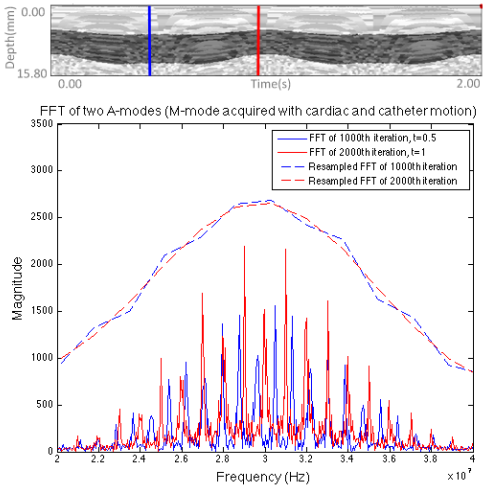

Figure 91: *Top: M-mode of tip transducer acquired with cardiac and catheter motion. Bottom: FFT of simulated RF data of A-mode at* $t = 0.5$ *sec and* $t = 1sec$

N.6. Test 8: Aliasing with artificial data

When the TSM algorithm was used on the simulated RF data aliasing occurred for too large angles. This phenomenon happens since there is a maximum velocity that can be measured with this algorithm, see Appendix F.2. It was tested if similar aliasing patterns occurred for simulated data as real US data. Therefore, the catheter was rotated on the tissue by hand with a frequency of 1Hz and an angle of approximately 0.3π. Figure 92 shows that for both simulated as real US data aliasing occurs, which can be indicated with two opposite velocity directions that are estimated within one A-mode. The aliasing patterns itself are not comparable since the simulated data is generated with a really smooth motion input signal instead of the motion controlled by hand for the real US data.

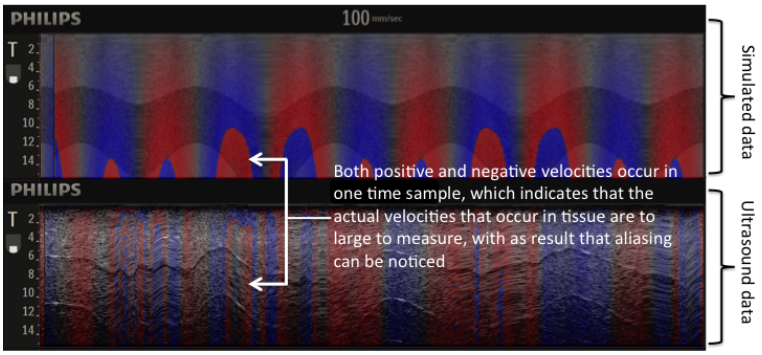

Figure 92: *Aliasing occurs as a result of too fast velocities that occur within the tissue*

O. Analysis of Output data from Simulation Model

O.1. Table of parameter settings of acquired output data

The simulation model was used to generate data that were uses for the analysis of the effect of catheter motion on M-mode images and corresponding TSM profile. The data that were generated with the simulation model were generated according the settings given in Table O.1. Test No. 3, 15, 16 and 17 were not used for the analysis, but were generated to test if the Strain rate algorithm would also work on the simulated data. This will be discussed in more detail in Appendix Q.5.

Table 8: *Parameter setting of acquisition samples, which were used for gaining insights in the effect of catheter motion on US M-modes*

Test No.	Amplitude Cardiac Signal	Amplitude Catheter Signal	Phase-shift Catheter signal
Only Cardiac motion			
1	0.5 mm		
2	1 mm		
3	0.5/0.6/0.75/0.65 mm		
Only Catheter motion			
4		0.125π	0π
5		0.25π	0π
5b		0.2π	0π
Cardiac & Catheter motion			
6	0.5 mm	0.125π	0π
7	0.5 mm	0.125π	0.25π
8	0.5 mm	0.125π	0.5π
9	1 mm	0.125π	0π
10	1 mm	0.125π	0.25π
11	1 mm	0.125π	0.5π
12	0.5 mm	0.25π	0π
13	0.5 mm	0.25π	0.25π
14	0.5 mm	0.25π	0.5π
12b	0.5 mm	0.2π	0π
13b	0.5 mm	0.2π	0.25π
14b	0.5 mm	0.2π	0.5π
15	0.5/0.6/0.75/0.65 mm	0.125π	0π
16	0.5/0.6/0.75/0.65 mm	0.125π	0.25π
17	0.5/0.6/0.75/0.65 mm	0.125π	0.5π

O.2. Output data

The data that were generated with the simulation model according the settings of Table O.1 were converted to data files that are compatible with the Cameleo software. Screenshots of the simulated data displayed in the Cameleo software are shown in Figure 93, 94 and 95.

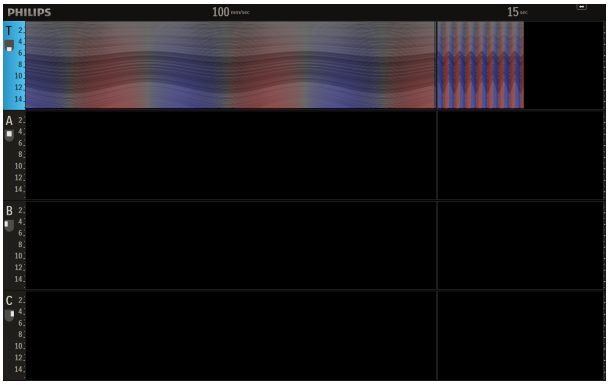

(a) Test No. 1

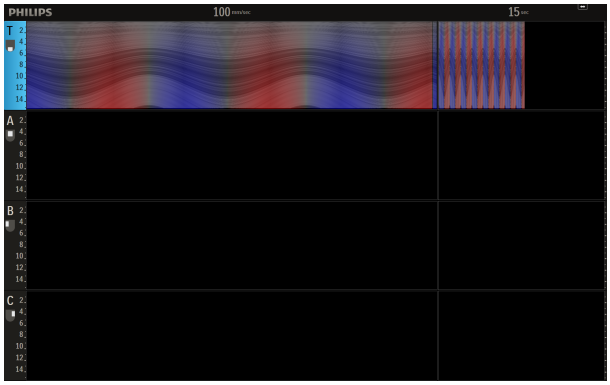

(b) Test No. 2

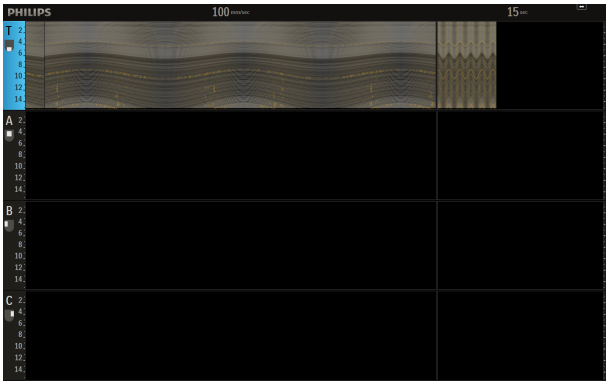

(c) Test No. 3, Strain algorithm

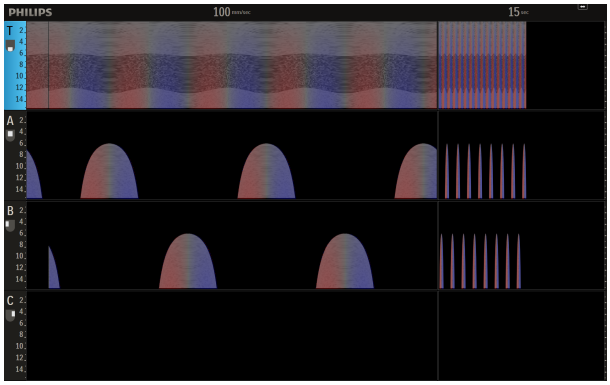

(d) Test No. 4

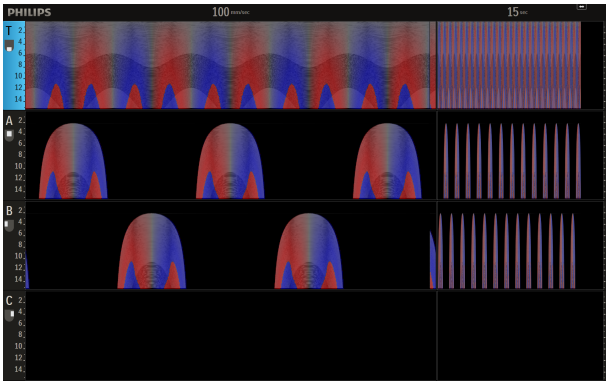

(e) Test No. 5

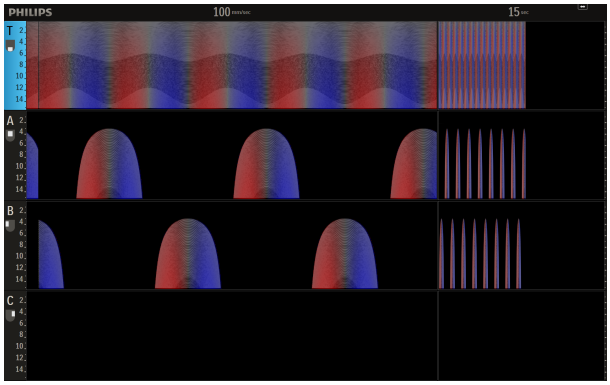

(f) Test No. 5b

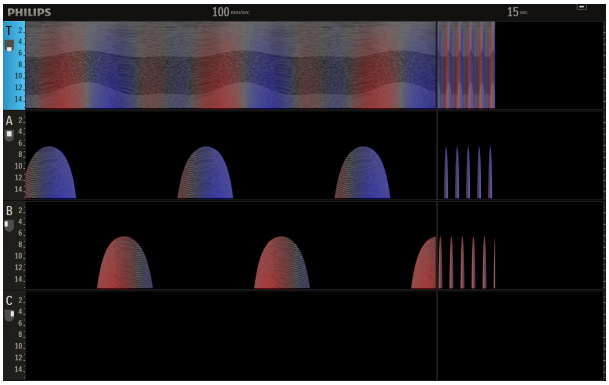

(g) Test No. 6

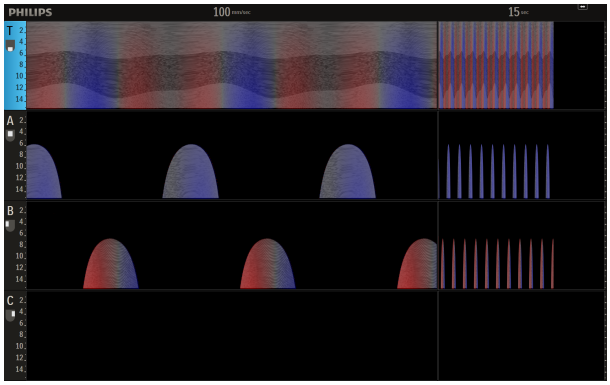

(h) Test No. 7

Figure 93: *Output data used for Analysis*

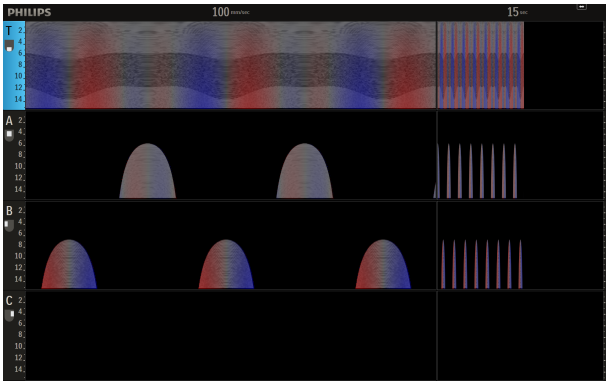

(a) Test No. 8

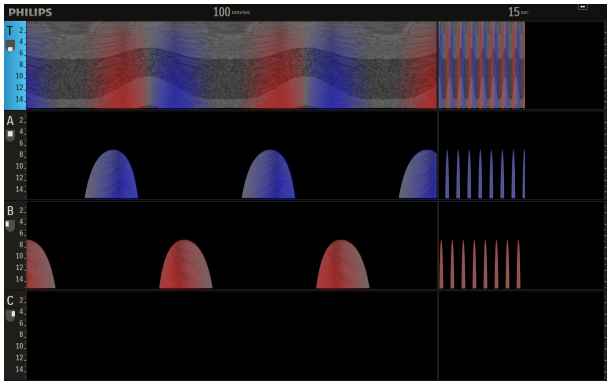

(b) Test No. 9

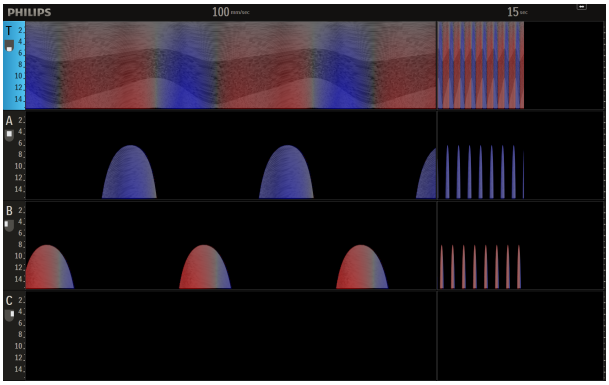

(c) Test No. 10

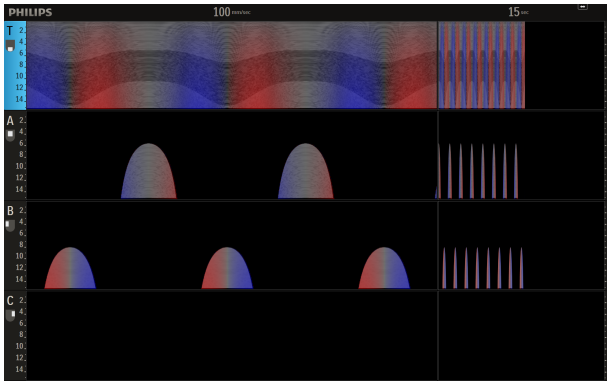

(d) Test No. 11

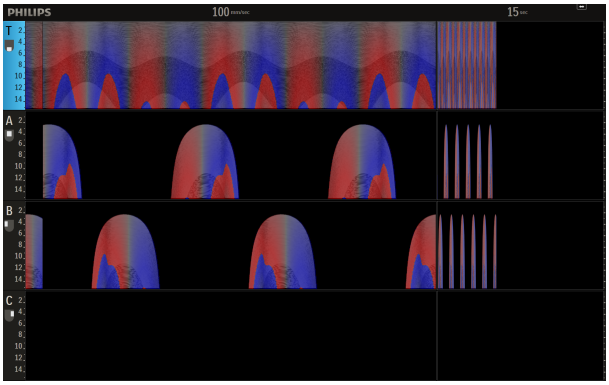

(e) Test No. 12

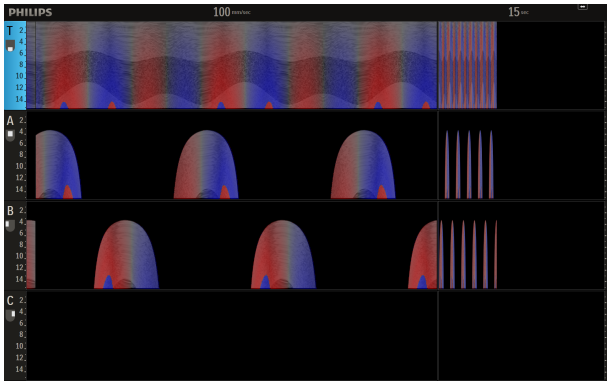

(f) Test No. 12b

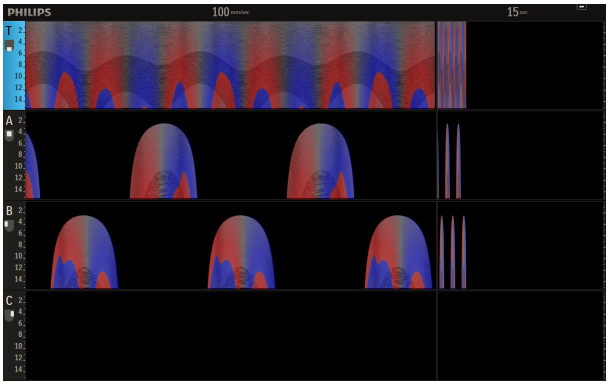

(g) Test No. 13

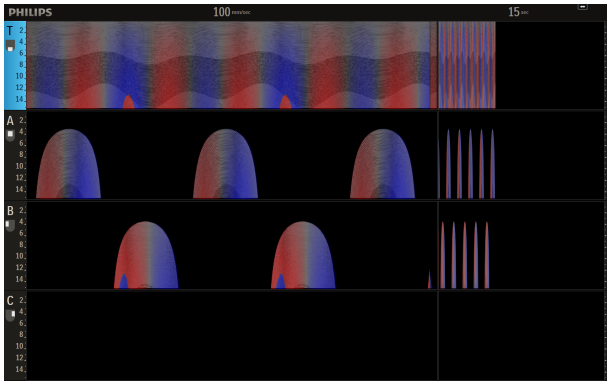

(h) Test No. 13b

Figure 94: *Output data used for Analysis*

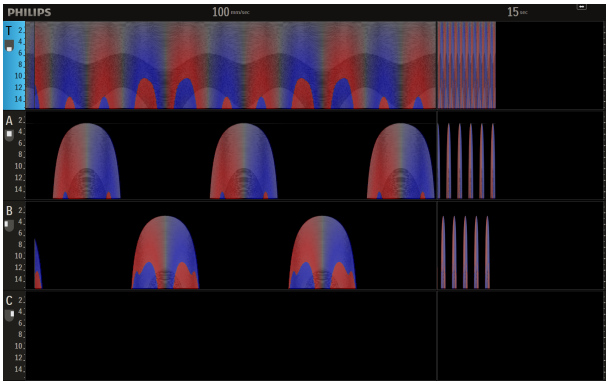

(a) Test No. 14

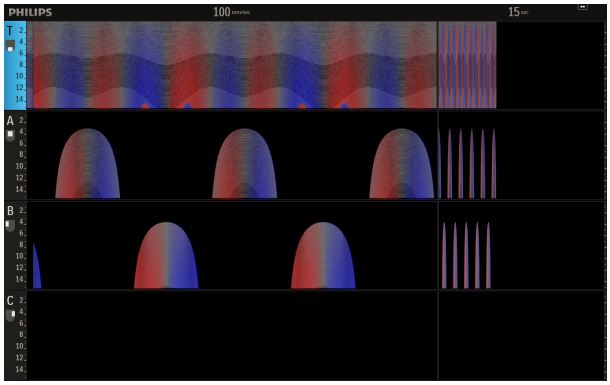

(b) Test No. 14b

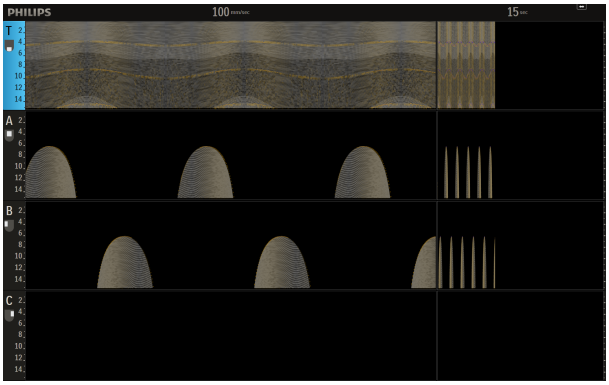

(c) Test No. 15, Strain algorithm

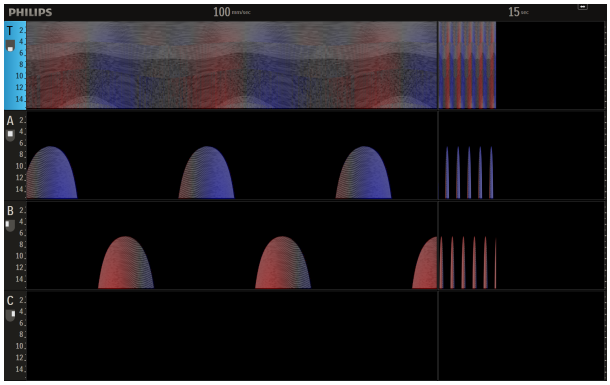

(d) Test No. 15, TSM algorithm

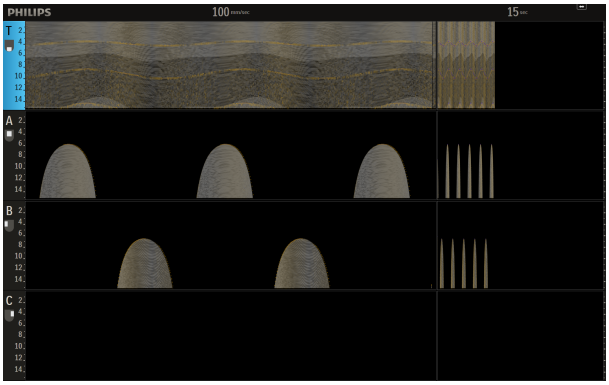

(e) Test No. 16, Strain algorithm

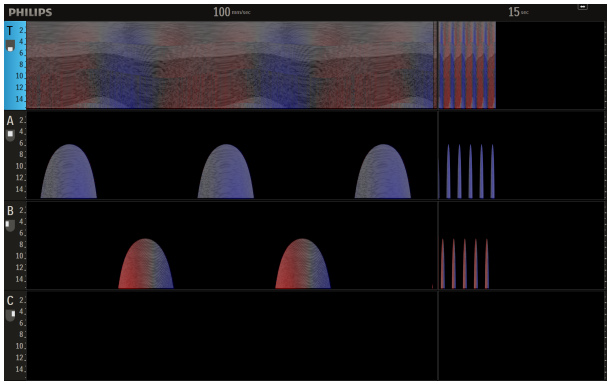

(f) Test No. 16, TSM algorithm

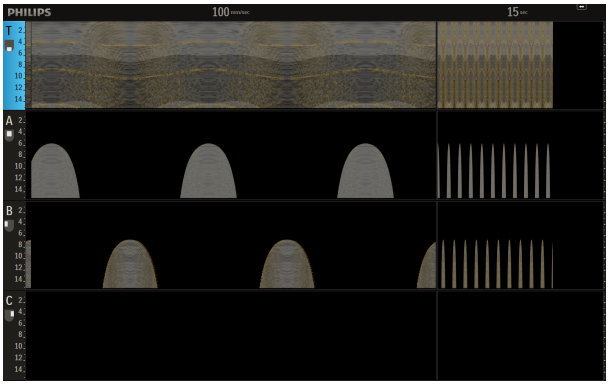

(g) Test No. 17, Strain algorithm

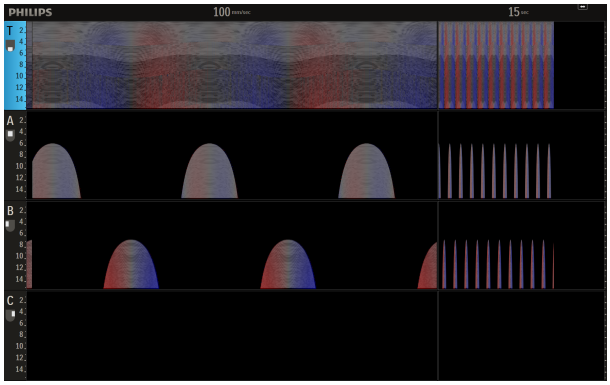

(h) Test No. 17, TSM algorithm

Figure 95: *Output data used for Analysis*

O.3. Overview of analysis with cardiac motion as starting point

The image displayed at the top of Figure 96 shows the M-mode image and TSM of the tip transducer when only cardiac motion is applied. This image is used as a base and from this starting point is shown which changes occur when also catheter motion is involved. If catheter motion is added to cardiac motion, the M-mode and TSM can be influenced in two different ways, this depends whether the catheter angle is increasing or decreasing between two time steps. If the catheter angle is decreasing the observed tissue seems to become less thick in the M-mode than it is in reality, as a result the velocity will increase. If the catheter angle is increasing the observed tissue seems to become even thicker than it is in reality, as a result the velocity will decrease.

When the velocity of catheter motion is larger, the effect on the M-mode and TSM would have obviously more impact, but when catheter motion is dominant over cardiac motion and these two motions have an opposite effect on the M-mode and TSM, the velocity direction of the catheter motion is estimated by the TSM instead of the velocity direction of the cardiac motion. This is the case when the heart wall becomes thicker while the catheter angle decreases or when the heart wall becomes thinner while the catheter angle increases.

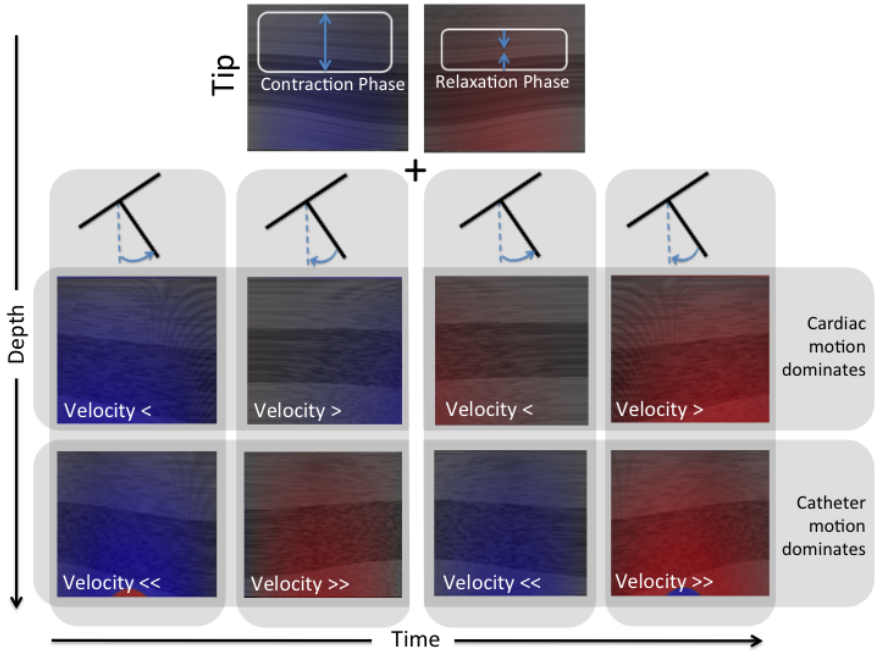

Figure 96: *Overview that shows how the M-mode and TSM of the tip transducer, acquired with only cardiac motion, can be influenced by catheter motion*

O.4. Example case 2

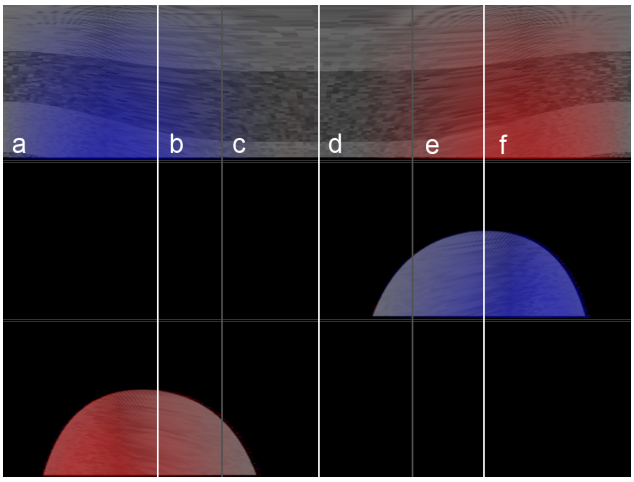

Figure 97: *Simulated output data, acquired with both cardiac motion and catheter motion, divided in six segments in order to evaluate effects of catheter motion and cardiac motion*

The segments shown in Figure 97 are evaluated based on the findings obtained with this study. The action plan, as discussed in this article, has been used to evaluate each segment.

a) Step 1) Catheter motion decreases the estimated velocity by the tip transducer.
Step 2) Side transducer is red, so it cannot be said for sure if cardiac motion is dominant.
Step 3) If cardiac motion is in contraction phase, the cardiac velocity direction is correct, but under-estimated, if cardiac motion is in relaxation phase, the cardiac velocity direction is cancelled out or even incorrect.

b) Step 1) Catheter motion increases the estimated velocity by the tip transducer.
Step 2) Side transducer is red, so it is for sure that cardiac motion is dominant. Cardiac velocity direction in tip transducer is correct, but overestimated due to catheter motion.

c) Step 1) Catheter motion increases the estimated velocity by the tip transducer.
Step 2) Side transducer has no colour, so it cannot be said for sure if cardiac motion is dominant.
Step 3) Nor cardiac nor catheter motion is dominant, so the cardiac velocity direction is correct, but overestimated due to catheter motion.

d) Step 1) Catheter motion decreases the estimated velocity by the tip transducer.
Step 2) Side transducer has no colour, so it cannot be said for sure if cardiac motion is dominant.
Step 3) Nor cardiac nor catheter motion is dominant, so the cardiac velocity direction is correct, but under-estimated due to catheter motion.

e) Step 1) Catheter motion decreases the estimated velocity by the tip transducer.
Step 2) Side transducer is blue, so it is for sure that cardiac motion is dominant. Cardiac velocity direction in tip transducer is correct, but underestimated due to catheter motion.

f) Step 1) Catheter motion increases the estimated velocity by the tip transducer.
Step 2) Side transducer is blue, so it cannot be said for sure if cardiac motion is dominant.
Step 3) If cardiac motion is in relaxation phase, the cardiac velocity direction is correct, but over-estimated, if cardiac motion is in contraction phase, the cardiac velocity direction is cancelled out or even incorrect.

O.5. Example case 3

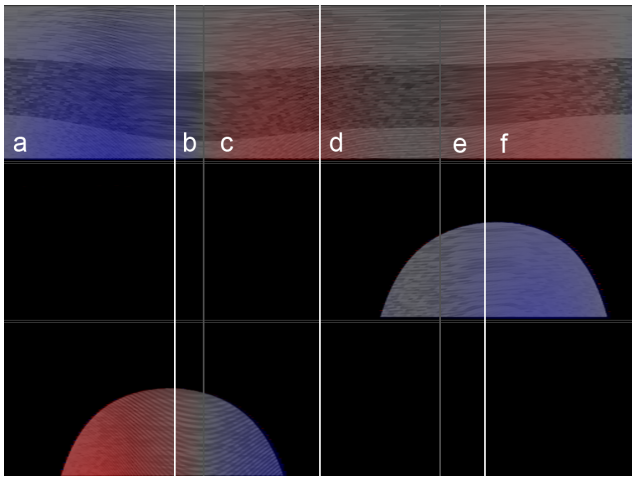

Figure 98: *Simulated output data, acquired with both cardiac motion and catheter motion, divided in six segments in order to evaluate effects of catheter motion and cardiac motion*

The segments shown in Figure 98 are evaluated based on the findings obtained with this study. The action plan, as discussed in this article, has been used to evaluate each segment.

a) Step 1) Catheter motion decreases the estimated velocity by the tip transducer.
Step 2) Side transducer is red, so it cannot be said for sure if cardiac motion is dominant.
Step 3) If cardiac motion is in contraction phase, the cardiac velocity direction is correct, but under-estimated, if cardiac motion is in relaxation phase, the cardiac velocity direction is cancelled out or even incorrect.

b) Step 1) Catheter motion increases the estimated velocity by the tip transducer.
Step 2) Side transducer is red, so it is for sure that cardiac motion is dominant. Cardiac velocity direction in tip transducer is correct, but overestimated due to catheter motion.

c) Step 1) Catheter motion increases the estimated velocity by the tip transducer.
Step 2) Side transducer is blue, so it cannot be said for sure if cardiac motion is dominant.
Step 3) If cardiac motion is in relaxation phase, the cardiac velocity direction is correct, but over-estimated, if cardiac motion is in contraction phase, the cardiac velocity direction is cancelled out or even incorrect.

d) Step 1) Catheter motion decreases the estimated velocity by the tip transducer.
Step 2) Side transducer has no colour, so it cannot be said for sure if cardiac motion is dominant.
Step 3) Nor cardiac nor catheter motion is dominant, so the cardiac velocity direction is correct, but under-estimated due to catheter motion.

e) Step 1) Catheter motion decreases the estimated velocity by the tip transducer.
Step 2) Side transducer is blue, so it is for sure that cardiac motion is dominant. Cardiac velocity direction in tip transducer is correct, but underestimated due to catheter motion.

f) Step 1) Catheter motion increases the estimated velocity by the tip transducer.
Step 2) Side transducer is blue, so it cannot be said for sure if cardiac motion is dominant.
Step 3) If cardiac motion is in relaxation phase, the cardiac velocity direction is correct, but over-estimated, if cardiac motion is in contraction phase, the cardiac velocity direction is cancelled out or even incorrect.

P. Discussion

P.1. Development of Simulation model

P.1.1. Carrier wave & translation

In the current simulation model the simulated carrier wave is only dependent on the catheter rotational motion and cardiac motion. This could be extended with X-translation and Y-translation. Since the assumptions was made that there is no X and Y motion during ablation, the decision was made to do not spend too much time on this process. Consequently, it is not possible to make a TSM of simulated data acquired with a translating catheter in X-direction and Y-direction.

P.1.2. Computation time

Related to the complexity of the wave equation, another reason for the simplified simulation was the calculation time. More complicated calculations are inherent to longer computation time. In conclusion, a consideration was made between a costly simulation that gives to much information for this research purpose or a simplified simulation that fulfils the requirements and gained enough information for this study objective.

P.2. Validation of Simulation Model

P.2.1. Add disturbances to motion input signals

Figure 99 shows the simulated output data when disturbances are added to the input signals. Although this gives similar effects as shown in Figure 15, the added disturbances to the input signals of the simulation model are a rough estimation, since the disturbances of the stepper motor are difficult to determine accurately.

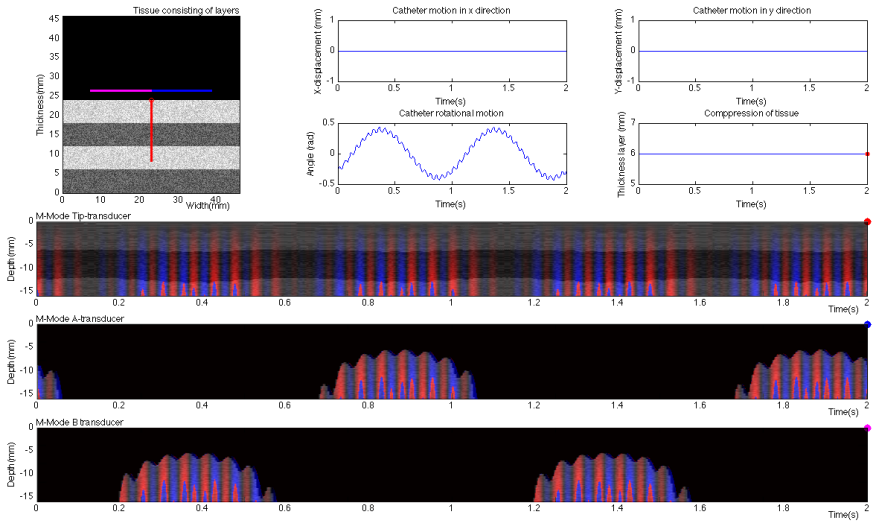

Figure 99: *Example how the input signal of the simulation model could be adapted in such a case that it corresponds to the undesired effects of the stepper motor (Figure 15) used in the test set-up*

P.2.2. One side transducer

Furthermore, the MUVIC 444-H catheter that was used for real US data acquisition contains three side transducers, while the 2D simulation model only contains two side transducers. For that reason, it was only possible to generate with one side transducer a real US M-mode image that was suitable for comparison with the simulation model. This was not really a problem since the applied catheter motion caused the same motion patterns in both the side transducers, but it should be taken into account when less homogeneous catheter motion is applied. In that case it is not possible to use the generated real US data of one side transducer as comparable data for the two side transducers of the simulation model.

P.2.3. Reflection coefficients

Another improvement for the validation tests is to better match the reflection coefficients of the observed tissues of the simulated data and real US data. In this study the tissues were matched based on a four-layer

structure of the tissue. Nevertheless, this could be even more coordinated when using reflection coefficients in the same range with as result that also the brightness levels of the simulated M-modes corresponds to the real US M-modes.

P.3. Analysis of Output data from Simulation Model

P.3.1. Transducer configuration

Figure 100 shows how multiple transducers could be used to calculate the catheter angle in case if the nearest transducer in relation to the catheter tip has been pushed into the tissue. In practise, the tissue surface is not a straight tissue surface, when using multiple transducers the transducer located with the largest distance in relation to the catheter tip would give the least accurate measurement of the catheter angle.

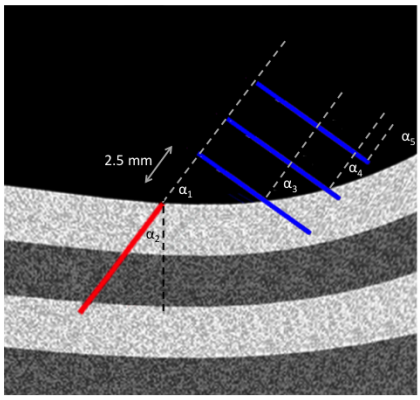

Figure 100: *Example how multiple transducer can be used to calculate the catheter angle if the nearest transducer is pushed into the tissue*

P.3.2. The term 'dominant'

In this simulation model the term 'dominant' is based on how the catheter and cardiac motion are modelled. Further research could give additional evidence that the distance between the Gaussian pulses are correctly modelled as a function of cardiac and catheter motion. Required improvements are not expected, since the RF data exactly follow the motion patterns of the M-mode image, see Figure 87, but if improvements are required to this way of modelling, then it is also required to have a critical view at when cardiac or catheter motion can be labelled with the term 'dominant'.

Q. Recommendations

Q.1. Simulate ablation process

In practise, the Cameleo catheter is used to ablate tissue. During ablation the tissue properties will change. Consequently, the acoustic impedance of the ablated tissue will change, the tissue becomes stiffer and the estimated velocities in the observed tissue will not be equal in the entire tissue. It would be interesting to add the possibility to also simulate this tissue ablation process. This simulation process can be used to gain even more insights about the effect of catheter motion on the assessment of lesion forming during ablation.

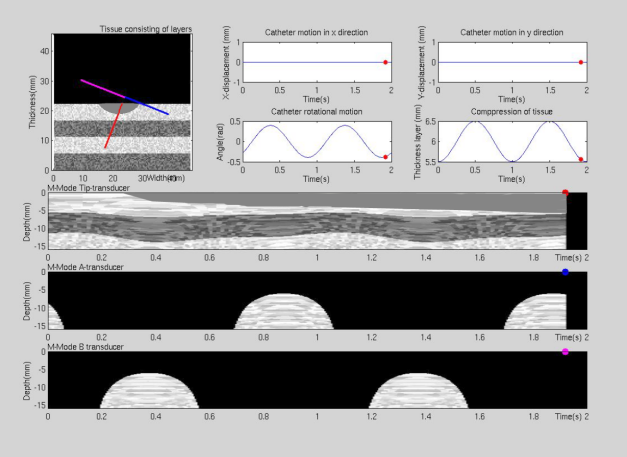

Figure 101: *Example of simulation output when a lesion formation is simulated*

Q.2. User interface

An user interface makes it possible for the user to adapt the input signals while running the simulation model. The effect of changes in the input signal will be directly visible in the M-mode images.

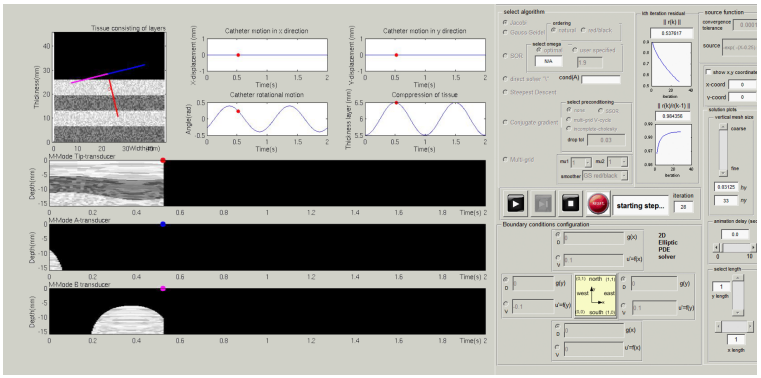

Figure 102: *Recommend is to add a user interface to the simulation model, which makes it possible for the user to adapt parameter settings while running the simulation model*

Q.3. X and Y translation

Another remark that should be mentioned is that in this study the influence of catheter translation in X and Y direction was not taken into account during the analysis. This decision was made based on the assumption that the catheter does not move in X or Y direction since a surgeon applies force on the catheter tip during ablation. Even though this is the case in the majority of cases, it could be interesting to also investigate the effect of these translations on the M-mode image and corresponding TSM, with as goal that these translations could be recognized if it happens anyway.

Q.4. Implement TSM in real-time in simulation model

It would also be recommended to implement the TSM algorithm in the simulation model. Currently, if a TSM is desired, the user first needs to generated RF data for a complete time period. The TSM of these generated RF data can then be calculated. It would be useful if the TSM can be calculated as an overlay of the M-mode image. Therefore the envelope of the generated RF data needs to be displayed over time, while the TSM also works in real time. This combination of monitoring will correspond more to the reality.

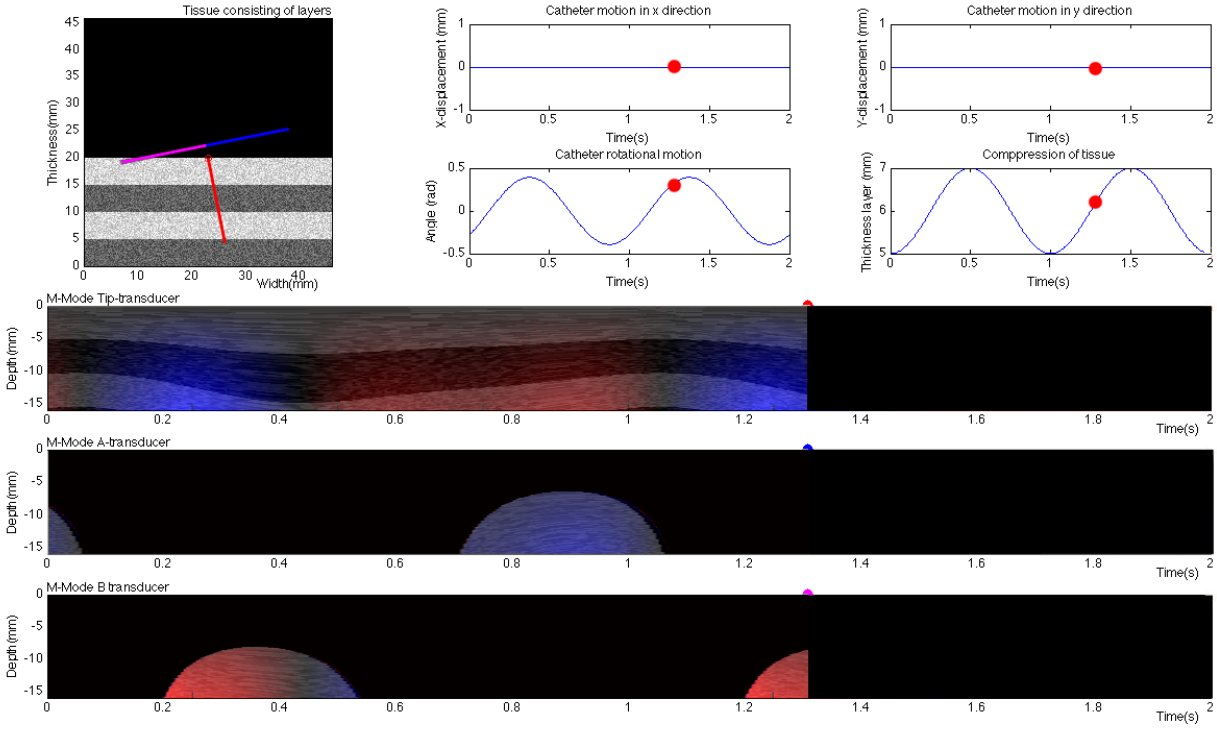

Figure 103: *It would be recommended to implement the TSM algorithm in the simulation model with as result that it could be used in real time.*

Q.5. Strain rate

The simulation model can also be extended by determine different motion input signals for different tissue layers. During this study a simple script has been written to test if the simulated RF data would also be suitable for the Strain rate algorithm, discussed in Appendix F. Therefore, the velocities within the tissue were varied as shown in Figure 104. In Figure 93 and 95 output data are shown that were generated with varying input signals for different tissue layers. As a result of a modelling mistake, the boundary of the different velocities corresponds not with the reflection boundaries, but these Figures show that the Strain rate algorithm can also be used on the simulated RF data.

```
for i = 1:N;

...
height = tissue.height(i);% Select the height of the layer for time=i

    factor_carrier = (height/abs(cos(rotZ(i))))/minheightlayer;

    factor_speckle = height/minheightlayer;
    factor_speckle = round(factor_speckle*1000)/1000;
    [Nom, Denom]=rat(factor_speckle);

  if Strain
    height2 = 1.2* height;
    height3 = 1.5* height;
    height4 = 1.3* height;

    factor_carrier2 = (height2/abs(cos(rotZ(i))))/minheightlayer;
    factor_carrier3 = (height3/abs(cos(rotZ(i))))/minheightlayer;
    factor_carrier4 = (height4/abs(cos(rotZ(i))))/minheightlayer;

    factor_speckle2 = height2/minheightlayer;
    factor_speckle2 = round(factor_speckle2*1000)/1000;
    [Nom2, Denom2]=rat(factor_speckle2);

    factor_speckle3 = height3/minheightlayer;
    factor_speckle3 = round(factor_speckle3*1000)/1000;
    [Nom3, Denom3]=rat(factor_speckle3);

    factor_speckle4 = height3/minheightlayer;
    factor_speckle4 = round(factor_speckle4*1000)/1000;
    [Nom4, Denom4]=rat(factor_speckle4);
  end
...
end
```

```
...
if Carrier
    if Strain
        a=resample(mmodeTip        (1:    end/4),Nom ,Denom ,0);
        b=resample(mmodeTip    (end/4:(2*end)/4),Nom2,Denom2,0);
        c=resample(mmodeTip((2*end)/4:(3*end)/4),Nom3,Denom3,0);
        d=resample(mmodeTip((3*end)/4:      end),Nom4,Denom4,0);

        time=1:(length(a)-1);
        time=time/fs_carrier;
        t = 0 : 1/100E6 : time(end); % 50khz sample rate, pulse train length 10msec
        d1 = (0 : 1/ (10e6 / factor_carrier)  : 2.0470e-05)'; % the prr is 1 kHz, pulse train length 10msec
        carriersignal  = pulstran(t,d1,'gauspuls',30e6,0.3); % 10kHz signal freq, with 50% bandwith

        time2=1:(length(b)-1);
        time2=time2/fs_carrier;
        t = 0 : 1/100E6 : time2(end); % 50khz sample rate, pulse train length 10msec
        d2 = (0 : 1/ (10e6 / factor_carrier2) : 2.0470e-05)'; % the prr is 1 kHz, pulse train length 10mses
        carriersignal2 = pulstran(t,d2,'gauspuls',30e6,0.3); % 10kHz signal freq, with 50% bandwith

        time3=1:(length(c)-1);
        time3=time3/fs_carrier;
        t = 0 : 1/100E6 : time3(end); % 50khz sample rate, pulse train length 10msec
        d3 = (0 : 1/ (10e6 / factor_carrier3) : 2.0470e-05)'; % the prr is 1 kHz, pulse train length 10msec
        carriersignal3 = pulstran(t,d3,'gauspuls',30e6,0.3); % 10kHz signal freq, with 50% bandwith

        time4=1:(length(d)-1);
        time4=time4/fs_carrier;
        t = 0 : 1/100E6 : time4(end); % 50khz sample rate, pulse train length 10msec
        d4 = (0 : 1/ (10e6 / factor_carrier4) : 2.0470e-05)'; % the prr is 1 kHz, pulse train length 10msec
        carriersignal4 = pulstran(t,d4,'gauspuls',30e6,0.3); % 10kHz signal freq, with 50% bandwith

        a=a.*carriersignal;
        b=b.*carriersignal2;
        c=c.*carriersignal3;
        d=d.*carriersignal4;

        mmodeTip = [a b c d];

    else

        time=1:lengthmmode;
        time=time/fs_carrier;
        t= 0 : 1/100E6 : time(end); % 50khz sample rate, pulse train length 10msec
        d1 = (0 : 1/ (10e6 / factor_carrier) : 2.0470e-05)'; % the prr is 1 kHz, pulse train length 10msec
        length(d1);
        carriersignal = pulstran(t,d1,'gauspuls',30e6,0.3); % 10kHz signal freq, with 50% bandwith
        mmodeTip=mmodeTip.*carriersignal;

    end
else
mmodeTip=resample(mmodeTip,Nom,Denom,0);
end
```

Figure 104: *Trial of implementing differences in tissue velocities, to test if the simulated RF data can also be used to obtain a strain rate image*